

155 P.

NASA CR-54023  
REPORT 108F



N 64 23947

NASA CR-54023

Code 1

Cat. 26

## INVESTIGATION OF ZEOLITE MEMBRANE ELECTROLYTES FOR FUEL CELLS

by

Dr. C. Berger (Principal Investigator)  
F. C. Arrance, Dr. D. W. Cleaves, and Dr. M. J. Plizga

prepared for

**NATIONAL AERONAUTICS AND SPACE ADMINISTRATION**

**CONTRACT NAS 7-150**

**ASTROPOWER LABORATORY**  
2121 PAULARINO AVE. NEWPORT BEACH, CALIFORNIA

**MISSILE & SPACE SYSTEMS DIVISION**  
**DOUGLAS AIRCRAFT COMPANY, INC.**  
SANTA MONICA/CALIFORNIA

OTS PRICE

XEROX \$ 11.50 ph.  
MICROFILM \$ \_\_\_\_\_



Report 108-F

**INVESTIGATION OF ZEOLITE MEMBRANE ELECTROLYTES  
FOR FUEL CELLS**

National Aeronautics and Space Administration  
Contract NAS 7-150  
Final Report

March 1964

Prepared By

Dr. C. Berger  
(Principal Investigator)  
Mr. F. C. Arrance  
Dr. D. W. Cleaves  
Dr. M. J. Plizga

MISSILE & SPACE SYSTEMS DIVISION  
ASTROPOWER LABORATORY  
Douglas Aircraft Company, Inc.  
Newport Beach, California

## FOREWARD

This report was prepared by Astropower Laboratory, Missile and Space Systems Division, Douglas Aircraft Company, Inc., for National Aeronautics and Space Administration, Lewis Research Center, Cleveland, Ohio under Contract No. NAS 7-150. It summarizes the work performed under this contract to date.

## TABLE OF CONTENTS

	<u>Page</u>
FORWARD	i
LIST OF ILLUSTRATIONS	iv
LIST OF TABLES	vii
1.0 INTRODUCTION AND SUMMARY	1-1
1.1 Technical Summation	1-2
1.1.1 Theory of Membrane Operation	1-2
1.1.2 Formulation Techniques	1-2
1.1.3 Conductivity	1-3
1.1.4 Fuel Cells	1-4
2.0 EXPERIMENTAL WORK AND DISCUSSION	2-1
2.1 Membrane Composition and Processing Studies	2-1
2.1.1 Zeolite Materials Investigated	2-2
2.1.2 Bonding Materials for Inorganic Fuel Cell Membranes	2-3
2.1.3 Membrane Preparation Techniques	2-4
2.2 Transverse Strength of Phosphate Bonded Inorganic Membranes	2-8
2.2.1 Membranes Prepared by Casting	2-8
2.2.2 Membranes Prepared by Pressing	2-9
2.2.3 Effect of Composition on the Transverse Strength of Pressed Inorganic Membranes	2-9
2.2.4 Effect of Sample Thickness on Transverse Strength of Pressed Inorganic Membranes	2-10
2.2.5 Effect of Pressing Pressure on the Trans- verse Strength of Pressed Inorganic Mem- branes	2-10
2.2.6 Effect of Sintering Temperature on the Transverse Strength of Pressed Inorganic Membranes	2-11
2.2.7 The Effect of Material Drying Time and Temperature on Transverse Strength of Phosphate Bonded Inorganic Membranes	2-12
2.2.8 Presintering Membrane Materials	2-14
2.3 Electrical Conductivity of Phosphate Bonded In- organic Membranes	2-15



## TABLE OF CONTENTS (CONT'D)

	<u>Page</u>
2.3.1 Measurement of Membrane Resistivity	2-16
2.3.2 Results of Resistivity Measurements	2-17
2.3.3 Effect of Composition on Resistivity	2-18
2.3.4 Effect of Sintering Temperature on Membrane Resistivity	2-21
2.3.5 Effect of Sintering Time on Membrane Resistivity	2-22
2.3.6 Effect of Drying Temperature on Membrane Resistivity	2-22
2.3.7 Effect of Drying Time on Membrane Resistivity	2-23
2.3.8 Conductivity for the Statistical Series of Membranes	2-23
2.4 Statistical Analysis of Composition and Processing Variables	2-25
2.4.1 Mathematical Model and Statistical Design	2-25
2.4.2 Experimental Results	2-27
2.4.3 Mathematical Results	2-28
2.5 H <sub>2</sub> -O <sub>2</sub> Fuel Cell Evaluation of Inorganic Membranes	2-29
2.5.1 Cell Design	2-29
2.5.2 Fuel Cell Operation	2-31
REFERENCES	R-1
APPENDIX A - STANDARD METHOD FOR PREPARATION OF INORGANIC MEMBRANE MATERIALS	A-1
APPENDIX B - TRANSVERSE STRENGTH MEASUREMENTS	B-1
APPENDIX C - OPERATING PROCEDURE FOR FUEL CELL	C-1
APPENDIX D - APPARATUS FOR MEASURING CONDUCTIVITY	D-1
APPENDIX E - RESISTIVITY DATA	E-1

## LIST OF ILLUSTRATIONS

<u>Figure</u>		<u>Follows Page</u>
1	Structure of Phosphate Bonded Inorganic Fuel Cell Membrane	2-1
2	Crystal Lattice Structure of Sodium Type A Synthetic Zeolite.	2-2
3	Hydrogen Ion Exchange of Linde 4A Zeolite	2-2
4	Hydrogen Ion Exchange of Linde AW-500 Zeolite	2-2
5	Effect of Zirconia Fiber Additions on the Transverse Strength of Zirconium Phosphate Membranes	2-8
6	Effect of Phosphoric Acid Content on Transverse Strength at 3 material drying Temperatures	2-9
7	Effect of Pressing Pressure on Transverse Strength of Inorganic Membranes	2-10
8	Effect of Pressing Pressure on the Apparent Density of Fired Inorganic Membranes	2-10
9	Effect of Sintering Temperature on Transverse Strength of Inorganic Fuel Cell Membranes	2-12
10	The Effect of Drying Time at 120°C on the Transverse Strength of Inorganic Fuel Cell Membranes	2-12
11	Effect of Material Drying Time at 3 Temperatures on Transverse Strength of Inorganic Fuel Cell Membranes	2-13
12	Effect of Material Drying Time on Transverse Strength	2-13
13	Effect of Material Drying Temperature on Transverse Strength (all data)	2-13
14	Photograph of Vacuum Drying Oven	2-14
15	Effect of ZrO <sub>2</sub> Fiber Additions and Sintering Temperature and Time on Membrane Resistivity	2-21
16	Effect of Alumino-Silicate Fiber Additions on Membrane Resistivity	2-21

LIST OF ILLUSTRATIONS (CONT'D)

<u>Figure</u>		<u>Follows Page</u>
17	Effect of Type of Zirconia Used on Inorganic Membrane Resistivity	2-21
18	Effect of Membrane Composition on Resistivity of Inorganic Membranes	2-24
19	Effect of Drying Temperature upon Resistivity at Constant Drying Time	2-25
20	Effect of Drying Time upon Resistivity at Constant Drying Temperature for Three Membrane Compositions	2-25
21	Statistical Design	2-27
22	Experimental Results	2-27
23	Smoothed Resistivity Data	2-28
24	Analytical Fuel Cell for Evaluation of Inorganic Membranes	2-29
25	Analytical Fuel Cell	2-29
26	Current Build-up in the Inorganic Membrane Fuel Cell During the Conditioning Period	2-31
27	Effect of Temperature on Inorganic Membrane Fuel Cell Operation at 20 Ma/Cm <sup>2</sup> Current Density	2-31
28	Polarization Curves for the Inorganic Membrane Analytical Fuel Cell Employing Membrane 191-050	2-32
29	Polarization Curves for the Inorganic Membrane Analytical Fuel Cell Employing Membrane No. 48-001 (Run 37)	2-32
30	Polarization Curves for the Inorganic Membrane Fuel, Showing the Effect of Modified Electrode-Membrane Assembly (Membrane: 191-050)	2-32
31	Mold and Hydraulic Press Used for Cold Pressing Inorganic Fuel Cell Membranes	A-3
32	Sintering Furnace for Inorganic Fuel Cell Membranes	A-3

LIST OF ILLUSTRATIONS (CONT'D)

<u>Figure</u>		<u>Follows Page</u>
33	Apparatus for Measuring Transverse Strength of Zeolite Membranes	B-1
34	Improved Modulus of Rupture Test Apparatus	B-2
35	Electrical Circuit of the Inorganic Membrane Analytical Fuel Cell	C-3
36	Controlled Atmosphere Thermobalance	D-1
37	Controlled Atmosphere Thermobalance	D-1
38	Electrode Assembly	E-1
39	High Temperature Conductivity Apparatus	E-1

## LIST OF TABLES

Tables are bound in numerical order  
following Appendix E.

### Table

I	Properties of Zeolite Materials Investigated
II	Evaluation of Organic Binders
III	Evaluation of Silicate Binders
IV	Effect of Type of Zirconia Used on Transverse Strength of Inorganic Membranes
V	Physical Properties of Calcia-Stabilized Zirconia Fibers
VI	Physical Properties of cast Oxide-Phosphate-Zeolite Mixtures Sintered at 500°C
VII	Effect of Sintering Temperature on the Transverse Strength of Inorganic Fuel Cell Membranes
VIII	Statistical Plan of Experiments
IX	Resistivities of Inorganic Membranes Prepared for Statistical Evaluation
X	Resistivities of Inorganic Fuel Cell Membranes at 50% and 100% Relative Humidity at Elevated Temperatures
XI	Analysis of Log Resistivity Data
XII	Analysis of Strength Data: Quadratic Surface
XIII	Analysis of Strength Data: Higher Order Surface
XIV	Inorganic Membrane Fuel Cell Operating Data
XV	The Effect of Membrane Sintering Temperature on Fuel Cell Operation
XVI	The Effect on Fuel Cell Operation of Omitting "Zeolon H" from the Inorganic Membrane Composition
XVII	The Effect of Alumino-Silicate Fiber Additions on the Fuel Cell Performance of Inorganic Membranes
XVIII	Resistivities at Three Temperatures (Membrane No. 191-047)

## LIST OF TABLES (CONT'D)

### Table

XIX	Resistivities at Three Temperatures (Membrane No. 191-017-1)
XX	Resistivities at Two Temperatures (Membrane No. 98-051-1)
XXI	Resistivities at Three Temperatures (Membrane No. 191-007)
XXII	Resistivities at Three Temperatures (Membrane No. 191-051)
XXIII	Resistivities at Three Temperatures (Membrane No. 191-042)
XXIV	Resistivities at Three Temperatures (Membrane No. 191-053)
XXV	Resistivities at Three Temperatures (Membrane No. 191-016)
XXVI	Resistivities at Three Temperatures (Membrane No. 191-032)
XXVII	Resistivities at Three Temperatures (Membrane No. 191-059)
XXVIII	Resistivities at Three Temperatures (Membrane No. 191-057)
XXIX	Resistivities at Three Temperatures (Membrane No. 191-019)
XXX	Resistivities at Three Temperatures (Membrane No. 131-021)
XXXI	Resistivities at Three Temperatures (Membrane No. 131-002)
XXXII	Resistivities at Three Temperatures (Membrane No. 131-023)
XXXIII	Resistivities at Three Temperatures (Membrane No. 131-024)
XXXIV	Resistivities at Three Temperatures (Membrane No. 131-025)
XXXV	Resistivities at Three Temperatures (Membrane No. 131-026)
XXXVI	Resistivities at Three Temperatures (Membrane No. 131-027)
XXXVII	Resistivities at Three Temperatures (Membrane No. 131-028)
XXXVIII	Resistivities at Three Temperatures (Membrane No. 131-029)
XXXIX	Resistivities at Three Temperatures (Membrane No. 131-030)
XL	Resistivities at Three Temperatures (Membrane No. 131-031)
XLI	Resistivities at Three Temperatures (Membrane No. 131-032)
XLII	Resistivities at Three Temperatures (Membrane No. 131-033)
XLIII	Resistivities at Three Temperatures (Membrane No. 131-035)

LIST OF TABLES (CONT'D)

Table

XLIV	Resistivities at Three Temperatures (Membrane No. 131-036)
XLV	Resistivities at Three Temperatures (Membrane No. 131-037)
XLVI	Resistivities at Three Temperatures (Membrane No. 131-038)
XLVII	Resistivities at Three Temperatures (Membrane No. 131-039)
XLVIII	Resistivities at Three Temperatures (Membrane No. 131-040)

## 1.0 INTRODUCTION AND SUMMARY

The importance of fuel cell auxiliary power for space missions has been well established in the selection by NASA of a liquid electrolyte  $\text{H}_2\text{O}_2$  system for Apollo and an organic ion exchange membrane system for the Gemini mission.

The organic membrane system was selected because of its advantages over the liquid electrolyte variety. Among these are, compactness, simple design, zero gravity compatibility (the absence of bulk liquid) and avoidance of electrode flooding problems. All systems however, have their detrimental and organic membranes number among these such problems as hydrolysis, radiation sensitivity, oxidation, and heat sensitivity, particularly above  $50\text{-}60^\circ\text{C}$ . All of these problems lead to changes in performance of the membrane, most of which are deleterious.

Astropower Laboratory felt that inorganic membranes could provide an avenue for markedly improving membrane fuel cell performance. Inorganic membrane advantages postulated were:

- a. Good resistance to oxidation, both chemical and electrolytic.
- b. Changes in solvation of inorganic membranes resulting in only minimal changes in dimensional stability.
- c. Resistance to high temperature without decomposition or change, (experimentally at these laboratories to about  $750^\circ\text{C}$ ).
- d. Inorganic ion exchange materials are hydrophilic and retain water at elevated temperatures.
- e. Inorganic ion exchange membranes can be cycled at various temperatures without impairment of physical characteristics.
- f. The ion exchange capability of effective inorganic materials is comparable to organic ion exchange membranes.
- g. Where a high radiation level in space exists, it is suggested that the radiation would not effect the inorganic membranes.

The advantages outlined above in (a) through (f) have been substantially validated during the course of our efforts on NASA project NAS 7-150. We have not had an opportunity to test (g) experimentally, however.



The general level of achievement has reached the point where serious development effort to establish practical fuel cell operating parameters is called for. The detail of the achievement to date is described below.

## 1.1 Technical Summation

### 1.1.1 Theory of Membrane Operation

Inorganic membranes have been utilized in the past for fuel cell applications (Reference 1). Their limitations in major part have been a result of a lack of recognition of the operative mechanism inherent in satisfactory performance of water based systems. We have evolved the concept that the inorganic membrane is bifunctional in character. A strong skeleton network is needed to provide required strength, said network containing ionizable groups for establishing an electrolytic conductive mechanism. The second feature is the requirement for an inherent or incorporated water balancing agent which can retain sufficient water in the membrane to allow suitable electrolytic conductance during fuel cell operation. Both work under this present program and Astropower proprietary efforts have given clear indications that this approach is valid. (Reference 2).

### 1.1.2 Formulation Techniques

Early efforts indicated that the reaction of zirconium dioxide, phosphoric acid and zeolite yielded reasonably cohesive membranes with an optimum composition of  $1\text{H}_3\text{PO}_4:1\text{ZrO}_2:1\text{Zeolite}$ . The strength of these membranes, however, (479 psi) were not satisfactory for rugged handling and practical performance in a fuel cell (Reference 3). Investigation of techniques to strengthen the membrane were channeled into two promising areas: an investigation of the reactivity of the hydrous zirconium oxide used and the material drying conditions utilized for the formulation prior to pressing and firing.

It was found in the case of the hydrous zirconium oxide (zirconia) that the degree of reactivity of the material played an important part in the ultimate strength of the membrane. (Reference 4). Strength

differences of as much as 1200 psi were observed as a function of initial starting materials. The reason for this was that if the reactivity of the starting materials has been dissipated by hydration of active zirconia sites, spontaneous formation of phosphate linkages with  $H_3PO_4$  is difficult due to the fact that suitable reaction sites have been taken up by water molecules. As a result of this effort, a standard optimal form of zirconia has been chosen for our formulations.

A corollary, in a sense, to the above efforts is the fact that the optimum point for reaction to occur between the zeolite, the zirconia and the phosphoric acid is the period after formation of the disc when it is fired in the furnace at 300 - 500°C. The formulations must be dried after mixing and if reaction is allowed to occur at this stage (as is manifested by high exotherms and rigidification), then the linkages which are formed do not contribute to the required geometric form of the membrane at the sintering stage where the permanent structure is determined and the ultimate strength developed. Efforts have been made, therefore, to minimize any reaction during the early stages of the formulative procedure. This has been done by trying to eliminate the water removal step entirely by "dry" mixing the ingredients (Reference 5), or by removing water from the mixture by vacuum drying (Reference 6). The latter approach has yielded large improvements in strength. Membranes prepared in such a manner have had transverse break strengths of 6000 psi, a 100% improvement over a comparable formulation dried at 150°C. These values represent a twelve-fold improvement in strength over a period of a year. Our target for improvement during the next year is to increase dry transverse strength to 10,000 psi and wet strength to 8500 - 9000 psi.

It is also important to note that increased sintering temperatures produce greater strength but that at temperatures above 500°C a consequent decrease in conductivity may result (Section 2.3).

#### 1.1.3 Conductivity

Many hundreds of membranes have been screened by conductivity measurements during the course of this program. A highly reliable apparatus described in this (Appendix D) and previous reports (Reference 7) has become a mainstay in making such measurements.

General conclusions that have been drawn relative to the influence of processing variables on conductivity are:

1. Conductivity of membranes sintered between 300 - 500°C is relatively constant e.g., membrane 191-007 sintered at 300°C had a resistivity of  $5.7 \times 10^1$  ohm-cm while a comparable membrane sintered at 500°C gave a value of  $6.4 \times 10^1$  ohm-cm. These do not represent the best resistivity values obtained and it is important to note that sintering at higher temperatures (500°C) will produce greater membrane strength.
2. The extent of drying or temperature has little effect on conductivity.
3. The ratio of  $H_3PO_4$  incorporated in the membrane as related to the zeolite and the zirconia is important in that the conductivity increases with the quantity of  $H_3PO_4$  incorporated. It is clear, of course, that if the ratio is too high (too much  $H_3PO_4$ ), the strength of the membrane will deteriorate.
4. Screening of membranes by conductivity measurements can be used as a semi-quantitative tool for determining the efficiency of such membranes in hydrogen-oxygen fuel cells.

#### 1.1.4 Fuel Cells

The major portion of our effort in fuel cell work has been directed toward the development of a device which could be used to compare, on a quantitative basis, the operability of various inorganic membranes which have been produced.

Our preliminary efforts were plagued with a number of mechanical difficulties and with catalyst-membrane contact problems. These problems were successfully resolved and the fuel cell proved useful in comparing test membranes. At the end of the current efforts, a fuel cell run was successfully extended on a daily basis for over eight days operation.

## 2.0 EXPERIMENTAL WORK AND DISCUSSION

### 2.1 Membrane Composition and Processing Studies

Early concepts (References 8 and 9) about suitable inorganic materials for the membranes to be developed under this project stressed:

1. The potential of synthetic zeolites in retaining water at elevated temperatures and acting as electrical conductors.
2. The necessity of finding a suitable binder to hold the zeolite in membrane form.

Exploratory work showed that synthetic zeolites (Linde "Molecular Sieves," Norton "Zeolon," etc.) were poor electrical conductors and emphasized the critical role of the binder in producing a conductive membrane. A variety of binders used in experimental membranes proved unsatisfactory by reason of poor conductivity and/or poor strength (References 3, 7).

The experimental insight necessary to move the project out of its exploratory stages involved the use of metallic oxide - phosphoric acid mixtures as binders, with the selection of zirconium oxide as the preferable oxide. The zirconium phosphate formed in the cementing reaction of these reactants is an ion-exchanger previously utilized by Kraus et.al. (Reference 10) and Hamlen (Reference 11).

The cementing effects achieved by phosphating oxides are recorded in the literature, (Reference 12). Even "Zeolon H" alone, being an alumino-silicate, can be cemented by phosphoric acid into a membrane of intermediate strength having conductive properties (Section 2.0). Thus a membrane made from equal amounts of zirconium dioxide, phosphoric acid and "Zeolon H," proved to have reasonable strength. Our conjecture is that the membrane consists of particles of "Zeolon H" and unreacted zirconia embedded in "acid-salt" cement. The cement forms when oxygen atoms of the phosphate tetrahedra in the phosphoric acid molecule occupy, by condensation or displacement during sintering, corners of the zirconate or aluminate tetrahedra in the metallic oxide structures. Figure 1 shows a structure in which the binding matrix contributes, by reason of the uncondensed acid groups in the acid-salt, significantly to the conductivity of the membrane.

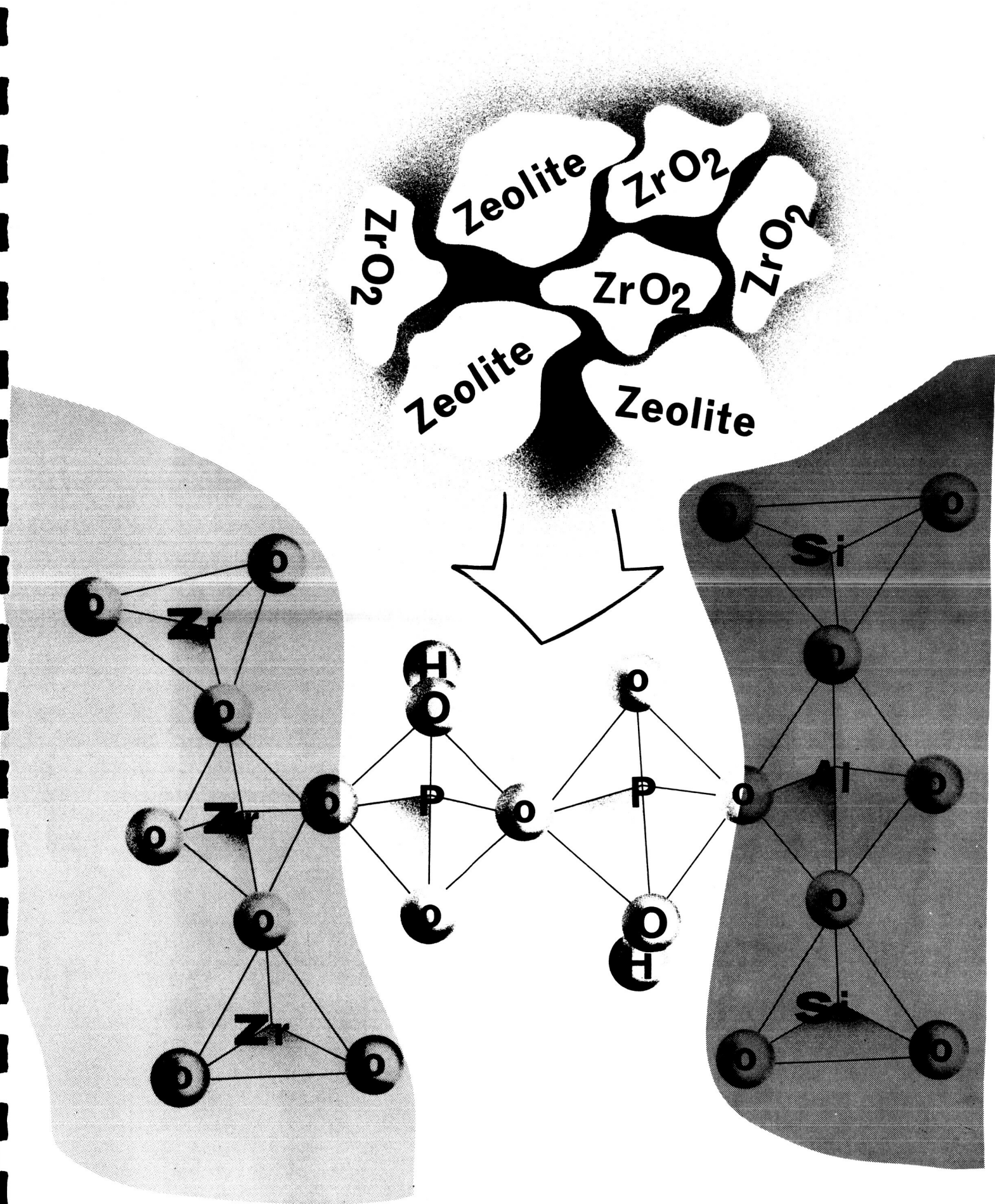


Figure 1. Structure of Phosphate Bonded Inorganic Fuel Cell Membrane

A further effect of the reactant phosphoric acid is likely. Figure 2 shows the structure of a typical zeolite, which has an open cage-like character. Conceivably, the phosphoric acid molecules enter the hollow interconnecting cavities, displacing some of the water of crystallization, possibly reacting with the inside walls of the cavities to become attached acid phosphate groups and enhancing the conductivity of the zeolite.

Thus the overall membrane appears to be constituted of a conductive structural element ( $\text{ZrPO}_4$ ) and a water retaining element, (zeolite). Proof of the validity of this approach is presented later.

#### 2.1.1 Zeolite Materials Investigated

Among the various materials investigated were zeolites manufactured by The Linde Company and "Zeolon" manufactured by The Norton Company.

The Linde zeolite materials have crystal structures consisting of hollow cubes with the internal cavities connected through openings on each of the faces of the cube. Two alumino-silicate structures are available and the pore openings which admit molecules into the interior cavity network are further varied by changing the associated cation. Linde "A" type zeolites have a unit cubic cell of 12.32 AU. These materials can be represented by the formula,  $\text{M}_{12}/\text{N}(\text{AlO}_2)_{12}(\text{SiO}_2)_{12} \cdot 27 \text{H}_2\text{O}$ . M being a univalent exchangeable cation. The sodium and calcium forms are stable at  $700^\circ\text{C}$  while the potassium forms are stable only to  $500^\circ\text{C}$  (Reference 13).

The Norton Company zeolite ("Zeolon") is reported to be synthetic mordenite,  $\text{M}_2\text{Al}_8\text{Si}_{40}\text{O}_{96} \cdot 24 \text{H}_2\text{O}$  and is available in hydrogen and sodium ion exchanged forms. The mordenite crystal structure consists of chains of four or five membered rings constructed of tetrahedra of either aluminum or silicon, each surrounded by four oxygen atoms which are linked together to form a network that results in a system of parallel channels possessing a structure similar to a tube bundle (Reference 14).

Figures 3 and 4 show the hydrogen ion exchange capacity of Linde 4A and AW-500 zeolites. Table I gives the properties of typical zeolites which were investigated.

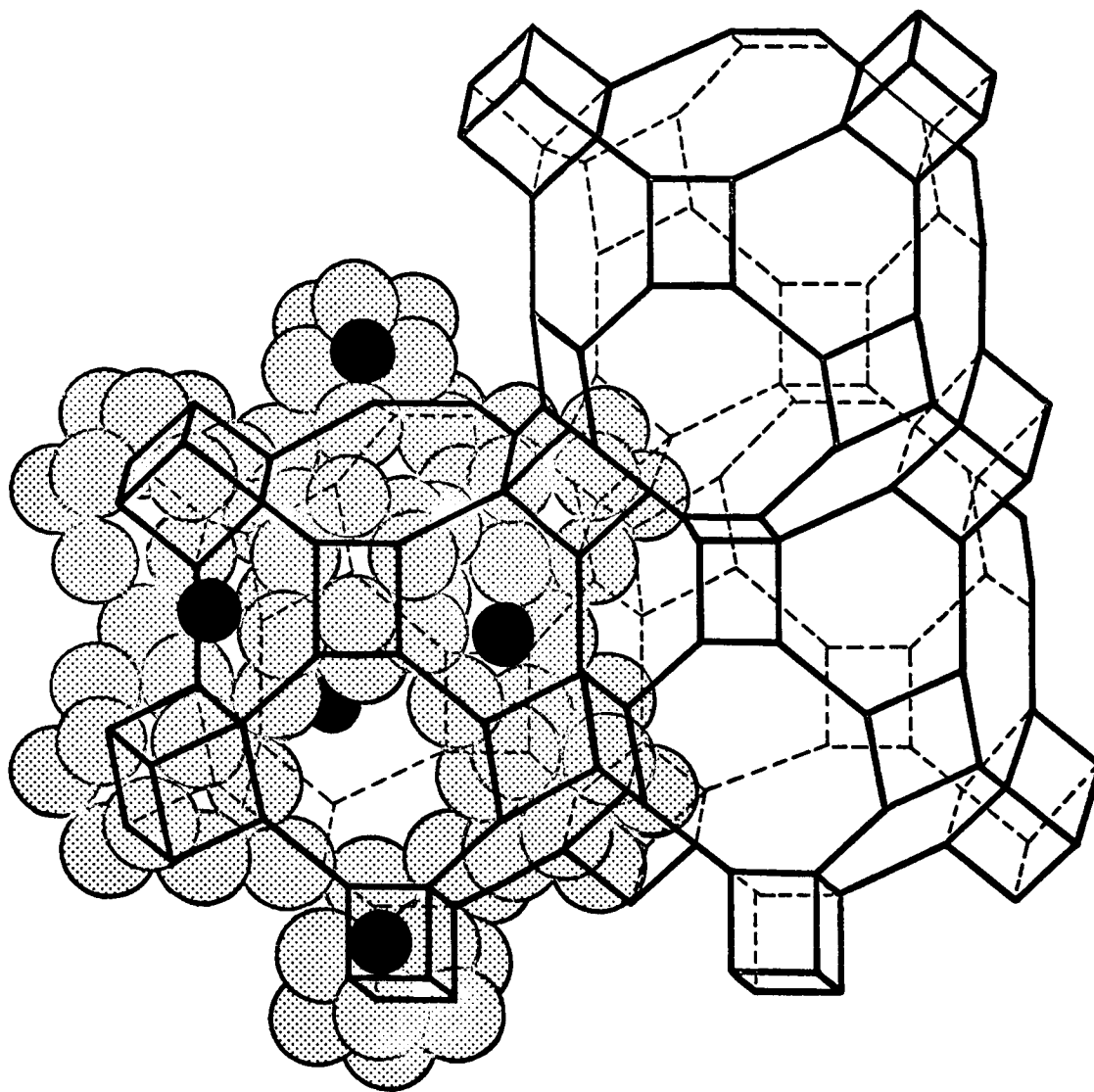


Figure 2. Crystal Lattice Structure of Sodium  
(Black) Type A Synthetic Zeolite.  
Oxygen Atoms are Shown in Gray.

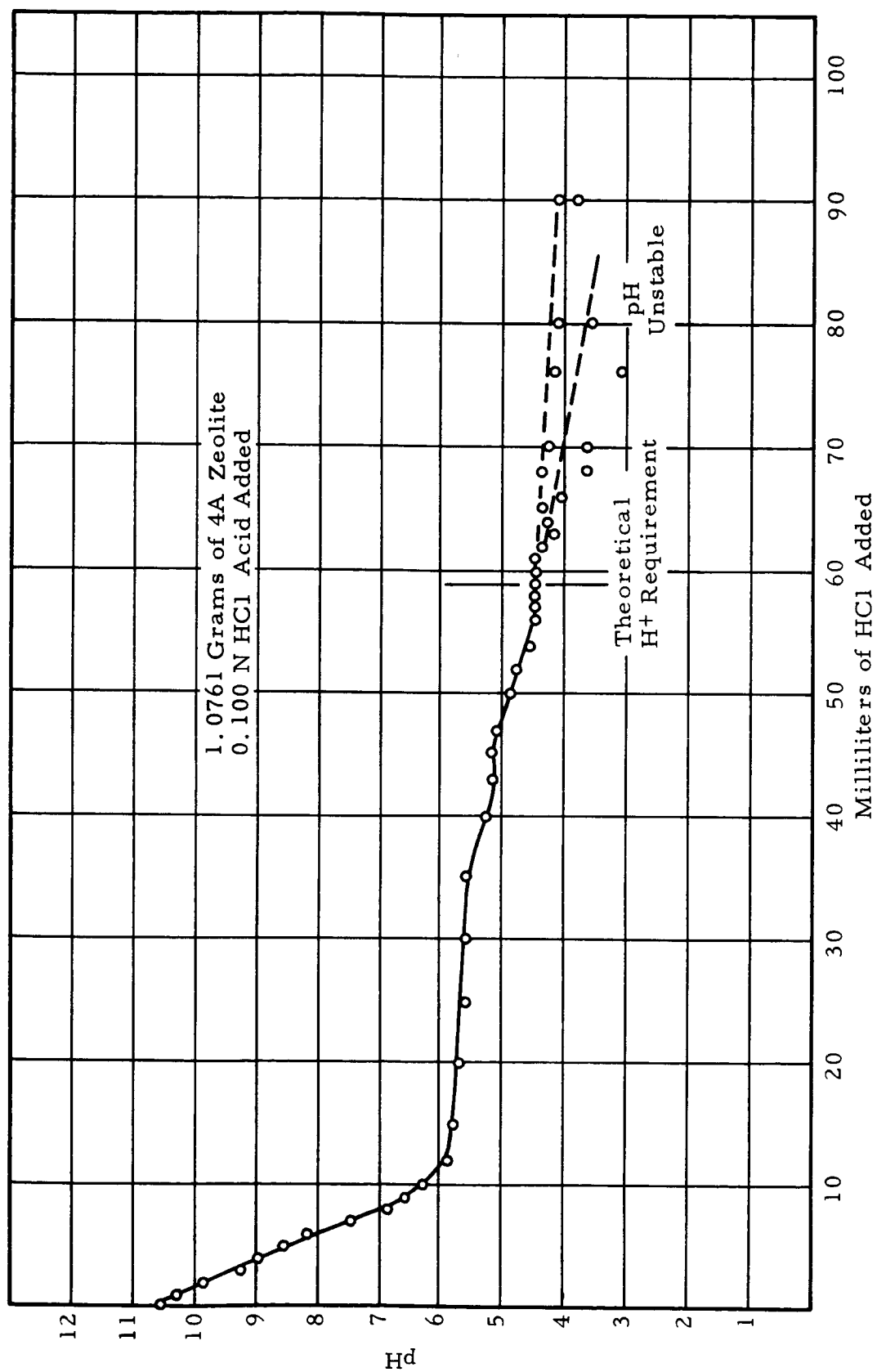


Figure 3. Hydrogen Ion Exchange of Linde 4A Zeolite



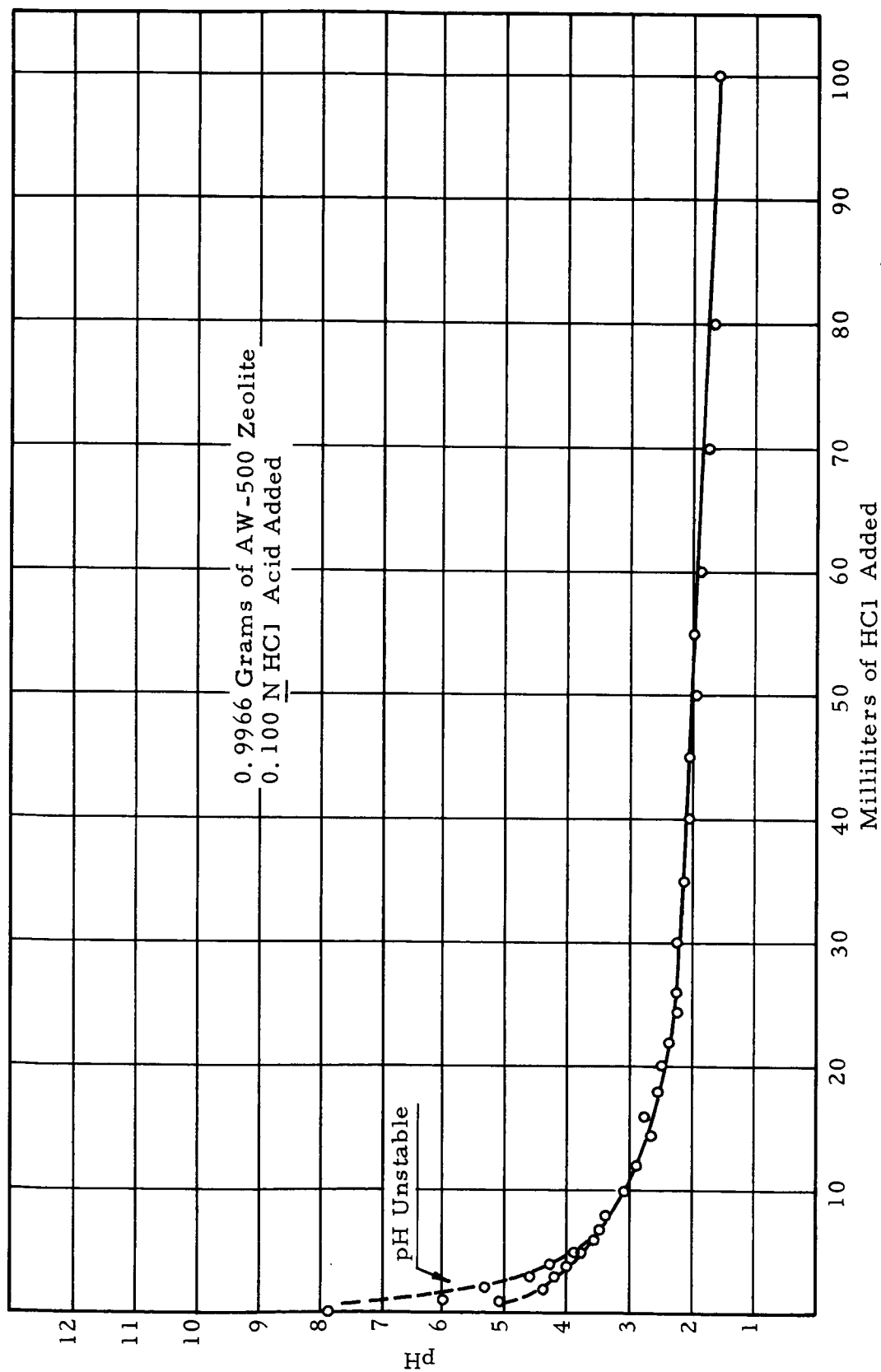


Figure 4. Hydrogen Ion Exchange of Linde AW-500 Zeolite

### 2.1.2 Bonding Materials for Inorganic Fuel Cell Membranes

In order to produce adequate strength for use in fuel cell membranes, it was necessary to develop suitable ion conductive binders to bond the water balancing materials used into thin fuel cell membranes. Bonding methods which were investigated included, organic binders, inorganic silicate binders, and inorganic phosphate binders.

Among the organic materials which were tested as binders for inorganic fuel cell membranes were Teflon, polyvinyl chloride, phenolics and silicone rubbers. They produced little or no strength when added to inorganic materials in amounts up to 30% by weight. Although modest strengths resulted from the use of various epoxy resins as binders, this work was discontinued when it was found that substantial amounts (20-30%) would be required to develop reasonable strength. As all of the organic binders tested were electrical insulators, had limited temperature resistance, and no ion conducting ability, only small additions could be tolerated in an inorganic fuel cell membrane. The results obtained are shown in Table II.

A number of experiments were carried out using various silicate based proprietary mixtures and sodium silicate as binders for zeolites. The results were generally unpromising as strong membranes were not produced and this work was discontinued. The results obtained are shown in Table III.

The bonding properties of phosphate materials have been recognized for many years. Phosphate bonded zinc oxide has been widely used as a dental cement (Reference 15) and there are numerous other applications utilizing phosphate bonding to produce strength at low and high temperatures (Reference 12).

Acid phosphate groups (such as  $\text{H}_2\text{PO}_4^{-2}$ ) have strong electron donor (ligand) properties and therefore readily coordinate with cations of periodic groups II and III and the transition element series. If the cations are already incorporated in the coordination compounds, they may still be reacted with acid phosphate groups by choosing an ion concentration sufficiently high to appreciably shift the reaction equilibrium in favor of

phosphate combinations. Thus when finally divided metal oxides are treated with concentrated phosphoric acid oxygen atoms are partly displaced by phosphate. On heating the phosphorylated oxides dehydrate condensing the acid phosphate groups into linkages between the phosphate tetrahedra. This results in fusion of the mixture into a solid mass. With at least one oxide, ZnO, furnace firing is not required to affect solidification or setting following reaction with acid phosphate. Possibly this is due to the exothermic nature of this particular reaction the heat required for condensing phosphate groups being self generated.

### 2.1.3 Membrane Preparation Techniques

Four methods for preparing inorganic fuel cell membranes were investigated.

- (a) Hot pressing
- (b) Cold pressing and sintering
- (c) Casting and sintering
- (d) Flame spraying

In hot pressing, heat and pressure are applied to the material while it is confined in a suitable mold. This method is used to produce maximum density in forming plastics and ceramics but is limited in its application.

Samples of Linde 4A zeolite bonded with 10-30% of various plastic materials such as Hysol 4314, Coraline 530, Teflon, Pliovic S-50, Durez 1400 and Eccosil 4712 were prepared by hot pressing. Only Coraline 530 and Hysol 4314 produced any appreciable strength, the other materials developing little or no bond in the percentages used (Reference 3). As organic materials are electrical insulators and provide no H<sup>+</sup> exchange capacity, no further hot pressing work was done in view of these unfavorable results.

Cold pressing is a conventional ceramic forming process permitting close dimensional tolerances and high production rates. Also, most materials can be formed by cold pressing. The pressed parts are sintered or fired after pressing to develop strength.

Casting is also a commonly used ceramic forming process and consists of making the materials up into a slurry or "slip" with water or an organic media. The slip is then poured into porous plaster of paris molds to dehydrate it and give it the desired form or may be poured or troweled into a suitable mold and dried. Cast parts are sintered after drying in order to develop strength. Flame spraying is carried out by passing powdered materials through a gas-oxygen flame or a d-c plasma arc. The softened particles are blown against a form or substrate and coalesce to form a porous material. A number of experimental inorganic fuel cell membranes were prepared during the course of a proprietary program (Reference 2) by flame spraying zirconia, alumina and other materials onto aluminum substrates. The sprayed materials were cylindrically ground to a diameter of  $2.000 \pm .001$  in and surface ground to a thickness of  $0.030 \pm .001$  in. After grinding, the flame sprayed membranes were removed from the substrate by dissolving the aluminum in hot caustic. As all inorganic membranes prepared in this manner exhibited very high resistivities and were highly porous, work with flame sprayed membranes was discontinued. As casting or cold pressing and sintering produced the best results with the materials being studied, these techniques were adopted for use in carrying out this investigation. Appendix A describes the procedures used in detail.

Zirconium oxide is manufactured by calcining ore which has been chemically treated. The conversion to  $ZrO_2$  is dependent on the heat treatment the batch receives and production variations in the process result in variations in the  $ZrO_2$  produced (Reference 16). When calcination temperatures are high and maintained for relatively long periods of time, the conversion is substantially complete and the zirconia produced is relatively free from hydrous  $ZrO_2$ . On the other hand, when the temperature of calcination is lower and calcining time is reduced, the product contains larger amounts of hydrate. Time-temperature relationships also determine the ultimate particle size of the crystalline zirconia formed. High calcining temperatures and long periods of time produce large crystals having relatively low reactivity while lower temperatures and shorter times produce smaller crystals and a more reactive product.

During the course of a proprietary investigation (Reference 2) a C.P. grade of zirconium oxide was used. Although of high chemical purity, it was recognized that the physical nature of this material and its reactivity varied considerably from lot to lot. As a result, significant variations in the properties of identical formulation were observed - especially variations in transverse strength after sintering. A 1  $\text{ZrO}_2$ : 1  $\text{H}_3\text{PO}_4$  composition, for example, prepared from two different lots of this zirconia, dried at  $120^\circ\text{C}$  and sintered at  $300^\circ\text{C}$  showed variations in transverse strength ranging from  $1300 \pm 51$  to  $2710 \pm 83$  psi. Similar results were obtained with a 1  $\text{ZrO}_2$ : 1  $\text{H}_3\text{PO}_4$ : "1 Zeolon H" formula prepared from two different lots of this zirconia, dried at  $120^\circ\text{C}$  and sintered at  $500^\circ\text{C}$ . In this case, transverse strength varied from  $517 \pm 25$  psi to  $2288 \pm 159$  psi as a result of lot to lot variation in the reactivity of the zirconia. In view of these findings, it was necessary to test a number of zirconium oxides obtained from various sources in order to find a material having a desirable degree of reactivity with phosphoric acid and a high level of uniformity from lot to lot. Among the materials tested were Seargent C.P.  $\text{ZrO}_2$ , TAM C.P  $\text{ZrO}_2$ , Zircoa A, and Zircoa B, which have approximately 5% CaO added to stabilize thermal expansion of the calcined product. It was found that Zircoa A and TAM C.P. had a high order of uniformity from lot to lot and resulted in reproducible values. Zircoa B, which was more reactive with phosphoric acid, was also very uniform and increased the strength of phosphoric acid bonded membranes when substituted for pure zirconia. This is probably a result of the presence of CaO which also reacts with the phosphoric acid. A comparison of transverse strengths for compositions using different types of zirconia is shown in Table IV.

The development of a strong bond between zirconia and phosphoric acid depends upon a chemical reaction between the two materials. It is important, however, that this reaction take place during sintering rather than during the mixing or material drying stages of the process. If the reaction between phosphoric acid and zirconia takes place to a significant degree during these operations, less bonding action is left to take place during membrane sintering and a weak membrane results. Highly reactive zirconias (those which have been calcined to relatively low temperatures for short

periods of time) react rapidly when mixed with phosphoric acid and generate substantial amounts of heat. There is also appreciable thickening of the slurry during mixing and the time and temperature required for material drying is substantially decreased. When formed into membranes and sintered, these materials have little strength. When zirconium hydroxide, for example, was mixed with equal parts of phosphoric acid and "Zeolon H," a large amount of heat was evolved and the slurry rapidly thickened forming a heavy paste as a result of reaction of the hydroxide with phosphoric acid. After 6 hours at room temperature, the material was "dry" enough to form into membranes which were sintered at 500°C. The sintered membrane had no measureable strength. When a reactive zirconia was used in a 1 ZrO<sub>2</sub>: 1 H<sub>3</sub>PO<sub>4</sub>: 1 "Zeolon H" composition, a moderate amount of heat was generated during mixing and the slurry thickened slightly due to reaction of the zirconia and phosphoric acid. After drying at 120°C, membranes were prepared and sintered at 500°C and had a transverse strength of 785<sub>±</sub><sup>55</sup> psi. When the same composition was prepared using a highly calcined zirconia, dried at 120°C and formed into membranes which were sintered at 500°C, the transverse strength was 2900<sub>±</sub><sup>154</sup> psi.

As a result of these experiments and tests of lot to lot uniformity, TAM C.P. and Zircoa A zirconium oxide were selected for use in the membrane compositions studied. Zirconia B (stabilized with 5% CaO) was also selected for further investigation on the basis of lot to lot uniformity and the high transverse strength values obtained with this material.

Fibrous materials of various types are commonly added to plastics and other materials to increase strength. Accordingly, it was deemed desirable to investigate the effects of adding inorganic fibers to fuel cell membrane compositions. Three types of inorganic fibers were used; acid washed asbestos, alumino-silicate fibers, and zirconia fibers. Both pure zirconia fibers and calcia stabilized zirconia fibers were evaluated. The introduction of inorganic fibers in phosphate bonded membrane mixes produced both a mechanical and a chemical effect. In addition to mechanical strengthening, the fibrous materials also reacted to various degrees with the phosphoric acid present in the membrane compositions increasing the chemical

bonding of the materials. This was particularly true of calcia stabilized zirconia fibers. The physical properties of calcia stabilized zirconia fibers are shown in Table V.

In order to investigate the effect of fibers on transverse strength, 5% zirconia fibers were added to phosphate bonded zirconia - "Zeolon H" membrane compositions. It was found that the fiber addition increased the transverse strength of a 1  $\text{ZrO}_2$ : 1  $\text{H}_3\text{PO}_4$ : 1 "Zeolon H" composition from  $1063 \pm 90$  psi to  $1910 \pm 210$  psi for samples sintered at  $300^\circ\text{C}$ . Sintering at  $500^\circ\text{C}$  resulted in an increase in strength from  $2381 \pm 85$  psi to  $2875 \pm 84$  psi as a result of the addition of 5% zirconia fibers. These results are shown in Figure 5.

Other fibrous materials such as alumino-silicates and acid washed asbestos were not significantly effective in increasing transverse strength after sintering. This is probably because these materials are relatively unreactive while the zirconia fibers act both as mechanical strengtheners and also increase strength through chemical reaction with the phosphoric acid present in the compositions.

## 2.2 Transverse Strength of Phosphate Bonded Inorganic Membranes

### 2.2.1 Membranes Prepared by Casting

Initially, in order to survey a wide range of membrane compositions made from metal oxides such as  $\text{Al}_2\text{O}_3$ ,  $\text{ZrO}_2$ ,  $\text{ZnO}$ , etc., phosphoric acid and "Zeolon H," test pieces were prepared by casting (Reference 3). The weighed ingredients were mixed with sufficient water to form a soft paste and then troweled into an open faced teflon mold to form 2 in diameter specimens 0.030 in thick. The filled molds were dried for several hours at  $150^\circ\text{C}$  and then removed from the mold and completely dried. Following this, they were sintered for 15 hours at  $500^\circ\text{C}$  and allowed to cool in the furnace.

The results of this preliminary survey of oxide-phosphate-zeolite mixtures are shown in Table VI. Except for one composition (0.5  $\text{ZnO}$ : 2.5  $\text{H}_3\text{PO}_4$ : 2.0 "Zeolon H"), which had a transverse strength of  $1223 \pm 456$  psi, only combinations of  $\text{ZrO}_2$ ,  $\text{H}_3\text{PO}_4$  and "Zeolon H" appeared promising.

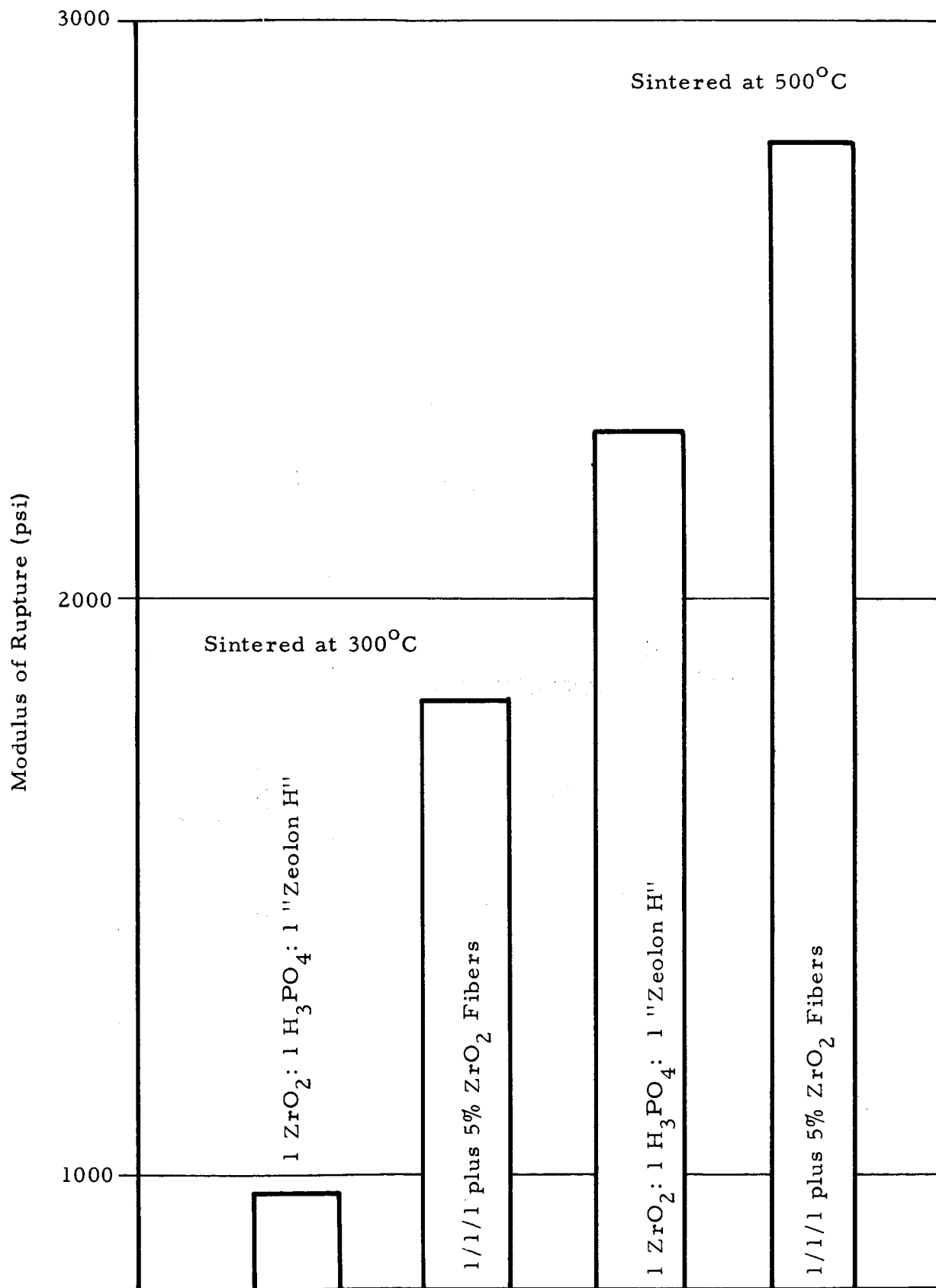


Figure 5. Effect of Zirconia Fiber Additions on the Transverse Strength of Zirconium Phosphate Membranes



The strongest combination was 1  $\text{ZrO}_2$ : 1  $\text{H}_3\text{PO}_4$  which had a transverse strength of  $1453 \pm 274$ , but other combinations also produced strengths above 1000 psi. The method for measuring transverse strength is given in Appendix B.

#### 2.2.2 Membranes Prepared by Pressing

Further investigation of oxide-phosphate-"Zeolon H" materials was carried out using cold pressed discs 2 in. in diameter, approximately 0.030 in. thick. Cold pressing was selected as the forming method since nearly all materials can be formed by this technique and samples having a high degree of uniformity and reproducibility can be made whereas, casting is somewhat limited in its application.

#### 2.2.3 Effect of Composition on the Transverse Strength of Pressed Inorganic Membranes

Along with drying time and temperature, pressing pressure and sintering temperature, membrane composition has a significant effect on transverse strength after sintering. As the development of membrane strength during sintering is a result of reactions between  $\text{ZrO}_2$ , "Zeolon H" and the phosphoric acid, it is apparent that the ratio between the  $\text{H}_3\text{PO}_4$  content and the solids will have an optimum range for high strength. Below this range low strength would be expected as there would be insufficient phosphoric acid to react as completely as possible with the solid materials. The bonding effect of the phosphoric acid content is also influenced by drying conditions - higher drying times and temperatures being required for higher acid contents.

The effect of  $\text{H}_3\text{PO}_4$  content on transverse strength for materials dried at several different temperatures is shown in Figure 6. It can be seen that material dried at  $150^\circ\text{C}$  for 20 hours, maximum transverse strength ( $3546 \pm 82$  psi) is obtained with a  $\text{H}_3\text{PO}_4$  content of 24%. Compositions containing between 18 and 30%  $\text{H}_3\text{PO}_4$  are also very strong and indicate this to be an optimum composition range for transverse strength. It can also be observed from Figure 6 that the range of maximum strength shifts depending upon the material drying temperature. Material dried at  $144^\circ\text{C}$ , for example,

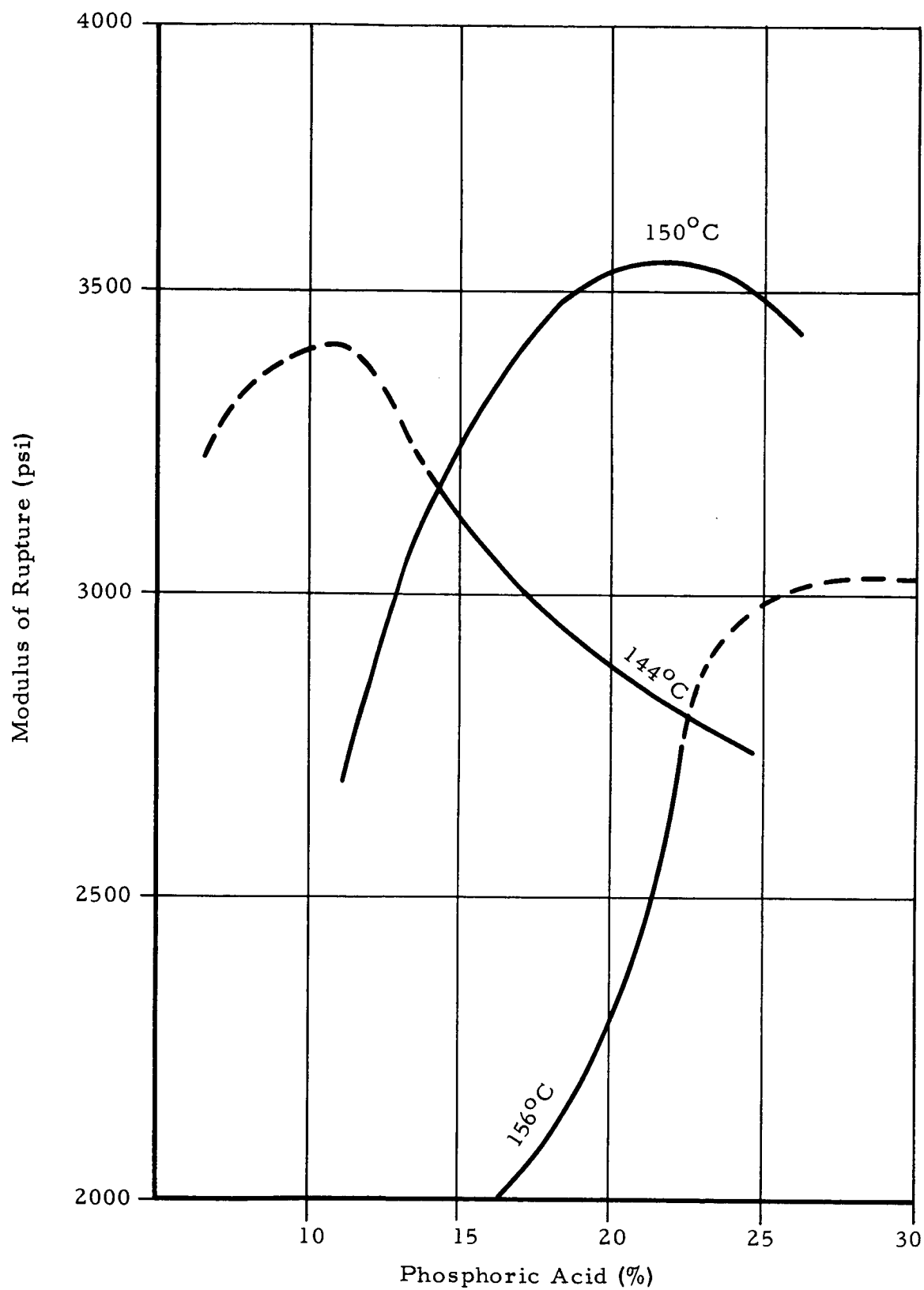


Figure 6. Effect of Phosphoric Acid Content on Transverse Strength at 3 Material Drying Temperatures.

shows decreasing strength as the  $\text{H}_3\text{PO}_4$  content is increased from 15 to 25%. This indicates that the maximum strength compositions for material dried at  $144^\circ\text{C}$  probably contains less than 15%  $\text{H}_3\text{PO}_4$  which is below the range investigated during this study. On the other hand, material dried at  $156^\circ\text{C}$  increases in transverse strength as the  $\text{H}_3\text{PO}_4$  content is increased from 18 to 23% indicating that the range of maximum strength for this material drying temperature is probably above the composition range studied.

#### 2.2.4 Effect of Sample Thickness on Transverse Strength of Pressed Inorganic Membranes

Variations in the density of different mixtures resulted in a corresponding small variation in sample thickness after pressing. To make certain that these small variations in thickness did not significantly affect modulus of rupture results, a series of samples were prepared ranging in thickness from 0.025 in. to 0.065 in. After sintering, the transverse strengths of these samples were measured. It was found that there was a maximum variation of only 10.9% between samples and it was concluded that modulus of rupture could be considered to be independent of sample thickness for the range being investigated.

#### 2.2.5 Effect of Pressing Pressure on the Transverse Strength of Pressed Inorganic Membranes

One of the factors which might logically be related to the strength of cold pressed inorganic membranes is pressing pressure. Accordingly, an investigation of the effect of pressing pressure on the transverse strength and apparent pressed density of phosphate bonded inorganic fuel cell membranes was made. Two groups of samples were prepared from a mixture composed of 1  $\text{ZrO}_2$ : 1  $\text{H}_3\text{PO}_4$ : 1 "Zeolon H" and dried for different lengths of time before pressing. The test pieces were pressed at 10, 15, 20, 25, 30 and 40 tons total load and sintered at  $500^\circ\text{C}$  for 15 hours. After sintering, modulus of rupture values were obtained. These results are shown in Figure 7. Figure 8 shows the apparent density of these samples. It was found that transverse strength was directly related to pressing pressure with stronger membranes resulting from increased pressure. The effect of the drying time used in the preparation of the pressing materials can also be seen in Figure 7.

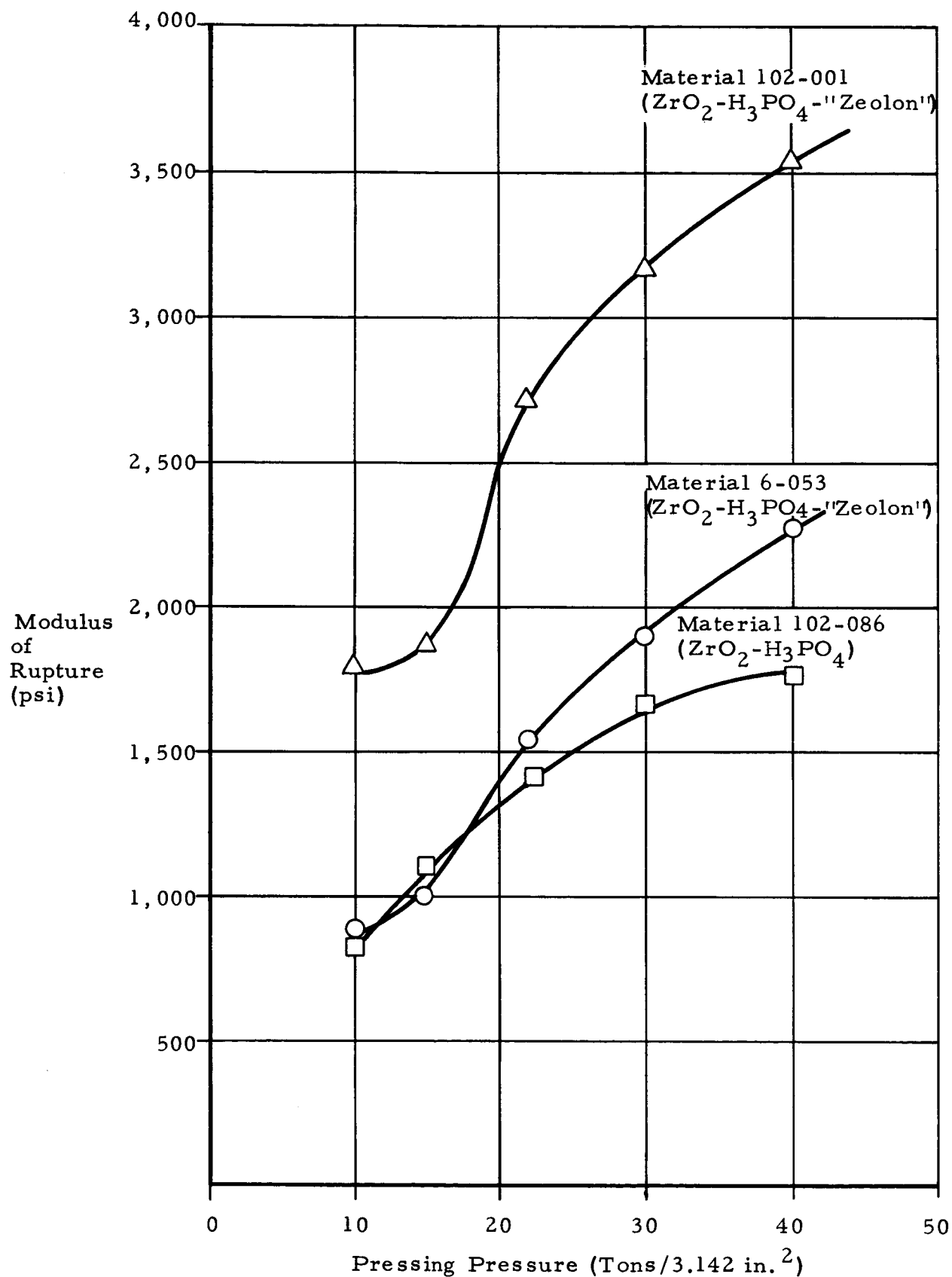


Figure 7. Effect of Pressing Pressure on Transverse Strength of Inorganic Membranes

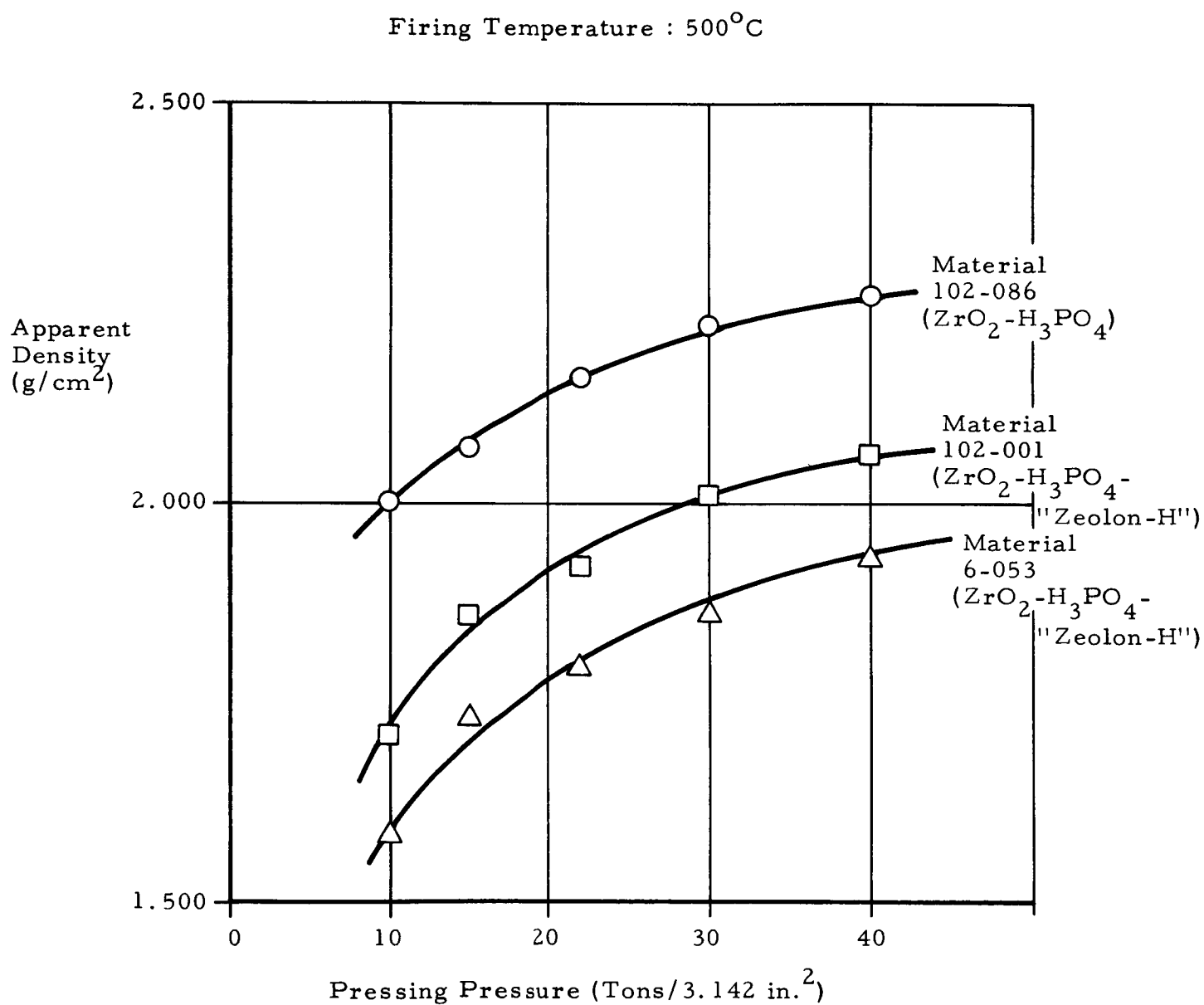


Figure 8. Effect of Pressing Pressure on the Apparent Density of Fired Inorganic Membranes

Although both materials No. 102-001 and No. 6-053 have the same composition, drying times were different. No. 102-001, which had the shorter drying time, had the greatest strength. Figure 7 also shows the effect of pressing pressure on the transverse strength of material No. 102-086 which was composed of 1  $\text{ZrO}_2$ : 1  $\text{H}_3\text{PO}_4$  without "Zeolon H." Increased forming pressure also increased the strength of this material after sintering although the shape of the curve is somewhat different and it shows no inflection in the 10 to 25 ton range. This is probably due to the fact that  $\text{ZrO}_2$  is composed of hard, non-plastic particles. The addition of "Zeolon H," which is clay-like and somewhat plastic in nature causes densification to increase rapidly with increased pressing pressure due to plastic flow. As the pressing pressure is raised further, less change takes place as most of the material flow has occurred at lower pressures.

Examination of Figure 8 shows that the density of the various materials studied increased as the forming pressure was increased. The density of material No. 102-086 was higher than materials No. 102-001 or No. 6-053 which contained "Zeolon H." Material No. 102-086 was dried for a shorter time than No. 6-053 and had higher transverse strength and higher density at all pressing pressures. It can be concluded from these observations that in general increased strength and density result from using higher pressing pressures and the presence of plastic and "soft" materials such as clays or "Zeolon H" improves pressed density. As transverse strength and pressed density are directly related, increasing pressing pressures will result in stronger membranes.

#### 2.2.6 Effect of Sintering Temperature on the Transverse Strength of Pressed Inorganic Membranes

The physical properties of most ceramic materials improve with increasing sintering or firing temperature to a maximum and then decline as the temperature is further increased. This relationship usually holds true for all characteristics including strength, electrical properties, chemical resistance, hardness, etc. It was reasonable to assume that a similar relationship might exist between transverse strength and sintering temperature

for phosphate bonded ceramics. In order to determine the effect of sintering temperature on the transverse strength of phosphate bonded membranes, a number of compositions were sintered at temperatures ranging from 250°C to 1000°C. Typical results are shown in Figure 9 and Table VII. Composition No. 048-001 which was 1 ZrO<sub>2</sub>: 1 H<sub>3</sub>PO<sub>4</sub>: 1 "Zeolon H" had a maximum strength of 4150 ± 115 psi when sintered at 450°C. Strengths were relatively high at sintering temperatures ranging between 350°C and 550°C. Material No. 191-050 which was 1 ZrO<sub>2</sub>: H<sub>3</sub>PO<sub>4</sub>: 1 H<sub>3</sub>PO<sub>4</sub>: 1 "Zeolon H" exhibited a maximum transverse strength of 2760 ± 90 psi when sintered at 500°C. Lower strength resulted when this composition was sintered at either higher or lower temperatures. The range of sintering temperatures resulting in relatively high transverse strength appears to be wider for this composition than for material No. 048-001 as high strength was obtained from sintering at temperatures between 400°C and 700°C.

It was found that there is an optimum sintering temperature range for phosphate bonded inorganic membrane compositions which results in maximum transverse strength. The optimum sintering range and sintering temperature for maximum transverse strength is related to composition but generally falls between 350°C and 700°C.

#### 2.2.7 The Effect of Material Drying Time and Temperature on Transverse Strength of Phosphate Bonded Inorganic Membranes

Along with composition, pressing pressure and sintering temperature, it was recognized that material drying time and temperature also had a significant effect on membrane strength. In order to investigate this variable, samples of 1 ZrO<sub>2</sub>: 1 H<sub>3</sub>PO<sub>4</sub>: 1 "Zeolon H" compositions were dried for times ranging from 10 to 100 hours at 120°C. After these various drying treatments, the materials were granulated, pressed into membranes at 10,000 psi and sintered for 15 hours at 500°C. The samples were then measured for transverse strength and the results are shown in Figure 10.

Examination of these data shows that increasing material drying time significantly decreases sintered strength. In a discussion of these results with the project officer he suggested that membranes be

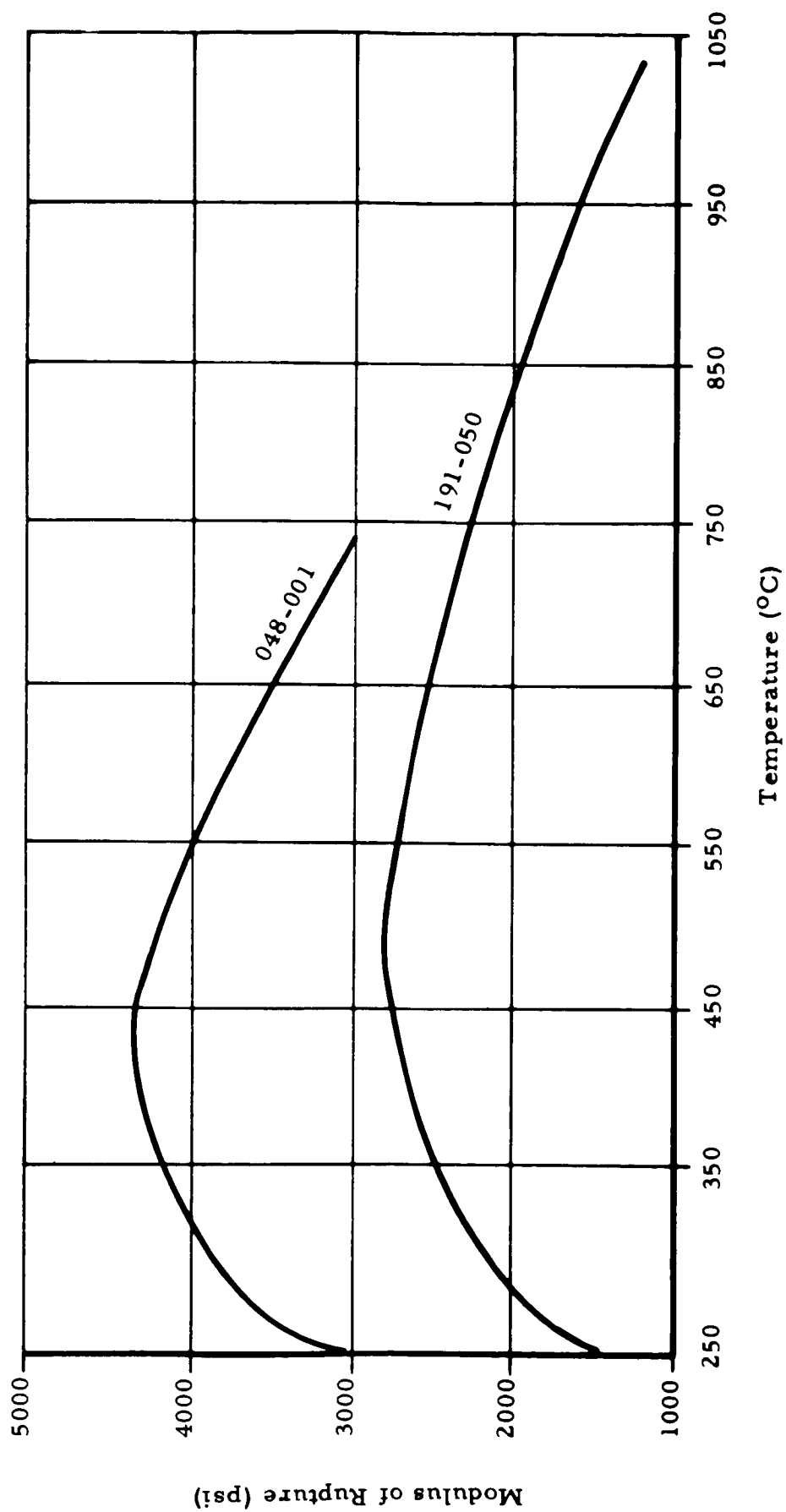


Figure 9. Effect of Sintering Temperature on Transverse Strength of Inorganic Fuel Cell Membranes



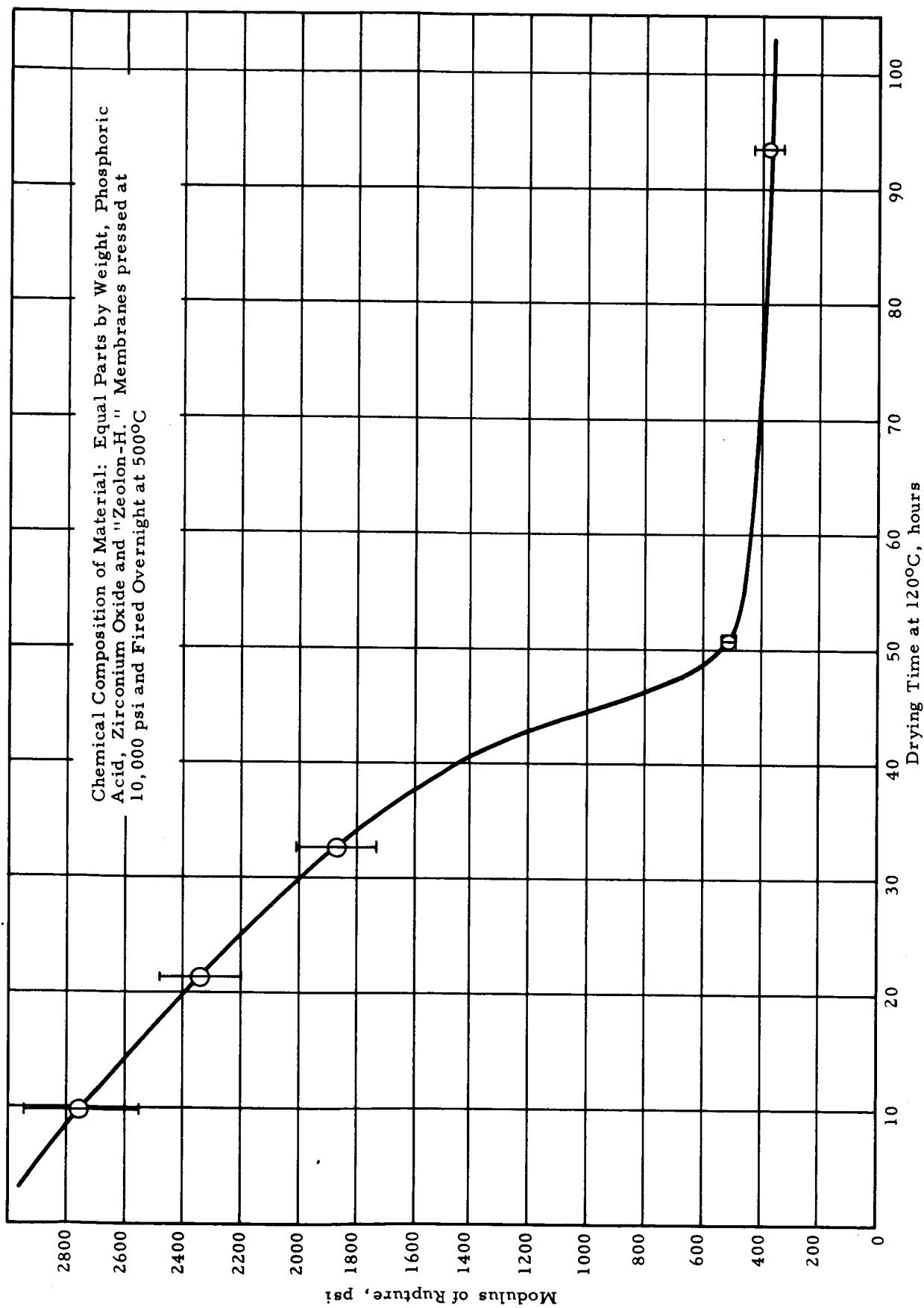


Figure 10. The effect of Drying Time at 120°C on the Transverse Strength of Inorganic Fuel Cell Membranes

prepared without material drying in order to verify the theory that minimum drying treatment would produce maximum strength. Accordingly, a composition consisting of 40% zirconia, 20% phosphoric acid and 40% "Zeolon H" was prepared by thoroughly mixing the ingredients and pressing 2" diameter membranes at 15 tons total load without material drying. The membranes were sintered for 15 hours at 500°C and their transverse strength was measured. These membranes were very strong having a transverse strength of  $3770 \pm 119$  psi. When the same composition was prepared by drying the material for 15 hours at 160°C, the strength was  $2433 \pm 250$ . The increase in strength resulting from elimination of the drying process is substantial. As it is impossible, however, to eliminate the material drying operation except for compositions which are very low in  $H_3PO_4$  content, investigation of vacuum drying of membrane materials was indicated.

Figures 11, 12, and 13 further illustrate the effects of drying procedure on transverse strength. Figure 11 shows the transverse strength obtained by drying the compositions shown in Table VIII at 144°, 150° and 156°C for various lengths of time. It can be seen that there is a marked decrease in sintered transverse strength as drying time is increased from 18 to 60 hours. As anticipated, the rate of decrease was greater for the higher drying temperatures even though the highest strength ( $3546 \pm 82$  psi) was obtained by drying the material at 150°C for 20 hours. The data indicate sharply increasing strength as drying time is decreased below 28 hours and it is probable that substantially stronger materials would result if the drying times and temperatures could be further reduced. In order to accomplish this, it is necessary to either reduce the moisture content of the phosphoric acid, or use vacuum drying to remove the moisture at low temperature.

In a proprietary Astropower Laboratory program, (Reference 2) the use of phosphorus pentoxide- $H_3PO_4$  mixtures for bonding inorganic material has been also investigated. This approach offers another means for reduction or elimination of material drying in order to increase sintered membrane strength.

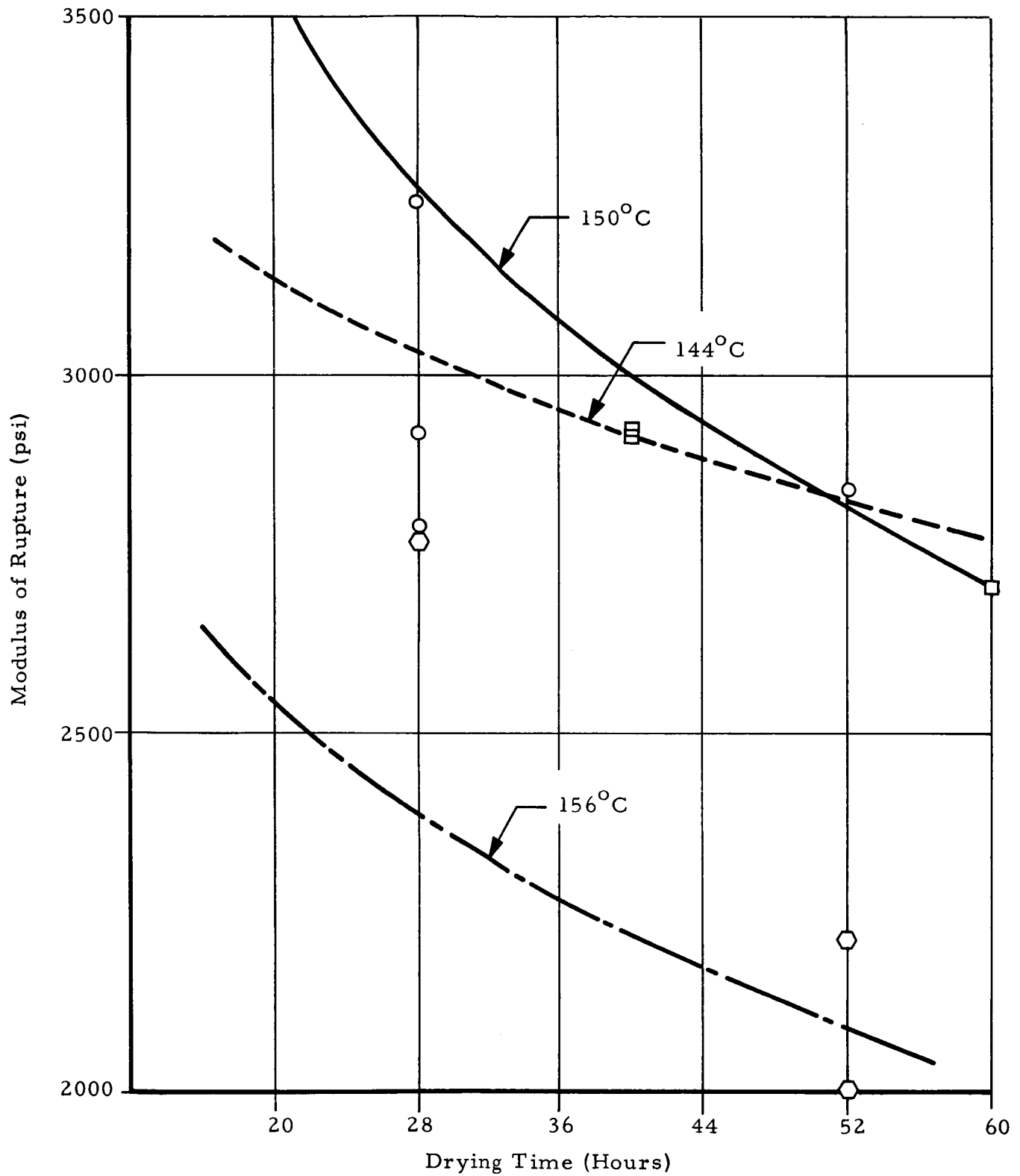


Figure 11. Effect of Material Drying Time at 3 Temperatures on Transverse Strength of Inorganic Fuel Cell Membranes

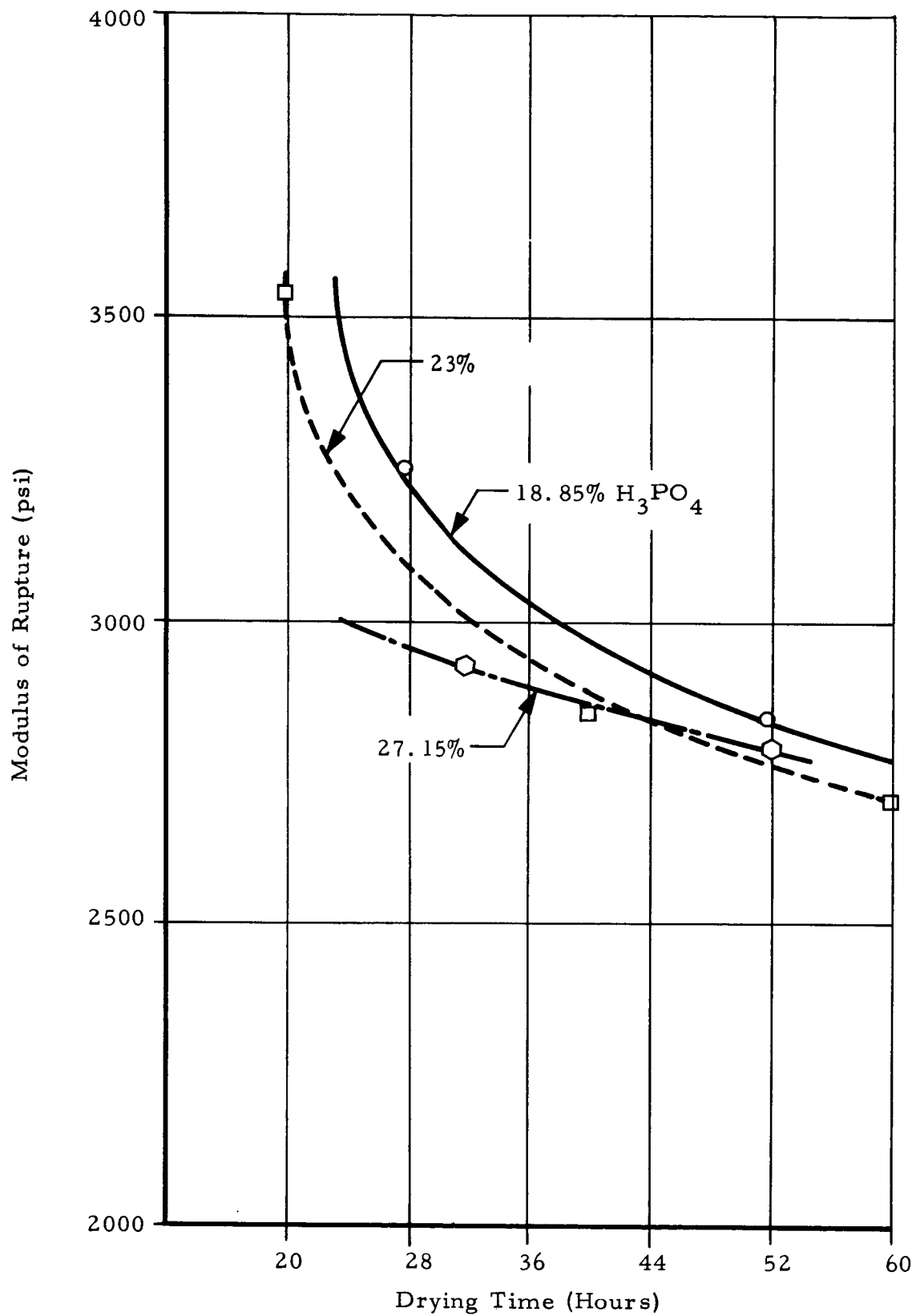


Figure 12. Effect of Material Drying Time on Transverse Strength.

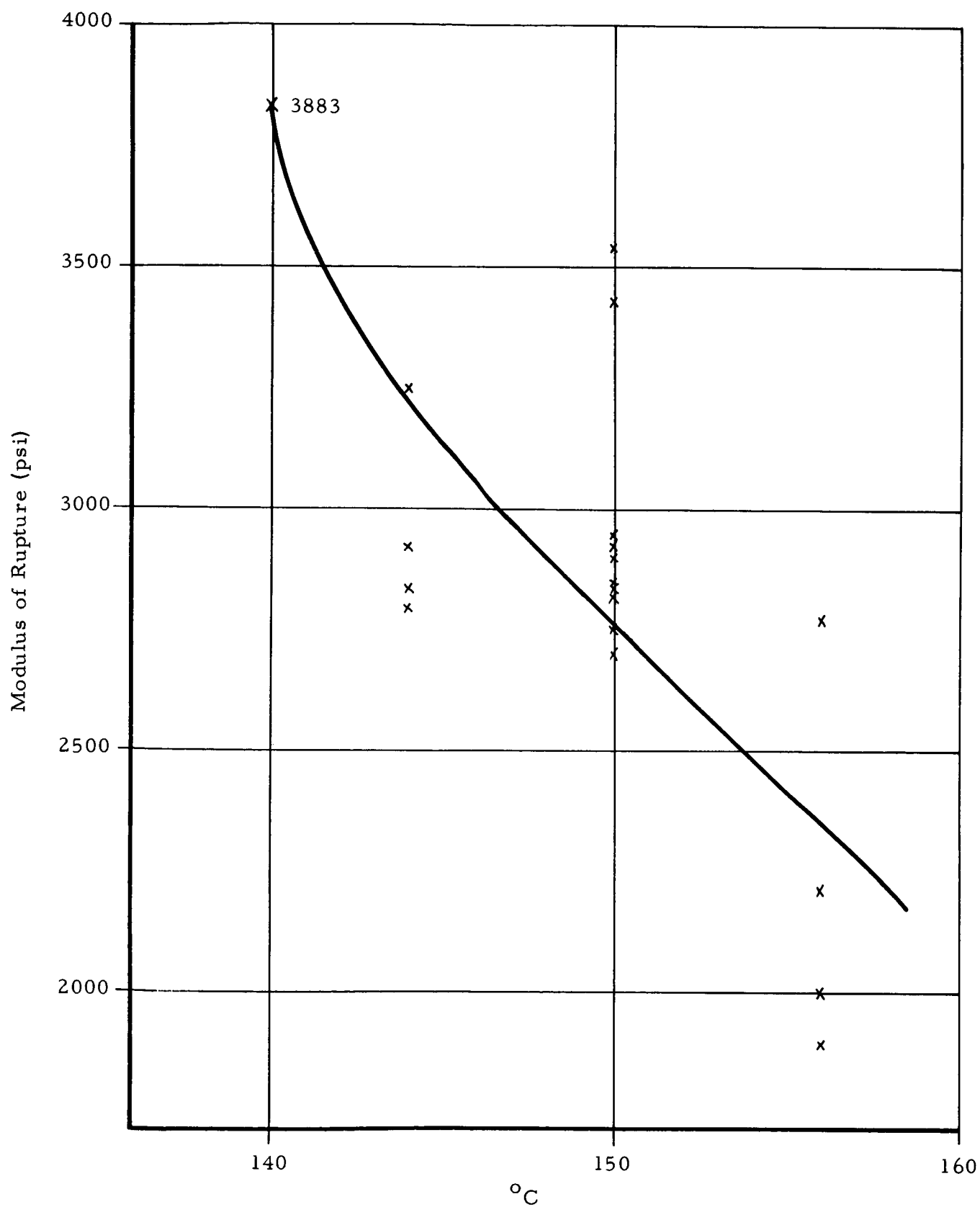


Figure 13. Effect of Material Drying Temperature on Transverse Strength (all data)

The effect of increasing drying temperature on transverse strength is shown in Figure 13. It can be seen that the highest strength (3883 ± 21 psi) was produced by drying the material for 40 hours at 140°C. Increasing drying temperature from 140° to 160°C resulted in a rapid decrease in sintered transverse strength for all compositions studied. Thus it is apparent that transverse strength can be increased by reducing both drying temperature and time and that high drying temperatures and long drying times are to be avoided. Figure 12 shows that the effect of drying time on strength is independent of composition. Transverse strength decreases significantly for all compositions ranging from 18 to 28%  $\text{H}_3\text{PO}_4$  as drying time is increased from 20 to 60 hours.

In order to evaluate the use of vacuum drying of membrane compositions, the drying oven used in this investigation was modified for vacuum drying by placing an aluminum dessicator in it. A hole drilled through the dessicator cover was attached to a suitable vacuum source. This permitted sample drying at controlled temperatures and vacuum conditions. Figure 14 is a photograph of the vacuum drying oven.

Vacuum drying a 1  $\text{ZrO}_2$ : 1  $\text{H}_3\text{PO}_4$ : 1 "Zeolon H" mixture for 40 hours at 90°C and 30 in of Hg increased the transverse strength to 5050 psi. This is more than a two fold increase in strength as compared to the same composition prepared by oven drying for 15 hours at 160°C. It is apparent from these favorable findings that vacuum drying can be significant in increasing membrane strength.

#### 2.2.8 Presintering Membrane Materials

As the experimental work progressed, it was found that the highest transverse strength (6025 psi) was obtained with a 2  $\text{ZrO}_2$ : 1  $\text{H}_3\text{PO}_4$  composition (Reference 6). This material also exhibited relatively good electrical conductivity. As a result of these findings, it was logical to expect that the substitution of pre-sintered  $\text{ZrO}_2$ - $\text{H}_3\text{PO}_4$  for  $\text{ZrO}_2$  in a composition along with equal parts of phosphoric acid and "Zeolon H" would result in high transverse strength and low resistivity. In order to investigate this assumption equal parts of  $\text{ZrO}_2$  and  $\text{H}_3\text{PO}_4$  were mixed, dried at 120°C and sintered for 15 hours at 500°C. The resulting material was hard and dense. It was

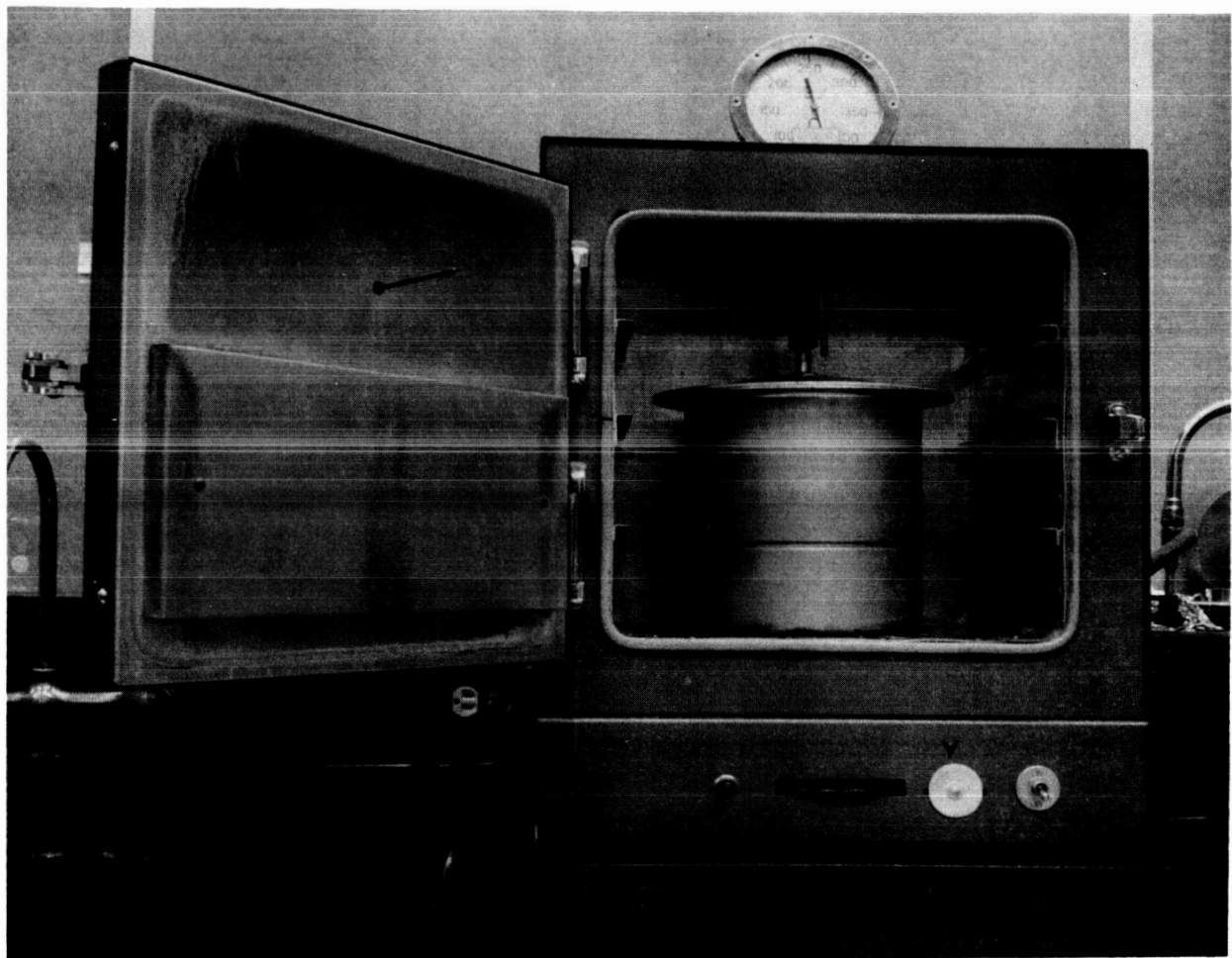


Figure 14. Photograph of Vacuum Drying Oven

crushed to minus 14 mesh in a mortar and after ball milling for 18 hours with porcelain balls, 5% calcia-stabilized zirconia fibers were blended into the slurry. The resulting composition was dried for 15 hours at 160°C, pressed into 2 inch membranes, 0.030 in. thick, at 15 tons load and sintered for 15 hours at 500°C. These membranes had a transverse strength of  $2895 \pm 84$  psi and the lowest resistivity of any composition tested in this program. Resistivity at 110°C and 100% R.H. was 4.0 ohm-cm; about twice the resistivity of phosphoric acid.

In addition to producing extremely low resistivity and good strength characteristics, the use of presintered  $\text{ZrO}_2\text{-H}_3\text{PO}_4$  resulted in phosphate bonded membranes which produced better results in the analytical fuel cell than the other compositions tested. The membrane containing presintered  $\text{ZrO}_2\text{-H}_3\text{PO}_4$  also had better high temperature performance in the fuel cell and performance at 97°C was as good or better than lower temperature performances for other membrane materials. It is apparent from these findings, that the concept of pre-reacting materials such as  $\text{ZrO}_2$  and  $\text{H}_3\text{PO}_4$  for use in inorganic fuel cell membranes represents a novel and promising approach in our efforts.

Application of this new development along with further optimization of materials, compositions and processing techniques can result in highly satisfactory inorganic membranes for fuel cell application.

### 2.3 Electrical Conductivity of Phosphate Bonded Inorganic Membranes

This investigation was concerned with the development of an inorganic membrane of sufficiently high electrolytic conductivity and mechanical strength to be employed in a hydrogen-oxygen membrane fuel cell. Such inorganic membranes would be particularly suited for fuel cell applications at temperatures of 100°C or above. The thermal stability of inorganic membranes would permit fuel cell operation at elevated temperatures in contrast to organic membranes which would deteriorate at these temperatures. Another important advantage of operating a fuel cell at elevated temperatures is the improved performance of the oxygen electrode with increasing temperature, since the oxygen overpotential is reduced.



The inorganic membrane system investigated was formed by chemical reaction of three materials;  $\text{ZrO}_2$ ,  $\text{H}_3\text{PO}_4$  and "Zeolon H." The resulting membranes consist of a mixture of zirconium phosphate polymer, "Zeolon H" and perhaps unreacted  $\text{ZrO}_2$  as well as amorphous products of unknown composition. These phosphate bonded inorganic membranes were investigated as they possessed much greater electrical conductivity than those prepared from other materials and also had high transverse strength.

### 2.3.1 Measurement of Membrane Resistivity

Membrane resistance was measured by means of an alternating current bridge. An Electro-Measurements Inc., Impedance Bridge Model 290R was employed in conjunction with an A.C. Generator Model 860R, which operates at a number of fixed tuned frequencies ranging from 400 to 10,000 cycles. Bridge balance was detected by a Hewlett Packard Vacuum Tube Voltmeter, Model 400D.

Experimental membranes were held between platinum electrodes having approximately 1.0 sq. cm surface area for measuring resistance. The membrane-electrode assembly was placed in a furnace held at constant temperature by an electronic temperature controller. Nitrogen gas of accurately controlled humidity was passed through the furnace to provide the desired relative humidity. This apparatus along with the auxiliary instrumentation is described in Appendix D.

Membrane resistance was measured at  $70^\circ$ ,  $90^\circ$  and  $105^\circ\text{C}$ . At each temperature, the relative humidity was varied from 0 to 70% and resistance measurements were made at each condition of temperature and humidity. Membrane resistance was expressed as resistivity (ohm-cm). Resistivity values representing the mean obtained from measurements of 2 or 3 individual membranes are reported with the error indicated as standard deviation.

An important relationship between the mean resistivity and relative humidity was deduced; namely, the logarithm of mean resistivity is a linear function of relative humidity at constant temperature. As a result,

resistivity values are reported from 50 to 100% relative humidity. Resistivity values reported for 100% relative humidity are extrapolated and less precise than those reported at lower relative humidity since the latter fall within the experimental range.

### 2.3.2 Results of Resistivity Measurements

For convenience of discussion, resistivity data are divided into two consecutive sections. In the first section, resistivity data previously reported are summarized and discussed in detail. These measurements were made on membranes which were produced by a number of different fabrication techniques and from a variety of compositions. Variations investigated included chemical composition, sintering time and temperature, the effect of additions of inorganic fibers and the effect of substituting presintered zirconium phosphate for  $\text{ZrO}_2$  in the membrane formula.

In the second section, the resistivities of 20 membrane compositions prepared for a statistical study of composition and processing variables are reported. The variables investigated in this series were chemical composition, drying temperature and the drying time. Two analyses of the statistical data were made. A discussion of these findings and graphical treatment of the data are presented in this report. A detailed analysis of the statistical series and the mathematical equations derived are presented in Section 2.4.

The most significant resistivity data accumulated for membranes formed from  $\text{ZrO}_2$ ,  $\text{H}_3\text{PO}_4$  and "Zeolon H" under different processing conditions are summarized in Table X. These data do not include measurements of the resistivities of the statistical series of membranes. These data are reported in Section 2.3.8.

Table X shows membrane resistivity at 50 and 100% relative humidity and at temperatures of  $105^\circ$  and  $110^\circ\text{C}$  for twelve membrane compositions. The basic resistivity measurements from which these data are obtained are shown in Appendix E, Tables XVIII through XXIX. Analysis of the effect of membrane composition and processing conditions on resistivity was made at 50% relative humidity because these resistivities lie

within the experimental range of measurement and are therefore more accurate than the values obtained by extrapolation to 100% relative humidity. Because of the strong dependence of resistivity upon the relative humidity, resistivities at 100% relative humidity are much lower than those obtained at 50% relative humidity. This is of major significance in fuel cell application as the water produced during operation of a hydrogen-oxygen cell provides high humidities in the vicinity of the oxygen electrode.

The resistivity data shown in Table X are arranged in order of increasing resistivity, ranging from a low value of 10 ohm-cm to  $1.8 \times 10^3$  ohm-cm at 50% relative humidity. This range of resistivity values is a result of variations in composition and processing techniques which were investigated.

### 2.3.3 Effect of Composition on Resistivity

This investigation was concerned with the effect of variations in composition and processing conditions on the resistivity of phosphate bonded inorganic membranes. Membranes formed from combinations of  $ZrO_2$ ,  $H_3PO_4$  and "Zeolon H" generally had much lower resistivities (10 ohm-cm to  $1.8 \times 10^3$  ohm-cm at 50% relative humidity and 105°C) than membranes formed from equal parts of  $ZrO_2$  and  $H_3PO_4$ . The substantially lower resistivity of membranes made from  $ZrO_2$ ,  $H_3PO_4$  and "Zeolon H" is ascribed to greater hydration of all temperatures. This membrane behaves as a quasi-solid electrolyte exhibiting a resistivity somewhat higher than, but approaching, the resistivity of a phosphoric acid solution. It was also found experimentally that membranes formed from  $ZrO_2$ ,  $H_3PO_4$  and "Zeolon H" retained much more water than membranes not containing "Zeolon H," at temperatures above 100°C (Reference 17). The presence of a water balancing agent is of significance in the application of inorganic membranes to fuel cells, especially at high temperatures.

Resistivity measurements of  $ZrO_2$  and "Zeolon H" established that both of these materials have very high resistivities in excess of  $10^5$  ohm-cm and therefore, make no significant contribution to electrolytic conductivity by themselves.

The nature of the membrane surface may also contribute to ionic transport of hydrogen ions through the membrane. The membrane surface consists of unreacted  $\text{ZrO}_2$  or zeolite and unidentified phases formed by chemical reaction of zeolite,  $\text{ZrO}_2$  and  $\text{H}_3\text{PO}_4$  at the sintering temperature resulting in new compounds. Although no new crystalline phases were detected by X-ray powder diffraction patterns, the presence of newly formed amorphous phases which can not be detected by X-ray techniques is a distinct probability. It can be concluded from the experimental work performed that conduction through phosphate bonded membranes is ionic and conduction is considerably improved by hydration (Reference 18). The objectives of this investigation however, were to determine the factors affecting ionic conduction rather than to develop a clear understanding of the mechanism or conduction.

The most highly conducting membrane developed in this investigation was No. 191-047, shown in Table X. This membrane had a resistivity of 10 ohm-cm at 50% relative humidity. Resistivity decreased to 4.0 ohm-cm (approximately twice the resistivity of an aqueous solution of  $\text{H}_3\text{PO}_4$ ) at 100% relative humidity. While the high  $\text{H}_3\text{PO}_4$  content included in the composition of this material may be partially responsible for its unusually high ionic conductivity, this membrane was prepared in a different manner from the other membranes shown in Table X. It was prepared using presintered zirconium phosphate ( $\text{ZrO}_2 : \text{H}_3\text{PO}_4$ ) in place of  $\text{ZrO}_2$  along with equal parts by weight of  $\text{H}_3\text{PO}_4$ , and "Zeolon H." Five percent  $\text{ZrO}_2$  fibers were added to the formulation for increased strength. Using presintered zirconium phosphate in place of  $\text{ZrO}_2$  resulted in extremely low resistivity compared with membranes made from  $\text{ZrO}_2$ ,  $\text{H}_3\text{PO}_4$  and "Zeolon H."

Presintered zirconium phosphate assures more complete reaction of the  $\text{ZrO}_2$  phase with  $\text{H}_3\text{PO}_4$  and may also result in a change in the structure of the zirconium phosphate polymer. Further experimental work will be required however, to fully explain the significant improvement in conductivity obtained.

As this membrane also contained 5%  $\text{ZrO}_2$  fibers, it is apparent that the presence of inorganic fibers did not adversely affect conductivity.

A number of other membranes shown in Table X exhibit unusually low resistivities ranging from  $2.6 \times 10^1$  to  $6.9 \times 10^1$  ohm-cm (50% humidity) and substantially lower values when extrapolated to 100% relative humidity. These range from 2 to 30 ohm-cm. All of the membranes have sufficiently low resistivity to be considered for use as fuel cell solid electrolytes. A common feature in the chemical composition of all of the highly conducting membranes is that they contain 30% or more incorporated  $\text{H}_3\text{PO}_4$ .

A more detailed examination of the effect of variations in the incorporated  $\text{H}_3\text{PO}_4$  content involves examining the effect upon membrane resistivity of variation in the ratio of  $\text{H}_3\text{PO}_4$  to  $\text{ZrO}_2$  and  $\text{H}_3\text{PO}_4$  to "Zeolon H" since both  $\text{ZrO}_2$  and "Zeolon H" phases are required in order to formulate highly conducting membranes. If the highly conducting membrane 191-007, in which both the  $\text{H}_3\text{PO}_4$  to  $\text{ZrO}_2$  and  $\text{H}_3\text{PO}_4$  to "Zeolon H" ratios are 1.0, is adopted as a reference, a comparison of the effect of variation in chemical composition of membranes is facilitated. Increasing either the ratio of  $\text{H}_3\text{PO}_4$  to  $\text{ZrO}_2$  or the ratio of  $\text{H}_3\text{PO}_4$  to "Zeolon H" decreases membrane resistivity. For example, an increase in the ratio of  $\text{H}_3\text{PO}_4$  to  $\text{ZrO}_2$  from 1.0 in the reference membrane to 2.0 at a constant ratio of  $\text{H}_3\text{PO}_4$  to "Zeolon H", decreases membrane resistivity from  $5.7 \times 10^1$  to  $3.8 \times 10^1$  ohm-cm. Moreover, if the  $\text{H}_3\text{PO}_4$  to  $\text{ZrO}_2$  ratio is held constant at 2.0, an increase in the ratio of  $\text{H}_3\text{PO}_4$  to "Zeolon H" decreases membrane resistance from  $3.8 \times 10^1$  to  $2.6 \times 10^1$  ohm-cm. In contradistinction to the preceding, a decrease of both ratios to 0.5 yields a resistivity of  $1.1 \times 10^2$  ohm-cm, which is nearly twice that of the reference membrane. Thus, it is clear that membranes with ratios of  $\text{H}_3\text{PO}_4$  to  $\text{ZrO}_2$  and  $\text{H}_3\text{PO}_4$  to "Zeolon H" below 0.5 would be expected to have too high a resistivity (greater than  $1.1 \times 10^2$ ) for application as fuel cell electrolytes. Therefore this ratio is a convenient tool for determining the lower limit of incorporated  $\text{H}_3\text{PO}_4$  content in membranes.

The amount of  $\text{H}_3\text{PO}_4$  which can be used in order to increase conductivity is limited by other factors. Figure 6, for example, shows that there is an optimum range of  $\text{H}_3\text{PO}_4$  content for maximum strength. Increasing the  $\text{H}_3\text{PO}_4$  content above this would decrease transverse strength even though conductivity might be improved.

The inclusion of 5% inorganic fibers in the membrane composition has been shown to substantially increase membrane strength. In addition to this important advantage, only a slight increase in membrane resistivity results when  $\text{ZrO}_2$  fibers are added. The three membranes shown in Figure 15 have the same chemical composition but 5%  $\text{ZrO}_2$  fibers were added during fabrication of membranes No. 191-042 and 191-051. Membrane No. 191-007 does not contain inorganic fibers. It can be concluded that  $\text{ZrO}_2$  fiber additions can be used to increase strength without significantly decreasing conductivity.

In contrast to  $\text{ZrO}_2$  fibers, the additions of 5% of aluminosilicate fibers in the membrane composition resulted in more than a two-fold increase in membrane resistivity as illustrated in Figure 16. Thus, the employment of aluminosilicate fiber offers no advantage since the two-fold increase in membrane strength resulting from their use is nullified by doubling the membrane resistivity.

In order to assess the effect of using different types of  $\text{ZrO}_2$  on membrane resistivity, Zircoa "B", a CaO stabilized  $\text{ZrO}_2$ , was used in place of the chemically pure  $\text{ZrO}_2$  normally used in membrane formulation. A three-fold increase in membrane resistivity resulted as shown in Figure 17. Consequently, it appears that the treatment employed to stabilize  $\text{ZrO}_2$  has an adverse effect and substantially increases resistivity.

#### 2.3.4 Effect of Sintering Temperature on Membrane Resistivity

Sintering at elevated temperature is required in order to form membranes of acceptable mechanical strength. A chemical reaction forming zirconium phosphate polymers takes place during sintering providing a matrix of zirconium phosphate bonds which produce membrane strength.

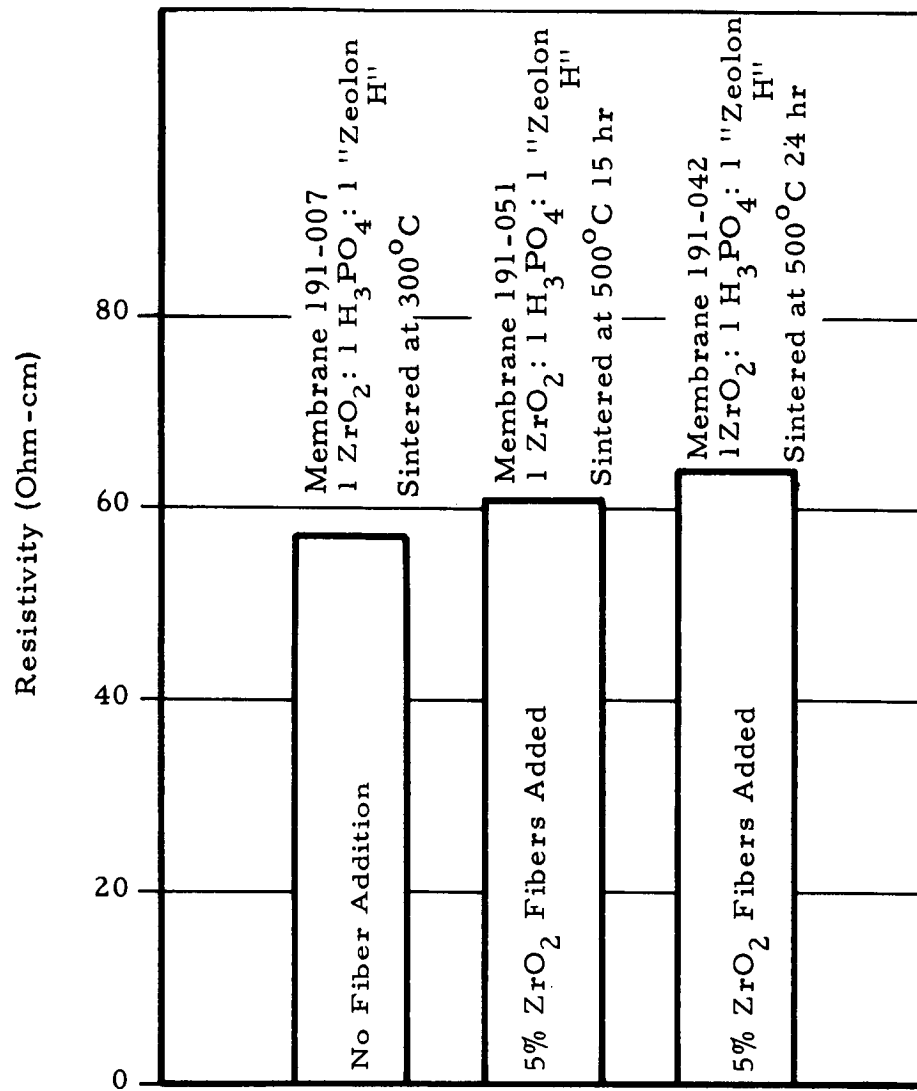


Figure 15. Effect of  $\text{ZrO}_2$  Fiber Additions and Sintering Temperature and Time on Membrane Resistivity

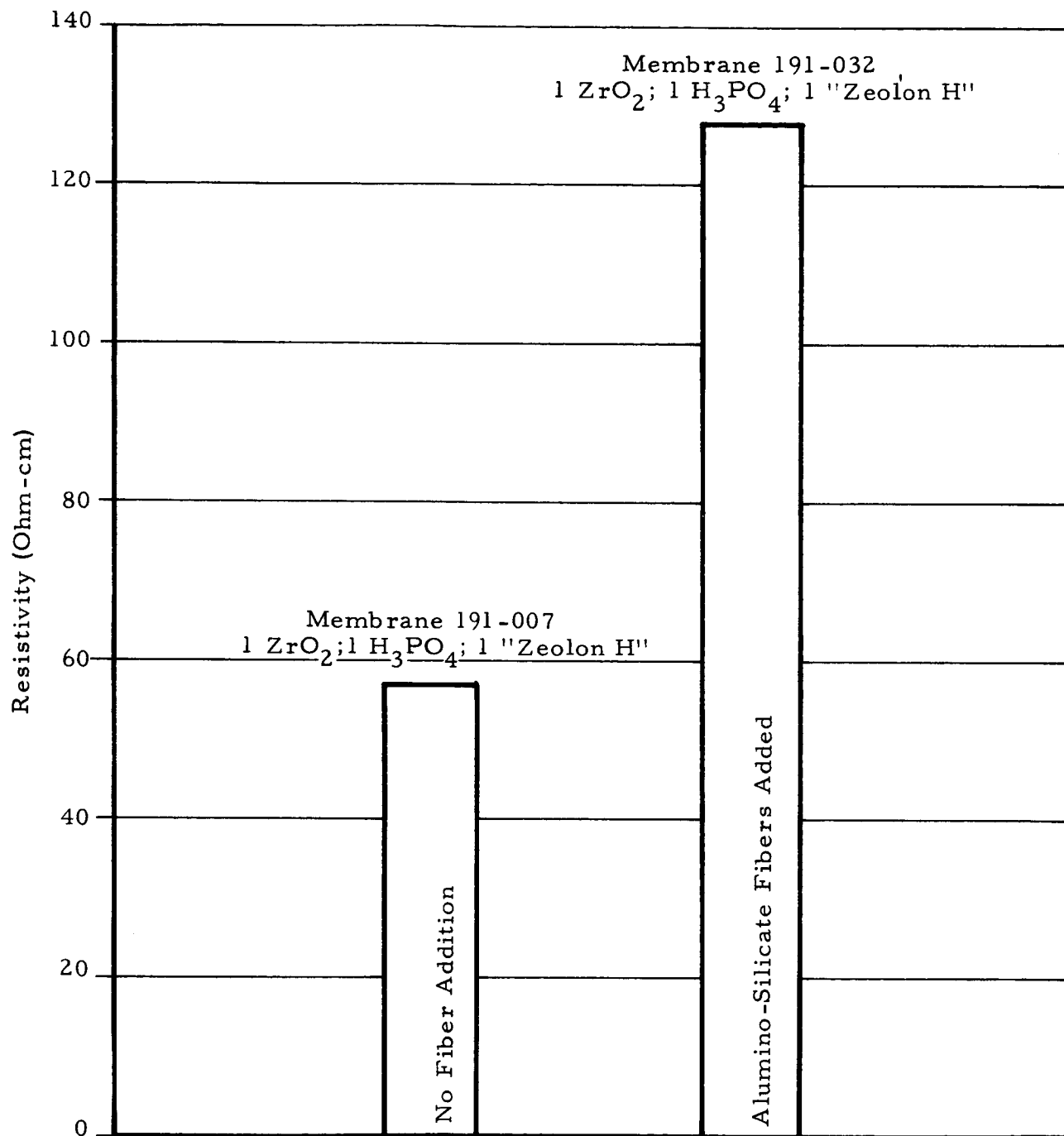


Figure 16. Effect of Alumino-Silicate Fiber Additions on Membrane Resistivity



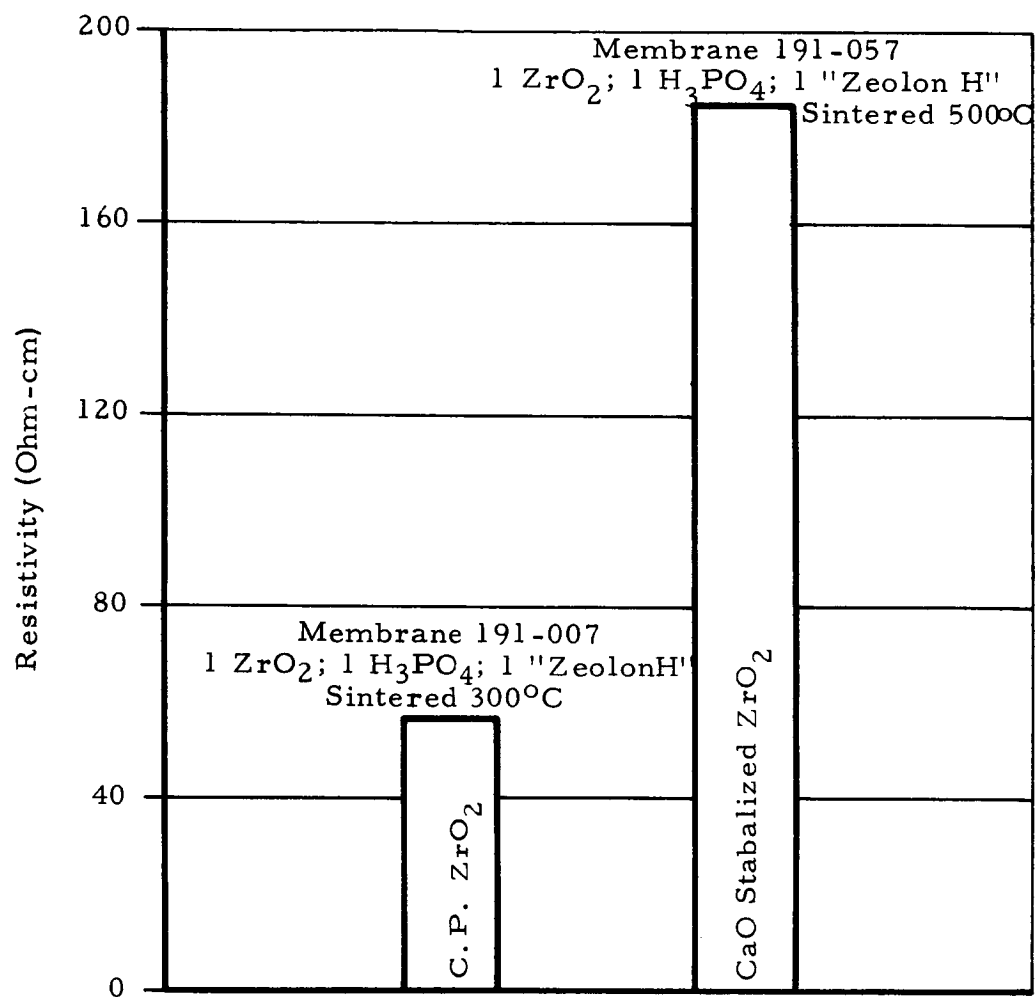


Figure 17. Effect of Type of Zirconia Used on Inorganic Membrane Resistivity

The use of a high sintering temperature such as 500°- 700°C, greatly increases membrane strength but it is expected that it would decrease membrane conductivity due to elimination of the ionic groups of the zirconium phosphate polymer in the membrane and the formation of a fused ceramic structure. The effect of increasing the sintering temperature from 300°C to 500°C, however, does not result in a significant increase in membrane resistivity. For example, membrane 191-007 sintered at 300°C exhibits a resistivity of  $5.7 \times 10^1$  ohm-cm, while membrane 191-042 sintered at 500°C for the same length of time exhibits a slightly higher resistivity of  $6.4 \times 10^1$  ohm-cm. The latter membrane contains 5% ZrO<sub>2</sub> fiber addition which may also account for the difference in resistivity of the two membranes. As a result of the lack of dependence of membrane conductivity upon sintering temperature in the range 300° to 500°C, sintering temperatures may be selected to optimize membrane strength.

#### 2.3.5 Effect of Sintering Time on Membrane Resistivity

The use of short sintering times would be expected to yield membranes of low mechanical strength due to incomplete formation of zirconium phosphate polymer which is responsible for membrane strength. On the other hand, while sintering for a longer time might result in improved membrane strength, the possible elimination of ionic groups in the zirconium phosphate polymer might result in membranes with poor conductivity. However, at a sintering temperature of 500°C, increasing sintering time from 15 to 24 hours resulted in an increase in membrane resistivity from  $6.1 \times 10^1$  to  $6.4 \times 10^1$  ohm-cm for membranes 191-051 and 191-042, (Table X ). Consequently, variations of sintering time in the range of 15 to 24 hours at 500°C do not appreciably affect membrane conductivity although more extended times might reduce membrane conductivity significantly.

#### 2.3.6 Effect of Drying Temperature on Membrane Resistivity

In drying membrane materials, in addition to water removal, a chemical reaction takes place forming zirconium phosphate polymer, particularly when the drying temperatures employed were sufficiently high (in the range 140 to 160°C). Thus the drying process involves the same

chemical reaction as that which occurs in the sintering process. However, at the lower temperatures employed in drying process the formation of zirconium-phosphate polymer may be expected to be rather incomplete. Since most membranes of similar chemical composition measured were dried at the same temperature ( $160^{\circ}\text{C}$ ), the effect of variation of drying temperature upon membrane resistivity cannot be deduced from the data in this table. However, in the statistical series section which follows, it was found that increasing drying temperatures increased membrane resistivity.

#### 2.3.7 Effect of Drying Time on Membrane Resistivity

Increasing the drying time from 20 to 40 hours at  $140^{\circ}\text{C}$  resulted in a two-fold increase in membrane resistivity as shown by the resistivities for membranes No. 191-053 and No. 191-059 in Table X. This increase in resistivity is not considered large in view of the unusual variations in the length of drying time involved. As shorter drying times at a given temperature result in increased strength, it is apparent that drying time should be kept to a minimum.

#### 2.3.8 Conductivity for the Statistical Series of Membranes

In order to evaluate thoroughly membranes formed from  $\text{ZrO}_2$ ,  $\text{H}_3\text{PO}_4$  and "Zeolon H," and to obtain optimum conductivity and strength consistently, a statistical program was established to evaluate the variables involved in membrane fabrication. As a large number of variables are encountered in membrane fabrication, it was necessary to arbitrarily fix values for certain variables maintaining them constant, in order to simplify the experimental program and study the more important variables. The range of the variables investigated was also necessarily restricted due to the time required for membrane fabrication and evaluation.

The statistical design adopted required the preparation of twenty membrane combinations for which the membrane resistivities are presented in Table IX. The basic resistivity data from which these results were obtained are shown in Appendix E, Tables XXIX through XLVIII. For the twenty combinations the variables in membrane preparation that were

maintained constant were:

1. Sintering temperature =  $500^{\circ}\text{C}$
2. Sintering time = 15 hours
3. All membranes were formed by cold pressing into 2-inch diameter discs at 15 tons total load.

The effect on resistivity and strength of the following variables was investigated:

1. Chemical composition,
2. Drying temperature,
3. Drying time.

The specific range over which these variables were investigated was:

1. Chemical Composition - All membranes contained 30% chemically pure  $\text{ZrO}_2$ . The ratio of  $\text{H}_3\text{PO}_4$  to "Zeolon H" in the membranes was varied so that the  $\text{H}_3\text{PO}_4$  content ranged from 16 to 30% and the "Zeolon H" content varied from 40 to 54%.
2. Drying Temperature - Materials used for membrane fabrication were dried at temperatures ranging from  $140^{\circ}$  to  $160^{\circ}\text{C}$ .
3. Drying Time - Materials used for membrane fabrication were dried for varying lengths of time ranging from 20-60 hours.

The effect of each of these variables on membrane resistivity is discussed in detail.

All membranes in the statistical series were fabricated from the same materials;  $\text{ZrO}_2$ ,  $\text{H}_3\text{PO}_4$  and "Zeolon H." As 30%  $\text{ZrO}_2$  is used throughout the series, the effect of variations in the ratio of  $\text{H}_3\text{PO}_4$  to "Zeolon H" may be deduced for membranes subjected to the same drying conditions. The decrease in membrane resistivity with an increase in the ratio of  $\text{H}_3\text{PO}_4$  to "Zeolon H" is illustrated in Figure 18. This figure shows that membrane resistivity decreases rapidly as the incorporated  $\text{H}_3\text{PO}_4$  to "Zeolon H" ratio increases.

Increasing drying temperature from  $140^{\circ}$  to  $160^{\circ}\text{C}$  with other variables held constant resulted in approximately a two-fold increase

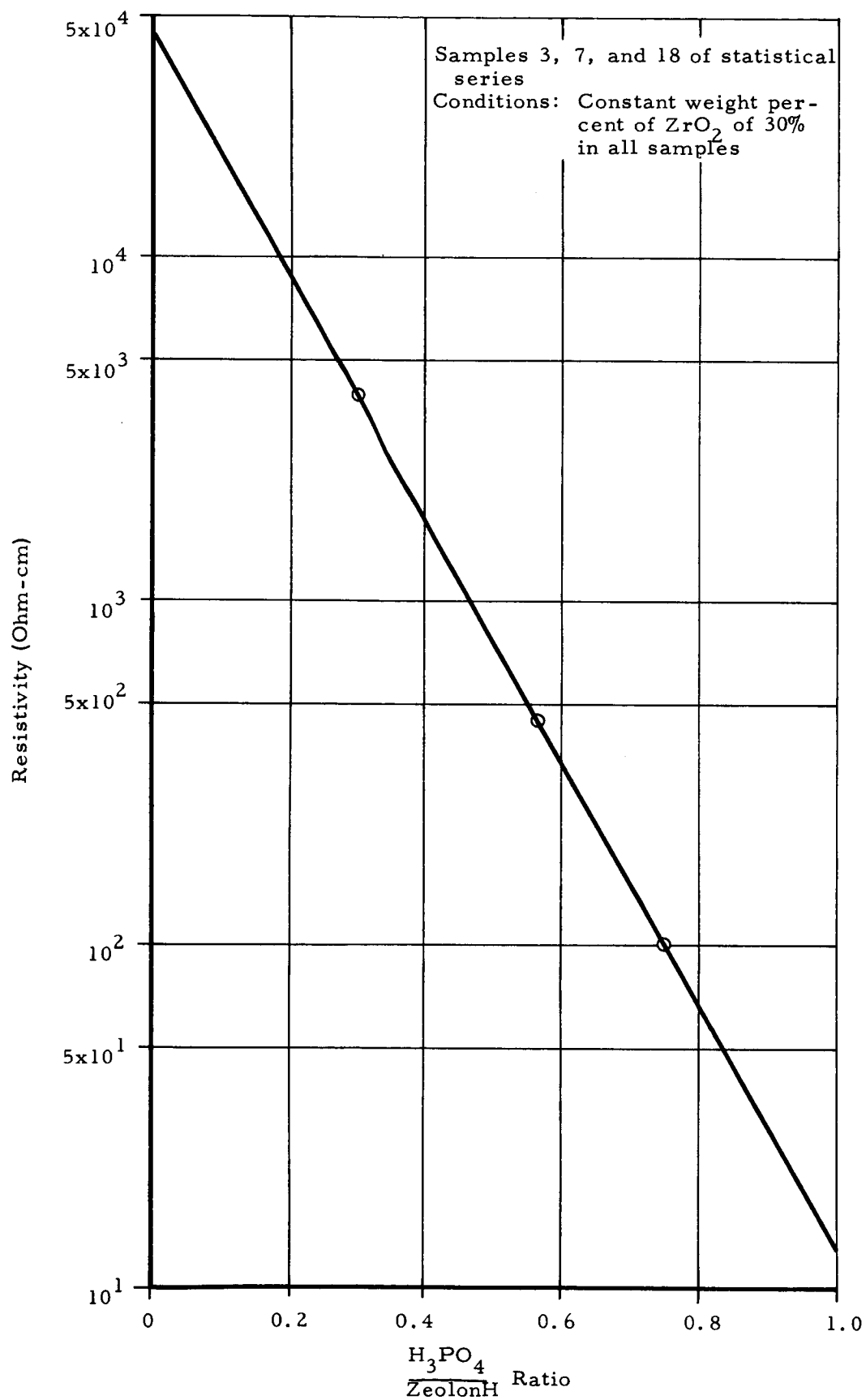


Figure 18. Effect of Membrane Composition on Resistivity of Inorganic Membranes

increase in membrane resistivity as shown in Figure 19. Consequently, it may be generalized that membrane materials should be dried at low temperatures, since this condition favors low resistivities as well as higher membrane strengths as shown in Figure 12.

The effect of drying time, with other variables constant, on membrane resistivity is shown in Figure 20. It is apparent from these data that there is a substantial dependence of membrane resistivity upon drying time at the highest drying temperature ( $156^{\circ}\text{C}$ ). Resistivities at drying temperatures of  $150^{\circ}\text{C}$  and  $144^{\circ}\text{C}$  are, for practical purposes, independent of drying time. At a drying temperature of  $156^{\circ}\text{C}$ , membrane resistivity increased almost five-fold as drying time was increased from 28 to 52 hours. It may be concluded therefore, that both membrane strength and conductivity decrease substantially with longer drying times, and that for optimum membrane characteristics drying should be minimized.

## 2.4 Statistical Analysis of Composition and Processing Variables

As the experimental work in this investigation indicated that certain compositional and processing variables had a significant effect on strength and conductivity, a statistical program was outlined so these variables could be investigated in depth. As the results obtained (Section 2.2) showed that composition, drying time and drying temperature were of major importance in the development of a high strength membrane having low resistivity, these factors were chosen as the variables for the statistical investigation. All other processing variables such as pressing pressure, sintering temperature, etc. were held constant.

### 2.4.1 Mathematical Model and Statistical Design

The foundation of an experimental investigation is the derivation of a mathematical model. The more precisely the model approximates physical reality, the smaller the number of experimental observations that are required, since interpolation becomes more accurate. On the other hand, if the number of observations taken is minimal, the dependence on the accuracy of the model becomes nearly absolute, due to the very large

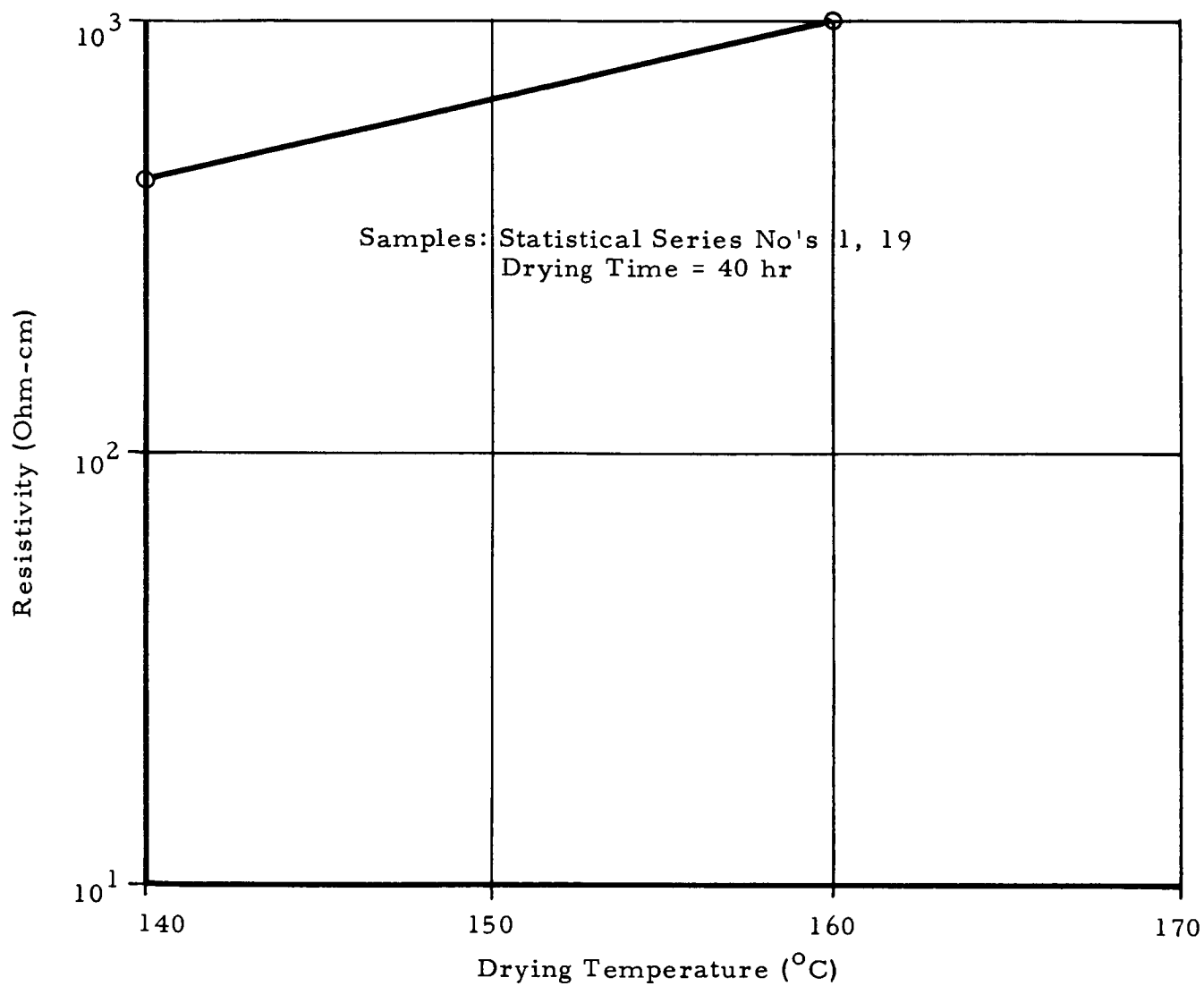


Figure 19. Effect of Drying Temperature upon Resistivity at Constant Drying Time.

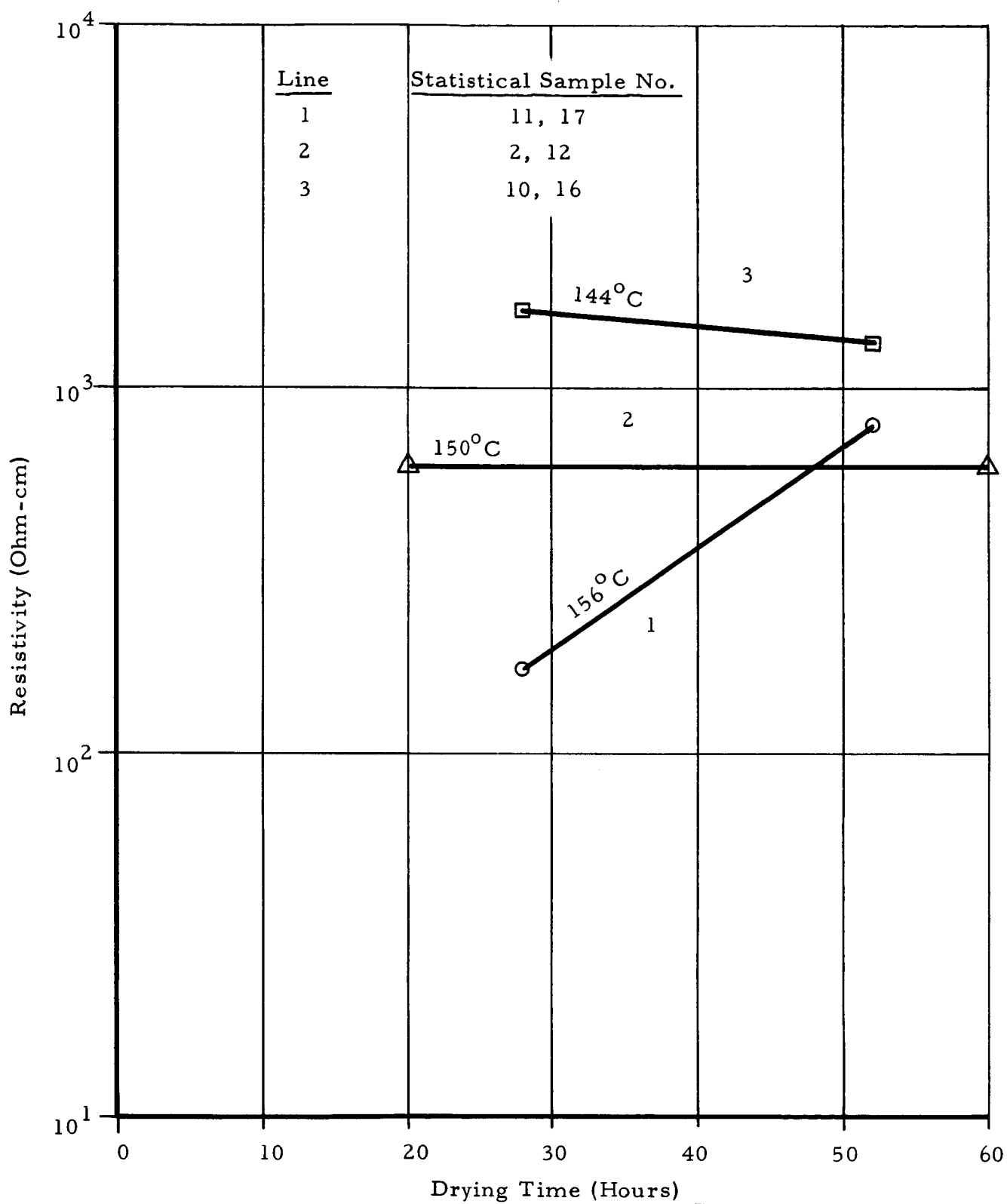


Figure 20. Effect of Drying Time upon Resistivity at Constant Drying Temperature for Three Membrane Compositions.



interpolation intervals which must be used.

The model must specify:

- (a) The dependent variables, or physical quantities, to be observed.
- (b) The physical parameters which are to be held constant.
- (c) The independent variables, or the physical parameters which are to be varied systematically.
- (d) The nature of the functional dependence of the observed results (dependent variables) on the parameters to be varied.

The dependent variables selected for this investigation were:

$y_1$  = the resistivity at 105°C and 50% humidity of the membranes fabricated

$y_2$  = the breaking strength of the membranes

The independent variables were:

C = Chemical composition, as measured by the  $H_3PO_4$  content

t = Drying time

T = Drying temperature

The functional dependence takes the form

$$y_1 = f_1 (C, t, T)$$

$$y_2 = f_2 (C, t, T)$$

The functions  $f_1$  and  $f_2$  are called response surfaces. In the model used, the response surfaces are assumed to be quadratic (in the case of resistivity, the dependent variable is placed on a logarithmic scale). For example

$$Z_1 = \log y_1 = b_0 + b_1 C + b_2 t + b_3 T + b_{11} C^2 + b_{22} t^2 + b_{33} T^2 + b_{12} Ct + b_{23} tT + b_{13} CT + \xi$$

where  $\xi$  is the experimental error. The coefficients b and the error are investigated experimentally.

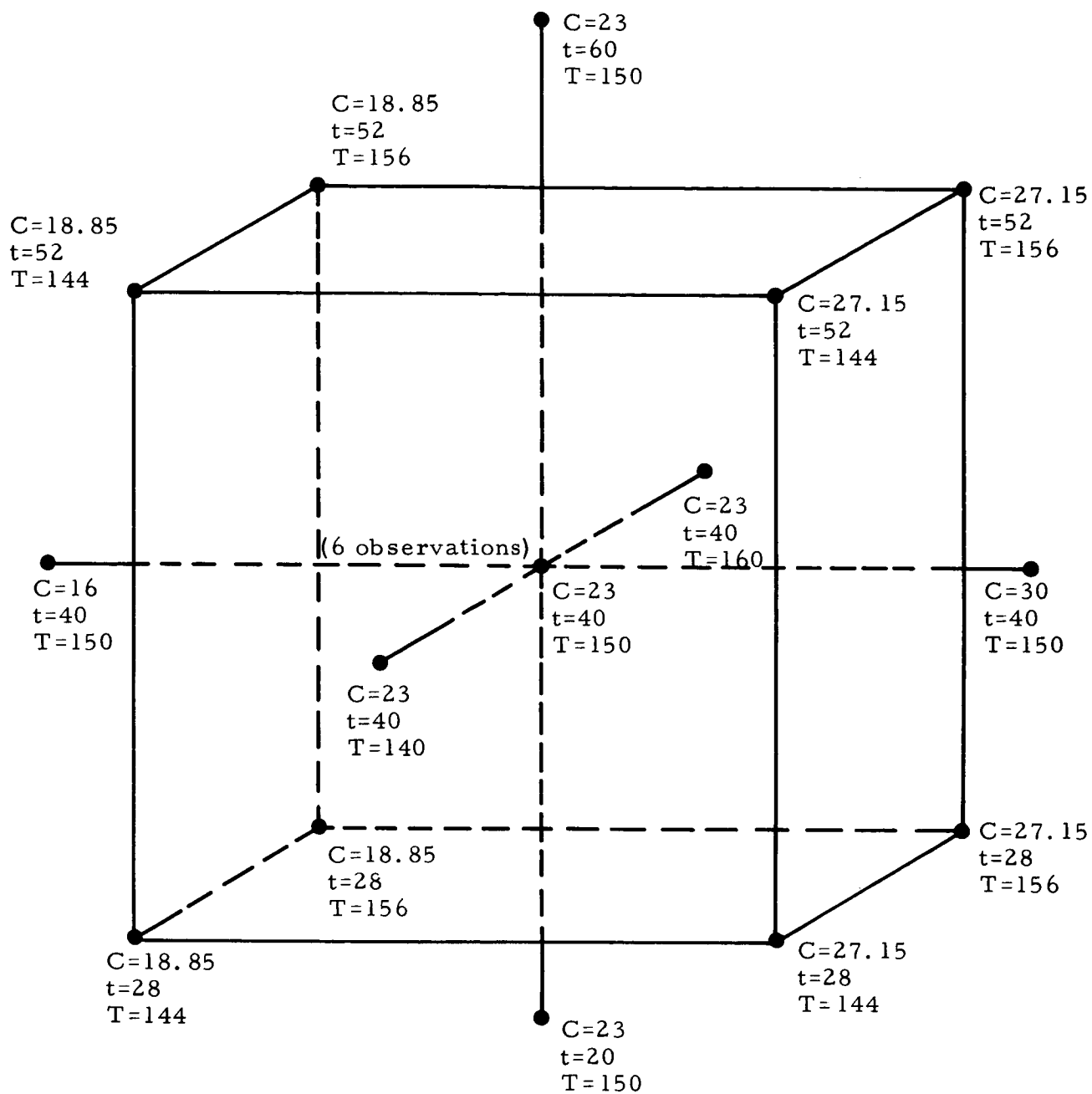
The statistical design that was chosen is called a "central composite rotatable design." It is described in more detail in Cochran and Cox (Reference 19). It was designed specifically for the investigation of quadratic response surfaces. The design is shown in Figure 21. The choice of six observations in the center provides nearly uniform interpolation accuracy within the central region being investigated. The model assumes that the experimental error in the logarithm of the resistivity is uniform over the design, and similarly the strength measurements have equal variances.

The experimental error is determined from the multiple measurements at the center. A sufficient number of observations are provided that the suitability of the quadratic response surface model may be determined.

The locations of the central point and the scaling of these axes were at the disposal of the experimenters. The experimental region to be investigated was determined from the results of previous studies and was selected with the hope of locating the optimum factor combination somewhere near the center of the design. In addition, preliminary tests demonstrated that fabricability of the membranes had to be considered. The attempt to predict an optimum point and locate it near the center was not too successful.

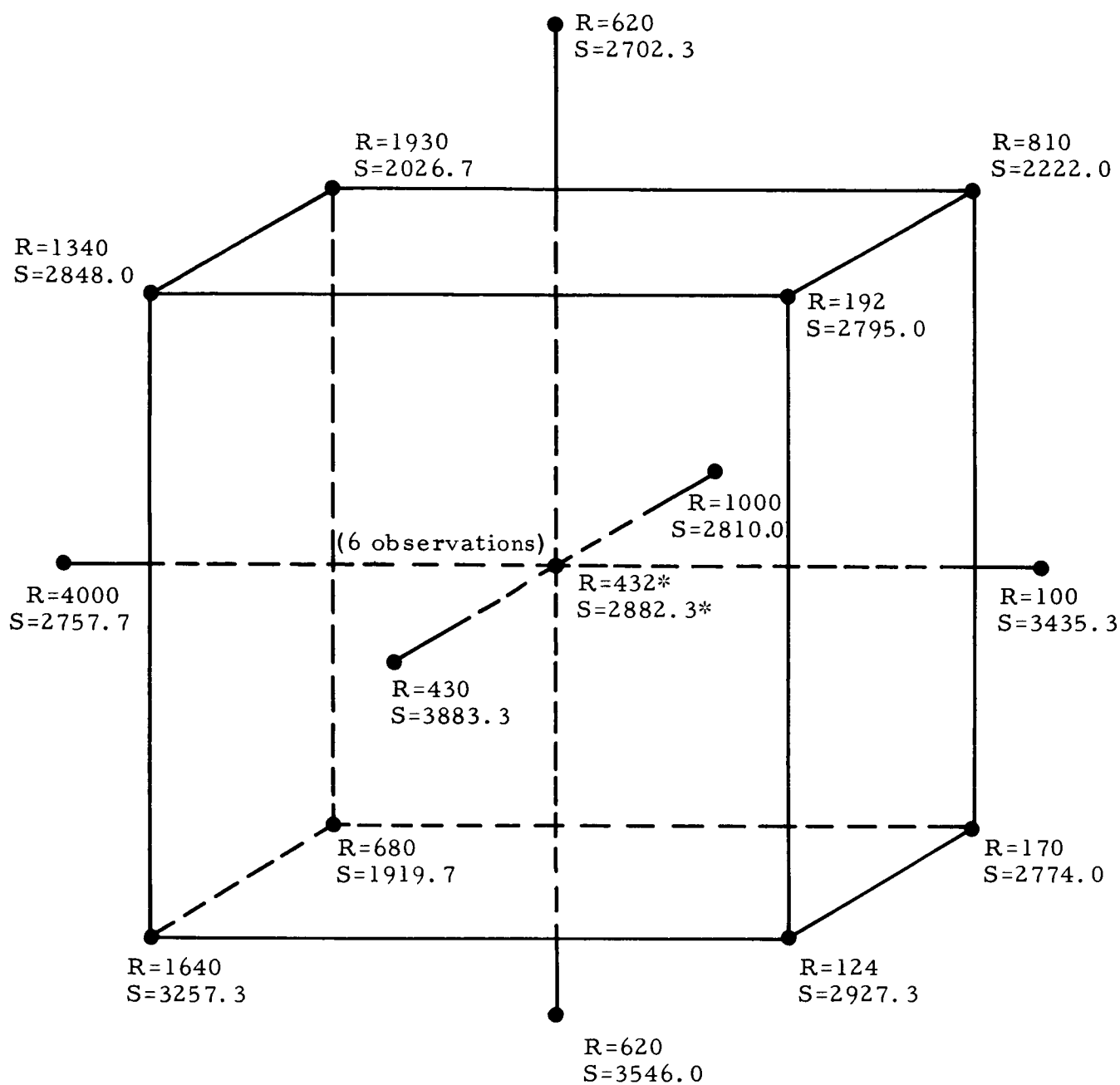
#### 2.4.2 Experimental Results

Figure 22 presents the experimental values observed for the statistical design of Figure 21. The strength data are the average breaking strength of three membranes and given in psi. The resistivity in ohm-cm was measured at several levels of humidity and interpolated to give the resistivity at 50% humidity. These resistivities are given in Figure 22. Data on resistivity for other levels of humidity and temperature are given in Section 2.3. The points on the back of the cube showing low strength are near the boundary of fabricability. One of the observations on the central point was not made for the resistivity data and an average over the other five observations was substituted instead.



C=Composition(%  $H_3PO_4$ )  
t=Drying Time (hrs)  
T=Drying Temp. ( $^{\circ}C$ )

Figure 21. Statistical Design



\*R=450, 640, 253, 295  
432 (est.), 520

\*S=2836.7, 2843.3, 2935.0,  
2851.7, 2922.3, 2905.0

Figure 22. Experimental Results

### 2.4.3 Mathematical Results

Table 11 presents the analysis of variance on the resistivity data. The mean square for lack of fit is equal to the mean square for error, indicating that the quadratic response surface provides an ideal fit to the data. This surface is given by:

$$\log_{10} R = 2.6119 - .4129X_1 + .0903X_2 + .0846X_3 + .0502X_1^2 + .0502X_2^2 + .0588X_3^2 + .0628X_1X_2 + .1233X_1X_3 + .1286X_2X_3$$

where  $X_1 = \frac{C - 23}{4.15}$

$$X_2 = \frac{t - 40}{12}$$

$$X_3 = \frac{T - 150}{6}$$

Figure 23 presents the resistivity data as smoothed by the quadratic surface. An analysis of the surface indicates that the predicted resistivity would be minimized at the point

$$C = 42.6\%$$

$$t = (-61.5) \text{ hrs.}$$

$$T = 171.5^\circ\text{C}$$

That the extrapolation is too great is clearly shown by the negative drying time. The direction of greatest improvement in resistivity suggests higher  $\text{H}_3\text{PO}_4$  content, shorter drying time, and higher drying temperature.

Table 12 presents the analysis of variance on the strength data. The comparison of the mean square for lack of fit and the mean square for error shows that the quadratic surface model does not provide an adequate fit to the experimental data. Higher degree surfaces may be fit to the data, but their use in interpolation leads to less uniform accuracy. Table 13 presents the analysis of variance for one such surface.

$$S = 2883 + 132X_1 - 176X_2 + 344X_3 + 179X_1X_3 - 117X_1X_2X_3 - 207(X_1^2 + X_2^2 + X_3^2) + 112(X_1^4 + X_2^4 + X_3^4)$$

This surface is not completely satisfactory, but is much better than the quadratic fit.

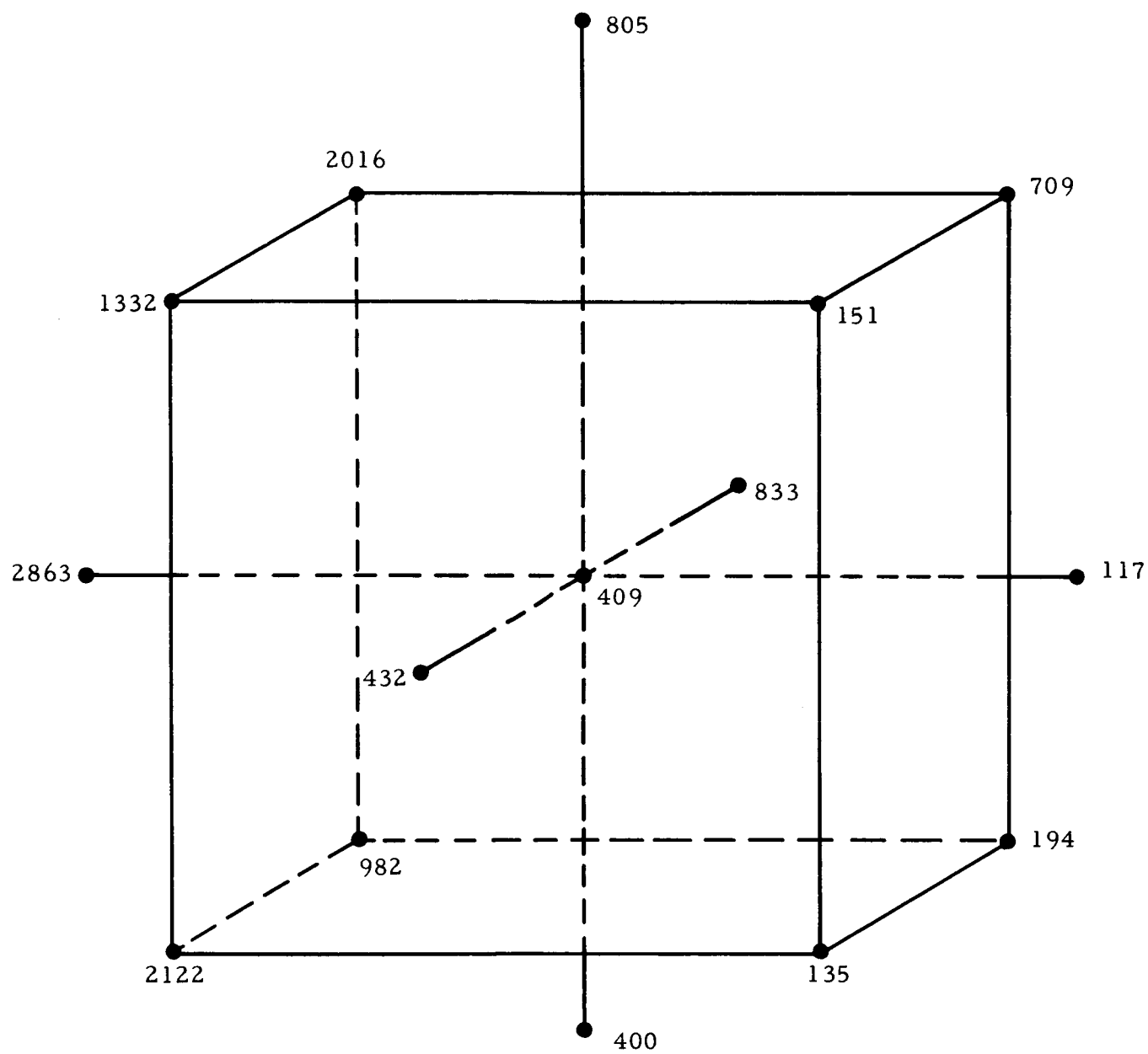


Figure 23. Smoothed Resistivity Data

The mathematical treatment of these data is tenuous, however, membranes fabricated with higher  $\text{H}_3\text{PO}_4$  content and shorter drying times appear to have high strength characteristics.

The quadratic surface provides a satisfactory fit to the log resistivity data and provides good interpolation and smoothing for  $X_1^2 + X_2^2 + X_3^2 - 1$ . As the optimum region does not fall within the area investigated, a further investigation of compositions containing more  $\text{H}_3\text{PO}_4$  and shorter drying times should yield membranes of lower resistivity. The indications are that such membranes will also have high breaking strength. These findings are in good general agreement with direct analysis of the experimental work done in this investigation except that the statistical analysis indicates that high drying temperatures should be helpful in producing strong inorganic membranes having low resistivity. This is in contrast to the experimental findings reported in Sections 2.2 and 2.3 which indicate that low temperature drying favors the development of high strength and good conductivity. The reason for this discrepancy in the statistical treatment of the data is not clear but will be investigated during the next phase of our endeavor.

## 2.5 $\text{H}_2\text{-O}_2$ Fuel Cell Evaluation of Inorganic Membranes

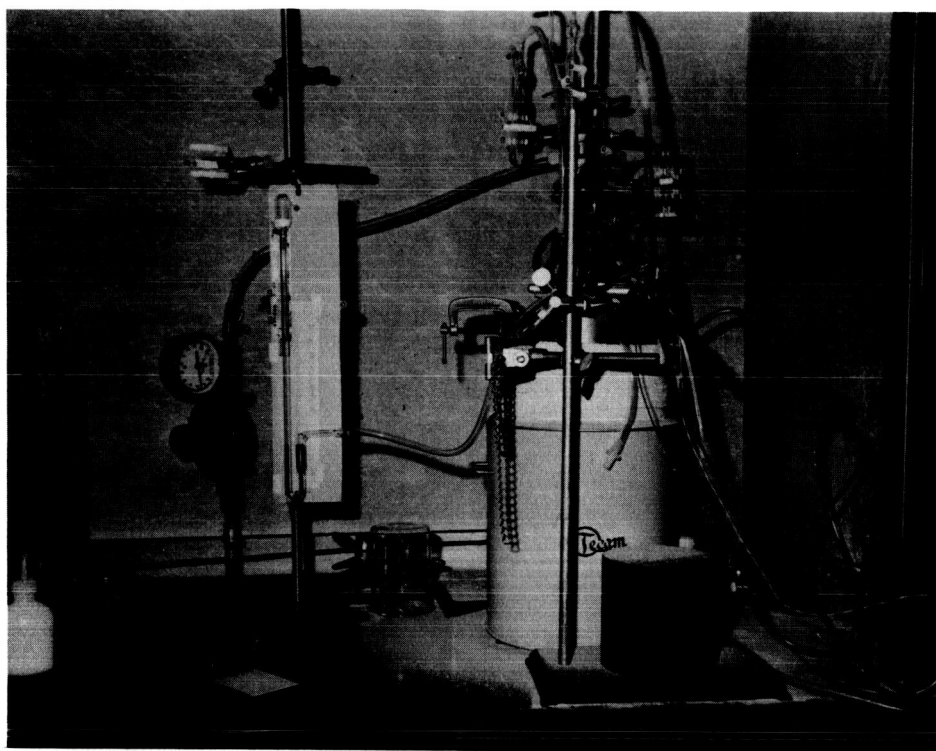
A simple test fuel cell was designed to measure performance of the inorganic membranes developed during this project. Figures 24 and 25 show the cell assembly. Appendix C discusses the cell operating procedure.

### 2.5.1 Cell Design

Since the contract specified a device for making a comparative evaluation of membranes, no attempt was made to emphasize optimization of weight, volume, or other structural aspects of the fuel cell. The steel casing was made sufficiently massive to insure good internal temperature control when the cell was immersed in a fluidized sand constant temperature bath.

Early cell operations revealed two main difficulties:

- (1) devising a stable electrode-catalyst-membrane assembly,
- (2) preventing gas leakage through the cell membrane gasket.



Assembled Fuel Cell

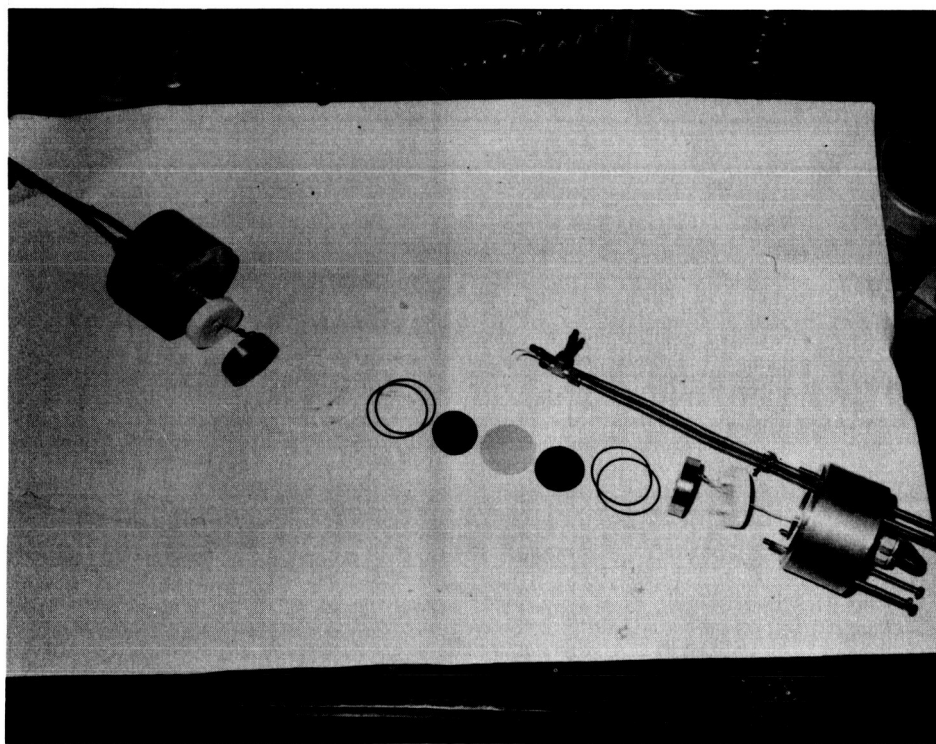


Figure 24. Analytical Fuel Cell for Evaluation of Inorganic Membranes



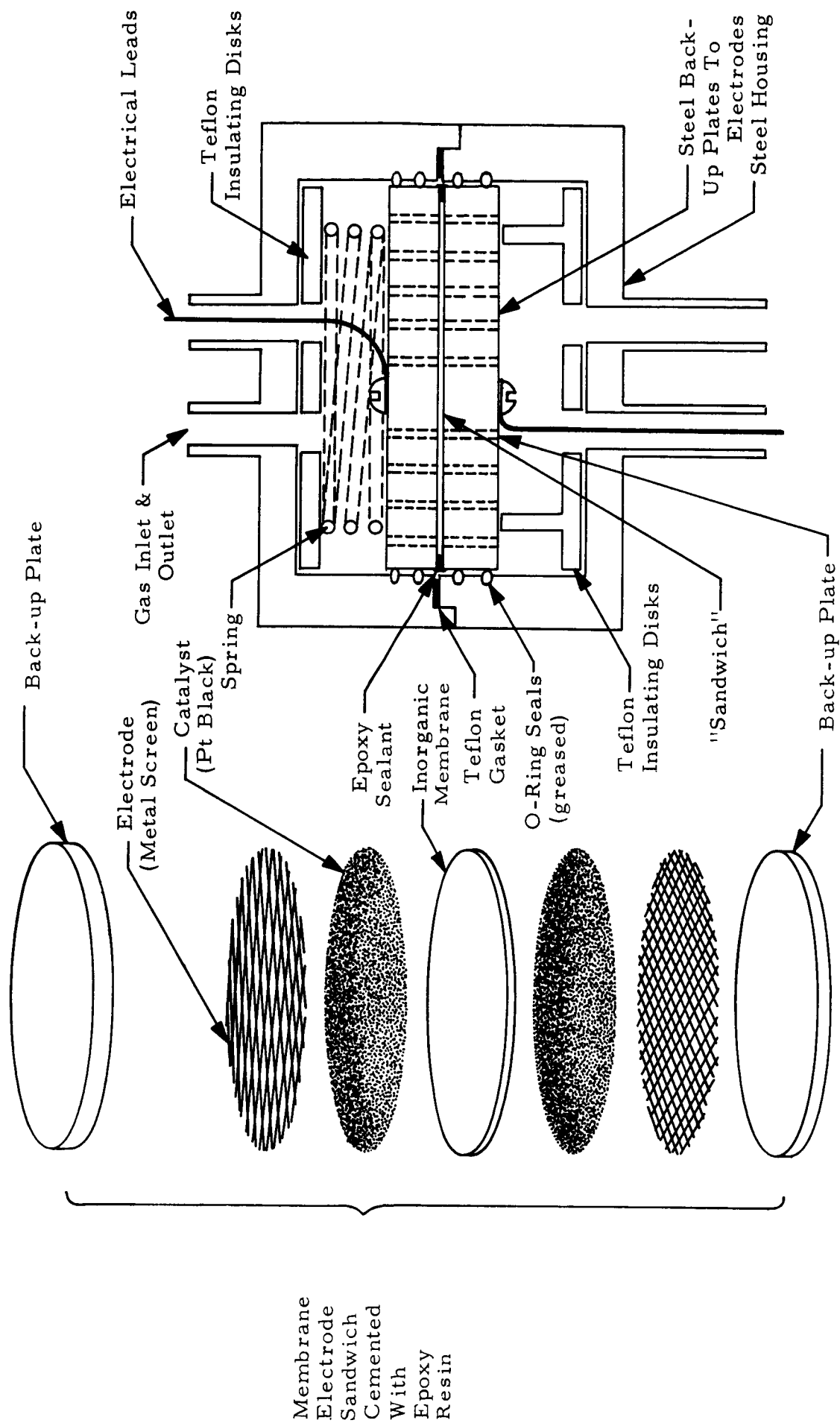


Figure 25 Analytical Fuel Cell

The first difficulty dominated early runs so that only one of the first 9 runs achieved both operating stability and a current density above  $20 \text{ ma/cm}^2$  at 0.5 volts.

In Run No. 10 and all succeeding runs, except a few using experimental electrodes, the platinum screen electrodes were replaced by a prefabricated Teflon-platinum black-tantalum screen electrode-catalyst matrix developed by American Cynamid for acidic aqueous-electrolyte fuel cells. Contact between the rough matrix sheet and the inorganic membrane was improved by maintaining a layer of platinum black ( $12\text{-}14 \text{ mg/cm}^2$ ) on each side of the membrane.

Following this change, successful operation occurred in Runs 10 and 11 (run 10 continued for 52 hours at  $67^\circ\text{C}$  and  $90^\circ\text{C}$  without failure). Then followed a series of cell failures traced eventually to an ineffective rubber sealer which had been used to fill the gap between the edges of the membrane and the Teflon cell gasket. To eliminate this difficulty, the rubber sealer was discarded and the electrode diameter was increased to match the membrane diameter (2.0"). During cell assembly the electrodes and membrane were sandwiched tightly between the steel backup plates (diameter 2.14") and held by a C-clamp while the juncture was sealed around the circumference with a gas-tight epoxy cement. The cemented "sandwich" was then fitted into the gas chamber O-ring seals which were greased with silicone to confine each gas to its proper compartment. (See Figure 25.)

The elimination of the difficulties described above revealed another problem concerning preconditioning of the electrode-catalyst-membrane assembly. Conclusion of the present experimental period precluded selection of a best preconditioning technique, but the nature of the problem and the preliminary attack on it can be described.

During membrane manufacture, the sintering operation dehydrates the membrane. The prefabricated electrode matrix and platinum black are also dry so that initial cell resistance may be very high, occasionally reaching values as high as  $10^6$  ohms. During earlier work with the fuel cell, rehydration was permitted to occur during initial cell operation on short circuit, during which current density rose slowly from very low values. However, it was possible to observe after Run No. 25 that occasionally a

presumably operable cell assembly would not begin to function, or would not rise to the expected performance.

Runs 19, 20 and 26, 27 compared membranes used as is with membranes exposed 24-48 hours to an atmosphere at 100% relative humidity to attempt a rehydration process before assembling the cell. No substantial effect was observed.

Runs 37 and 38 employed a brief (10 sec.) immersion of the entire back-up plate-electrode-membrane sandwich in water, followed by removal of visible water from the back-up plate holes by an air stream. The superior cell performance during these runs suggests that hydration of the electrode-catalyst-membrane interface may be particularly important in cell behavior. Figure 26 compares the improved rate of cell current buildup in Run 37 to the unpreconditioned behavior of Run 35.

#### 2.5.2 Fuel Cell Operation

Table 14 gives data obtained from fuel cell operations. The sharp improvement in general cell performance in the later runs requires conclusions based on earlier runs to be viewed with caution as discussed above.

In the fuel cell program, 4 runs showed stable cell operation at 95-97°C. Two of these runs (37 and 38) used assemblies preconditioned by brief water immersion (suggesting that the condition of the electrode-catalyst-membrane interface may be a crucial factor at high temperatures) and showed a lower level of operation at 97°C and 90°C.

The other 2 runs (11 and 25) both used a membrane in which presintered zirconium phosphate, phosphoric acid, and "Zeolon H" were used in equal proportions; and both runs showed optimal operation at 97°C. Figure 27 compares at a convenient current density cell voltages in these runs with those of several other runs.

It should be noted that Runs 33, 34 and 35 employ the same type of membrane as Runs 11 and 25. In contrast to the latter two runs, Runs 33, 34 and 35 all show decreased or poor performance at 90°C and no performance at 95°C. The membranes used in Runs 11 and 25 were pressed

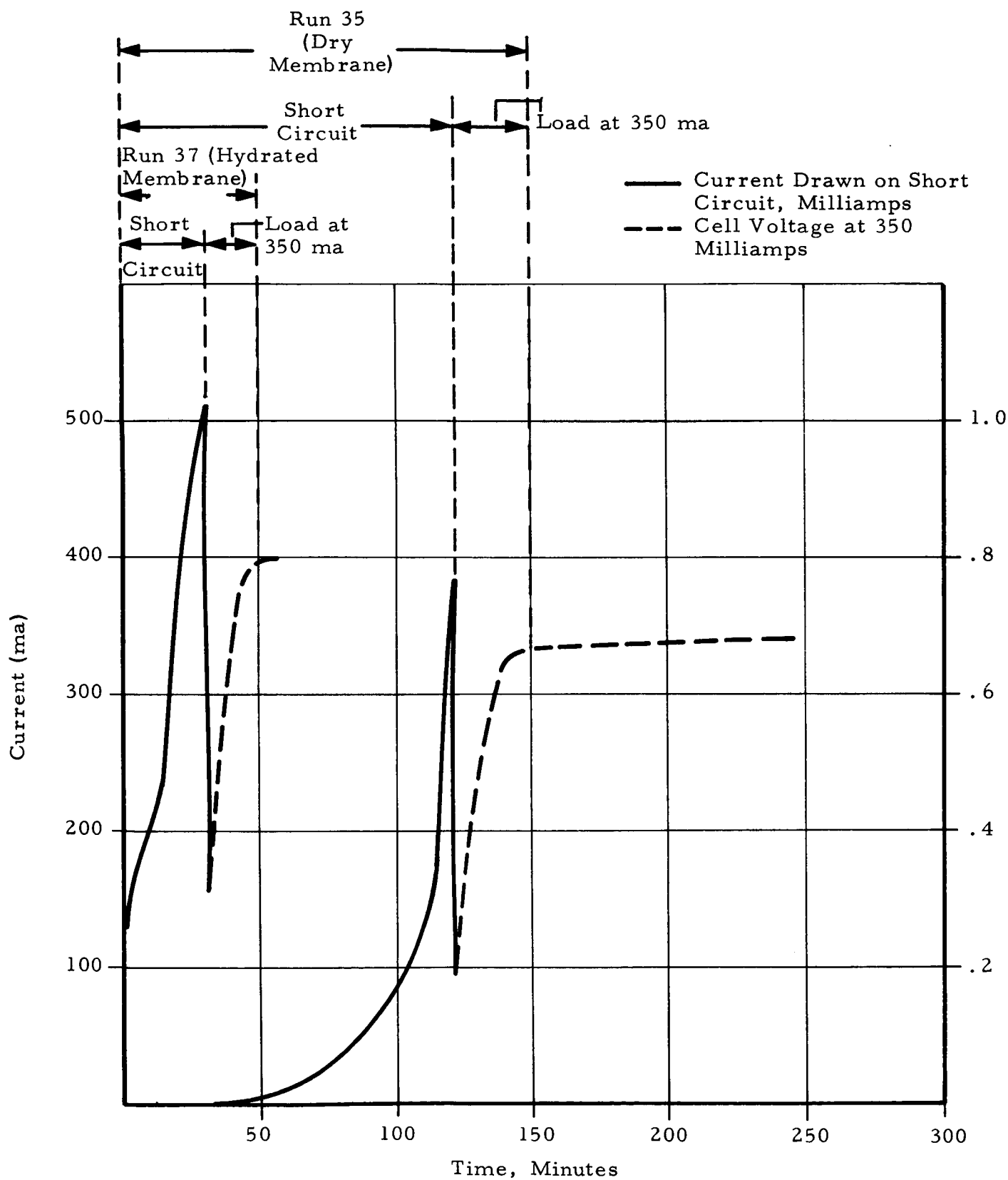


Figure 26. Current Build-up on Circuit in the Inorganic Membrane Fuel Cell During the Conditioning Period.

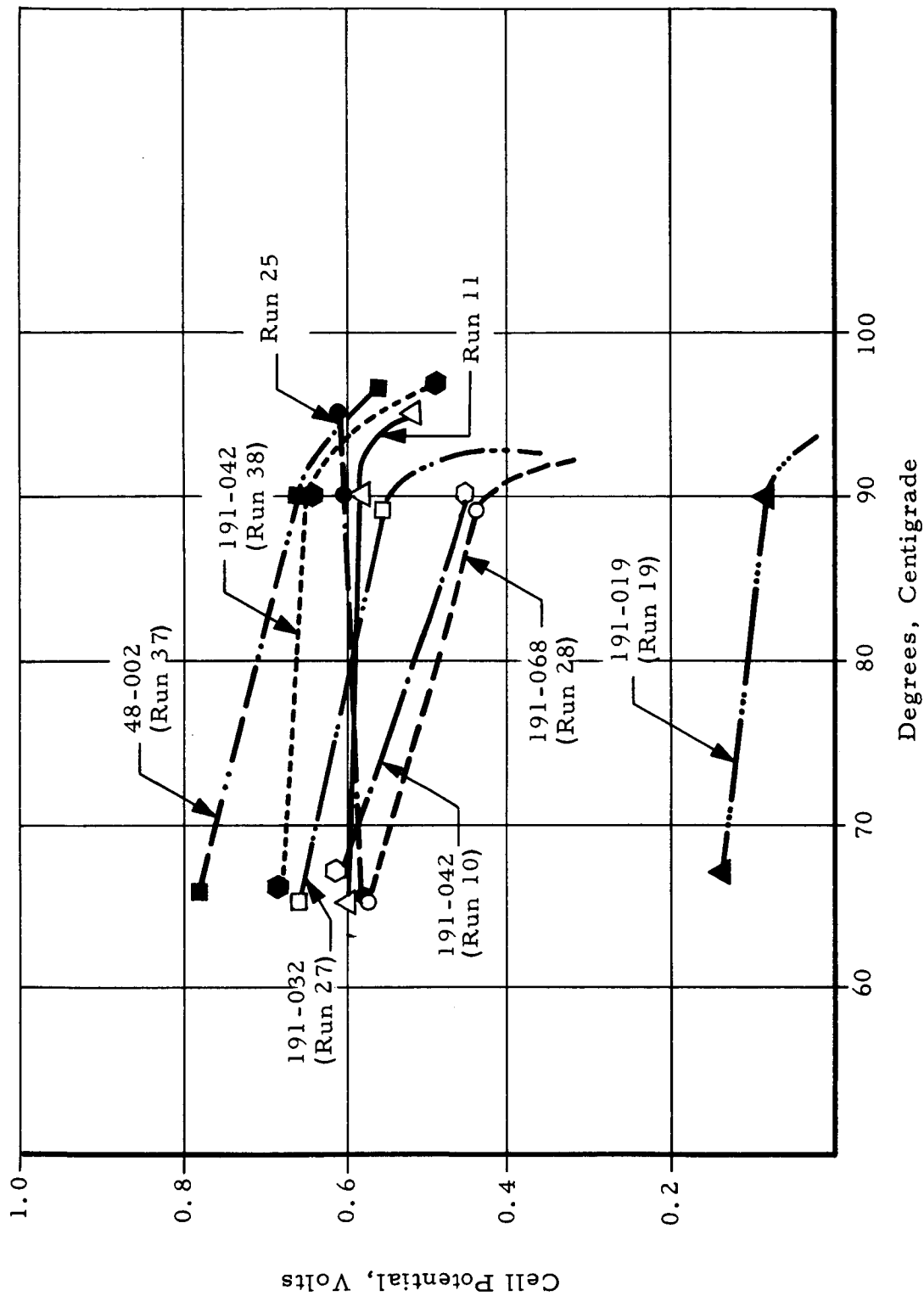


Figure 27. Effect of Temperature on Inorganic Membrane Fuel Cell Operation at 20 Ma/Cm<sup>2</sup> Current Density

and sintered within a few days after preparation, by ball-milling and oven-drying the membrane material. The membranes used in Runs 33, 34 and 35 were pressed and sintered after storage of the material in a sealed glass jar for approximately 90 days. Possibly a slow chemical alteration of the unsintered material is responsible for the behavior of the membranes made from the stored material.

The evidence although inconclusive, warrants the observation that not only the condition of the electrode-membrane contact but also the chemical nature of the membranes may be a factor in successful cell operation at 97°C.

As above, Runs 33, 34 and 35 used membranes of the same composition. They differed in sintering temperatures, which ranged from 250°C to 750°C. A membrane of a different composition sintered at 350°C was used in Run 37. Table 15 compares membrane sintering temperature and current densities at 65°C for all runs in which electrode diameter or membrane composition do not have a major influence on current density. (Runs 37 and 38 are included although they differ from other runs by a preconditioning immersion in water, which possibly has an independent effect on current densities.)

The data suggests that lowered membrane sintering temperature may improve fuel cell operation.

Figures 28 and 29 show polarization curves whose slopes indicate virtually identical internal cell resistances, but whose total current carrying capacities at a given voltage vary. For instance:

<u>Run</u>	<u>Temp. °C</u>	<u>Resistance, Ohms</u>	<u>Current Density<sub>2</sub> 0.5 Volts, Ma/Cm<sup>2</sup></u>
33	65	0.42	50.0
33	90	0.38	25.2
37 (1st day)	65	0.33	63.2
37 (2nd day)	66	0.35	51.4

Another and perhaps related, peculiarity of these polarization curves involves the absence of activation polarization in many cases where the open-circuit potential falls below 0.9 volts., (e.g., Figure 30). In a majority of fuel

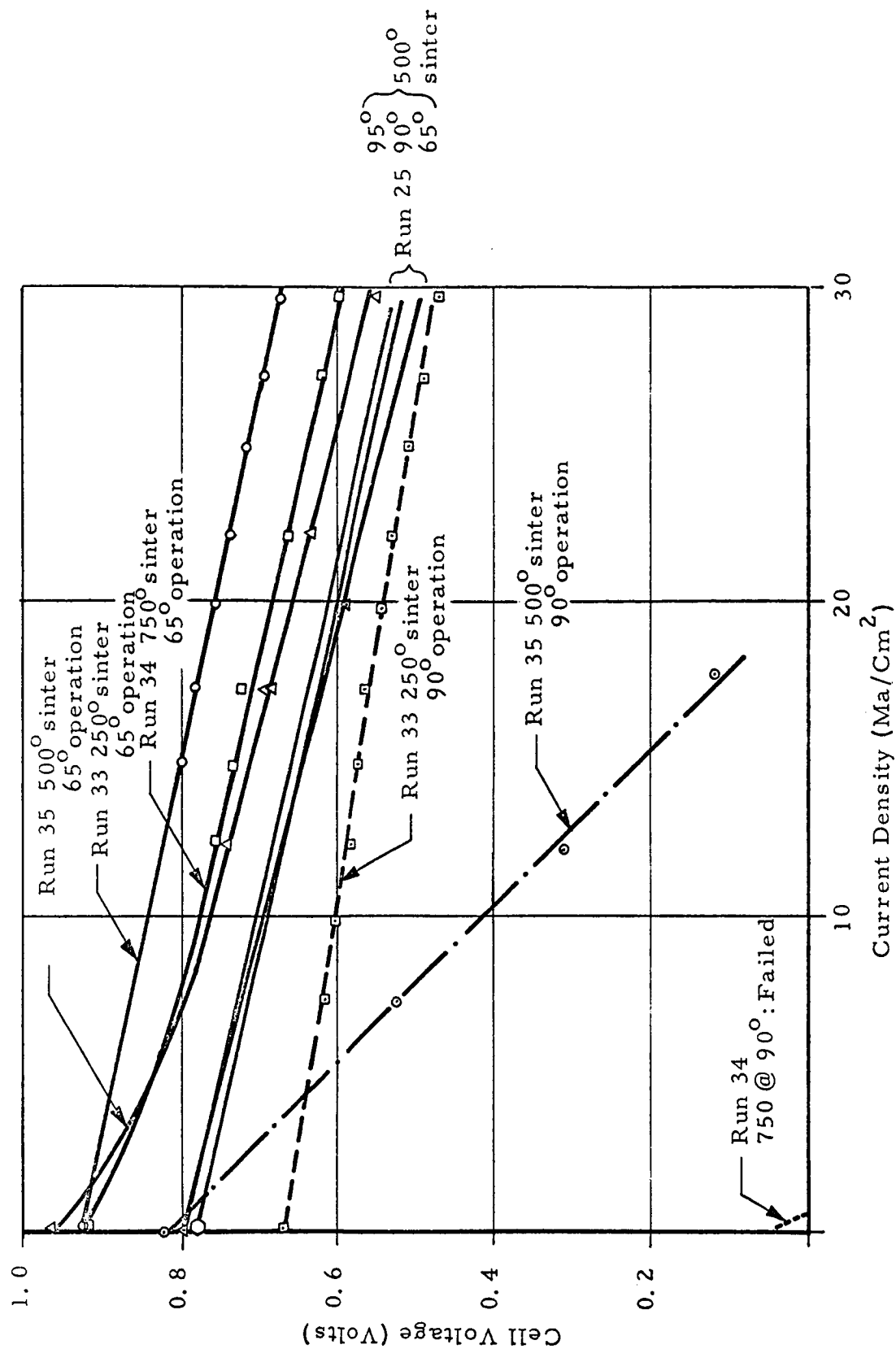


Figure 28. Polarization Curves for the Inorganic Membrane Analytical Fuel Cell Employing Membrane 191-050.

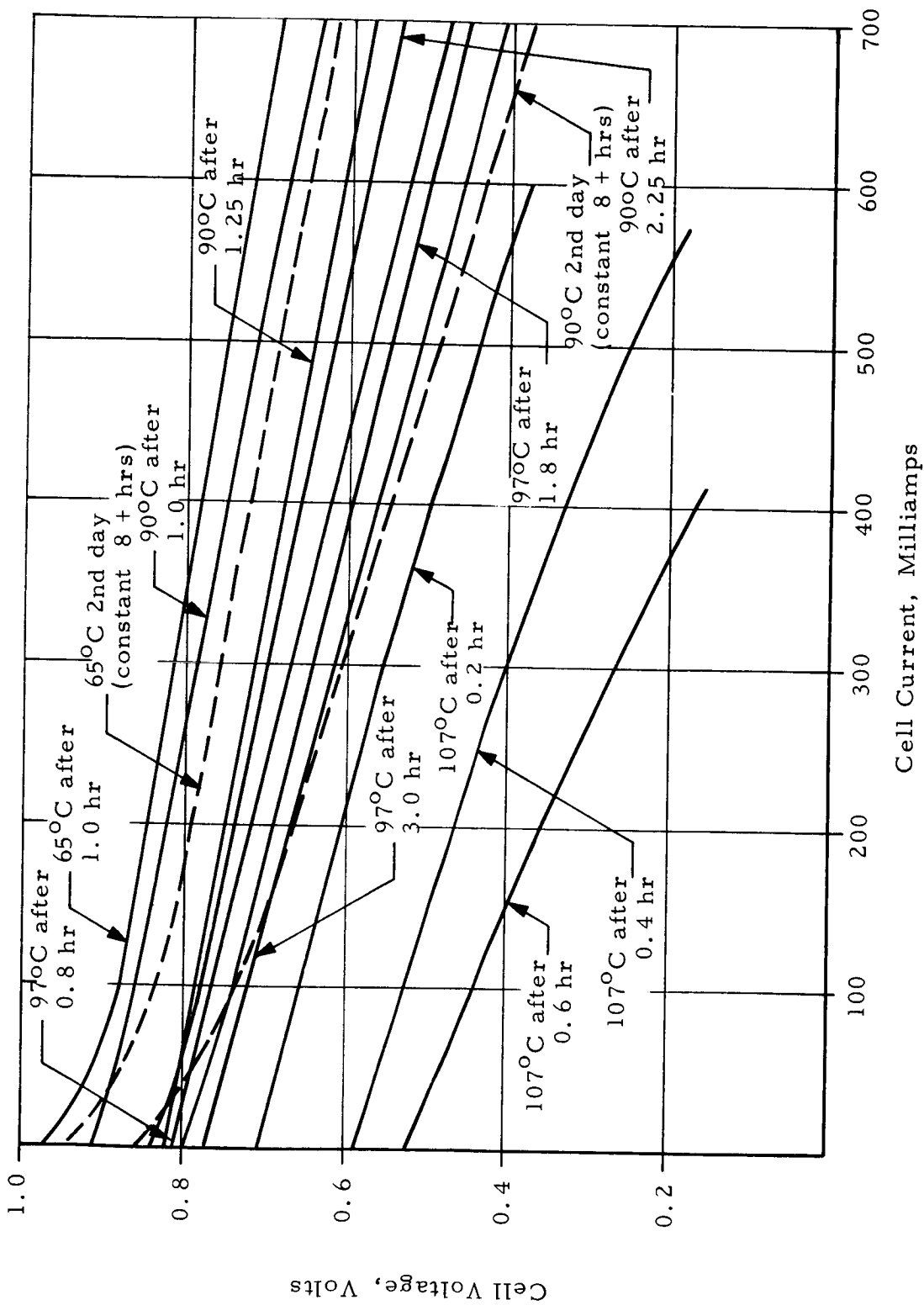


Figure 29. Polarization Curves for the Inorganic Membrane Analytical Fuel Cell Employing Membrane No. 48-001 (Run 37).



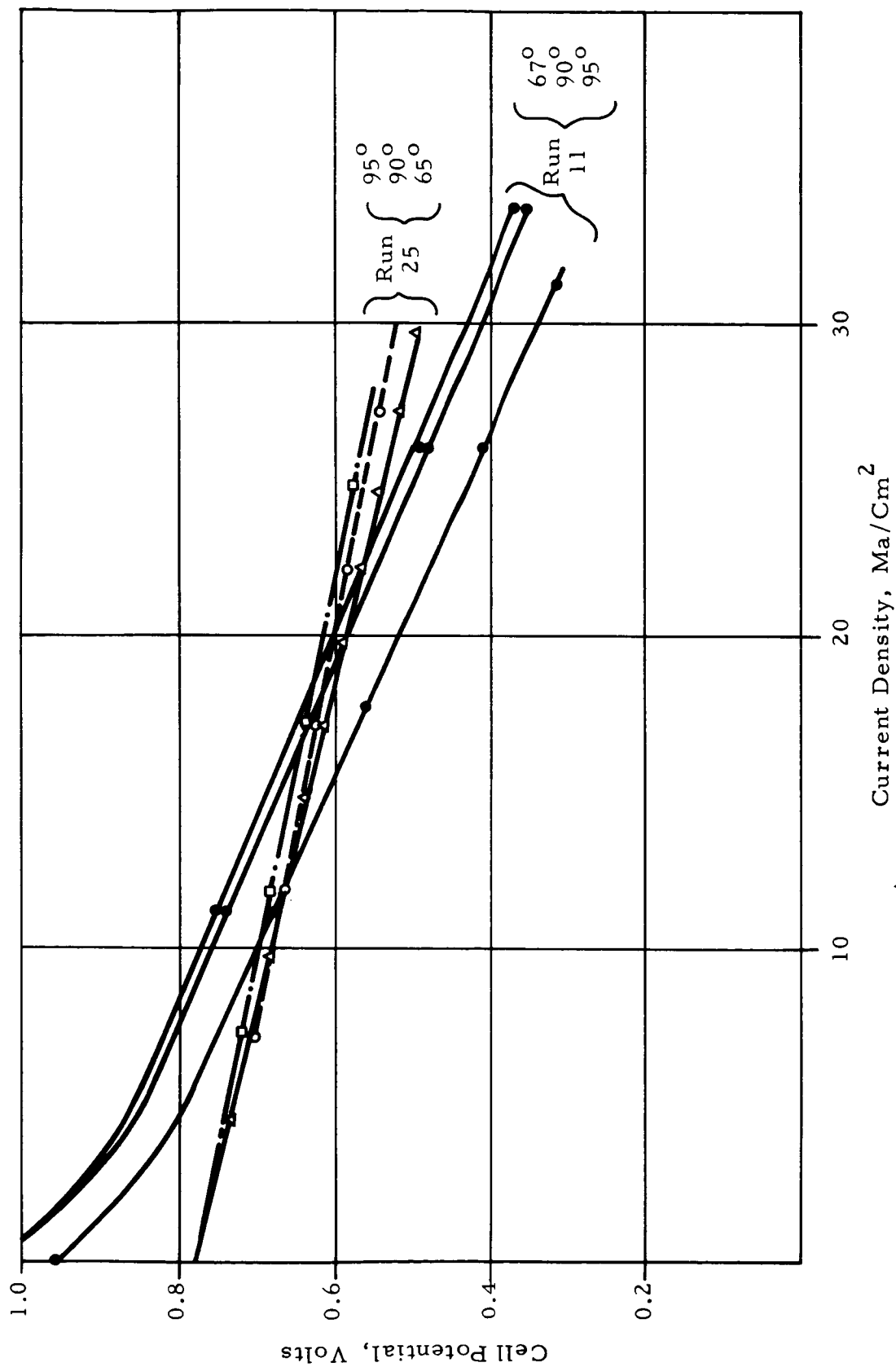


Figure 30. Polarization Curves for the Inorganic Membrane Fuel, Showing the Effect of Modified Electrode-Membrane Assembly (Membrane: 191-050)

fuel cell assemblies showing an open circuit potential above 0.9 volts, activation polarization occurs (i. e. the polarization curve departs from a straight line as the current density approaches zero). Presumably electrode phenomena such as flooding are responsible for these effects.

The effect of composition on fuel cell operation has been discussed briefly. In general, the variety of factors influencing fuel cell performance has made evaluation of small effects due to membrane composition difficult thus far. However, some additional observations merit comment.

A. The Effect of Eliminating "Zeolon H" from the Membrane:

Run 19 using membrane 191-019 containing 50%  $\text{ZrO}_2$  and 50%  $\text{H}_3\text{PO}_4$ , showed an average 3.1 fold increase in cell resistance over that observed with "normal" membrane compositions, as shown in Table 16 providing a measure of correlation between fuel cell and conductivity data.

B. The Effect of Inert Fibers in the Membrane:

Comparison in Table 16 of Runs 10, 11, and 28 show that addition of 5% zirconium oxide fibers has little effect on cell resistance. However, the addition of 5% alumino-silicate fibers increased cell resistance approximately 1.6 fold, as shown in Table 17. This is in agreement with the results reported in Section 2.3.

C. The Effect of Eliminating  $\text{ZrO}_2$  from the Membrane:

In membrane 200-011, zirconia was omitted from the composition, the material being 1.3 parts of "Zeolon H" and 1.0 parts of concentrated phosphoric acid. This membrane had intermediate strength (1300-1600 psi) and in the fuel cell, developed a current density at 0.5 volts of  $5.7 \text{ ma/cm}^2$ . Cell resistance was 2.74 ohms; about 5-fold greater than normal membranes in comparable runs (nos. 34, 37, 38, etc.). The run demonstrated a moderately conductive membrane with properties less satisfactory for fuel cell operation than membranes containing zirconia, "Zeolon H," and phosphoric acid.

## REFERENCES

1. Anon., Chemical and Engineering News (16 Oct 1961) pg 40.
2. Astropower Laboratories, Project No. 8017-1.
3. "Investigation of Zeolite Membrane Electrolytes for Fuel Cells," Astropower, Inc., Report 108-Q1 NASA Contract NAS 7-150 (9-1-62) pp 2-12.
4. "Investigation of Zeolite Membrane Electrolytes for Fuel Cells," Astropower, Inc., Report 108-M4 NASA Contract NAS 7-150 (10-7-63) p 1.
5. "Investigation of Zeolite Membrane Electrolytes for Fuel Cells," Astropower, Inc., Report 108-M6 NASA Contract NAS 7-150 (12-7-63) p 3.
6. "Investigation of Zeolite Membrane Electrolytes for Fuel Cells," Astropower, Inc., Report 108-M7 NASA Contract NAS 7-150 (1-7-64) p 2.
7. "Investigation of Zeolite Membrane Electrolytes for Fuel Cells," Astropower, Inc., Report 108-Q2 NASA Contract NAS 7-150 (12-18-62) pp 2-26.
8. "Compact Fuel Cell," Astropower, Inc., Proposal A61108 (Dec. 1961).
9. "Investigation of Zeolite Membrane Electrolytes for Fuel Cells," Astropower, Inc., Proposal A62026 (Mar. 1962).
10. Kraus, K. A., Phillips, H. O., Carlson, T. A., Johnson, T. S., Proc. International Cont. Geneva (1958) p 1832.
11. Hamlen, R. P., J. Electrochem. Soc. 109, 746-749.
12. Kingery, W. D., "Fundamental Study of Phosphate Bonding," J. Amer. Ceram. Soc. 33, (8) 239 (1950).
13. Thomas, T. L., and Mays, R. L., "Separations with Molecular Sieves," Physical Methods in Chemical Analysis, IV (1961) pp 45-96.
14. Keough, A. H., and Sand, L. B., J. Am. Chem. Soc., 83, 3536 (1961).
15. Souder, W. and Paffenbarger, G. C., "Physical Properties of Dental Materials," Nat. Bur. Standards (U.S.) Circ., No. 433 (1942).
16. Ryshkewitch, E., "Oxide Ceramics," Academic Press, New York (1960).

17. "Investigation of Zeolite Membrane Electrolytes for Fuel Cells," Astropower, Inc. Report 108-Q3 NASA Contract NAS 7-150 (3-18-63).
18. "Investigation of Zeolite Membrane Electrolytes for Fuel Cells," Astropower, Inc. Report 108-M2, NASA Contract NAS 7-150 (8-7-63).
19. Cochrane, W. G. and Cox, G. M., Experimental Designs, Second Edition, John Wiley & Sons, New York (1962).

APPENDIX A

STANDARD METHOD FOR PREPARATION  
OF INORGANIC MATERIALS

## APPENDIX A

### STANDARD METHOD FOR PREPARATION OF INORGANIC MATERIALS

In order to produce satisfactory inorganic membranes for fuel cell application, it was necessary to rigidly standardize all procedures used in the preparation of membrane materials. This was accomplished by the application of adequate quality control practice to all phases of membrane preparation to produce membranes of uniform physical, electrical and chemical characteristics. The following procedures were established:

#### A. Ball Milling Membrane Compositions

Clean grinding jar, cover, gaskets and grinding balls by washing thoroughly. Place balls in grinding jar, cover with water, secure cover and grind for 15 minutes. Empty mill and rinse with clean water. Repeat twice. Place grinding jar, cover and balls in oven at 120°C until completely dry.

The level of the grinding balls should be just above the midpoint of the jar (55% of the jar volume). For small grinding jar (1 gallon and under) use 1 inch and smaller grinding balls. A gradation of sizes is preferable.

Weigh raw materials carefully and accurately so as to avoid spillage or contamination. Keep the grinding jar covered at all times during weighing in order to avoid pick up of airborne dust. Add dry materials to the grinding jar first, liquids last.

Milling time must be exact to a total variation of five minutes. After grinding empty the milled materials and balls through an 8 mesh screen into a clean container. Screen the slurry through an 80 mesh screen. Place the screened slurry in suitable containers for drying.

Wash, dry and return all equipment to storage.

## B. Mixing Membrane Compositions

As all of the materials presently used in the preparation of inorganic membranes were finally divided (less than 10 microns ultimate particle size) grinding in a ball mill was unnecessary. Accordingly, the results of mixing raw materials in a high speed blender were compared with ball mill preparation and it was found that satisfactory results were obtained. As a result ball milling was discontinued after the early part of the investigation and replaced with mixing in a Waring Laboratory Blendor for 15 minutes. Preparation of inorganic membrane materials by mixing not only greatly reduces preparation time and permits the preparation of large numbers of samples, but also offers the advantage of being able to introduce materials into the composition without significantly altering their physical form. Fibers, for example, can be added to the mixture by this means whereas ball milling largely destroys fiber structure due to the grinding action of the media.

When particle size reduction was desired, a combination of the two techniques was used, especially when fibers or similar materials were to be added to the composition. In these cases, ball milling was used to grind the raw materials to the desired degree of fineness and the fibers or other additives were then introduced into the compositions by high speed mixing.

## C. Preparation of Membrane Materials for Compaction

The dried materials were crushed with a porcelain mortar and pestal and then screened through a 32 mesh screen. The fines were then removed from this material by screening over an 80 mesh screen resulting in a -32 mesh +80 mesh product. This size granulation was chosen because of the large diameter thin discs being pressed. Proper granulation is essential to uniform die filling and the avoidance of air entrapment which results in substandard quality of the pressed compact.

#### D. Compacting Membrane Materials

The membrane materials were pressed into 2 in. diameter 0.030 in. thick membranes using Carboloy dies and punches. A very thin film of kerosene was used as a die and punch lubricant. During pressing, the die was arranged in the hydraulic press so as to apply pressure to both the top and bottom punches, floating the die cavity. This resulted in very uniform pressing and the production of sound membranes. Figure 31 shows the die and press used for making inorganic fuel cell membranes.

After pressing, the compacted materials were quite fragile and care had to be used to avoid cracking, breakage or distortion. The membranes were transferred to a flat firing plate by means of a wide spatula. After compacting, the pressed membranes were stored in a drying oven at 110°C until they could be loaded in the furnace for sintering.

#### E. Sintering Inorganic Membranes

The pressed membranes were sintered by loading them on smooth, flat refractory surfaces and placing them in the electric furnace. Refractory setters commonly used for firing ceramic wall tile were found to be highly satisfactory for this purpose. Nine membranes could be loaded on each setter and the setters could be stacked four high in the sintering furnace so as many as 36 membranes could be sintered at one time. More important, the setters provided a constant thermal load (mass) for the furnace which increased the uniformity of sintering within a given run and from load to load. After sintering at the desired temperature and time, the furnace was allowed to cool to 110°C and the refractory setting and sintered membranes were removed. The automatically controlled sintering furnace is shown in Figure 32.



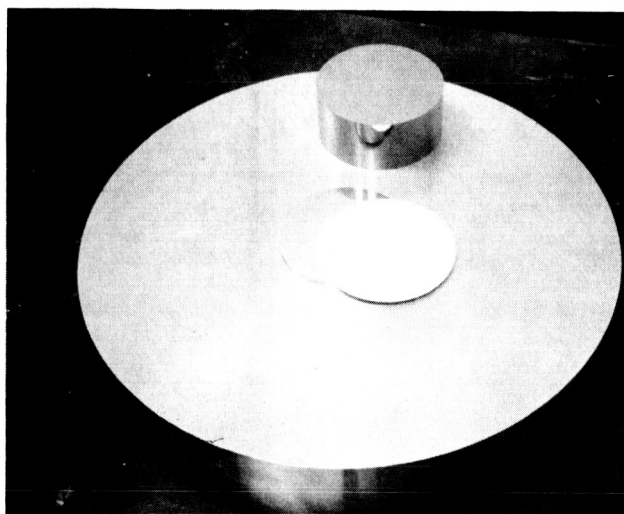


Figure 31. Mold and Hydraulic Press Used for Cold Pressing Inorganic Fuel Cell Membranes

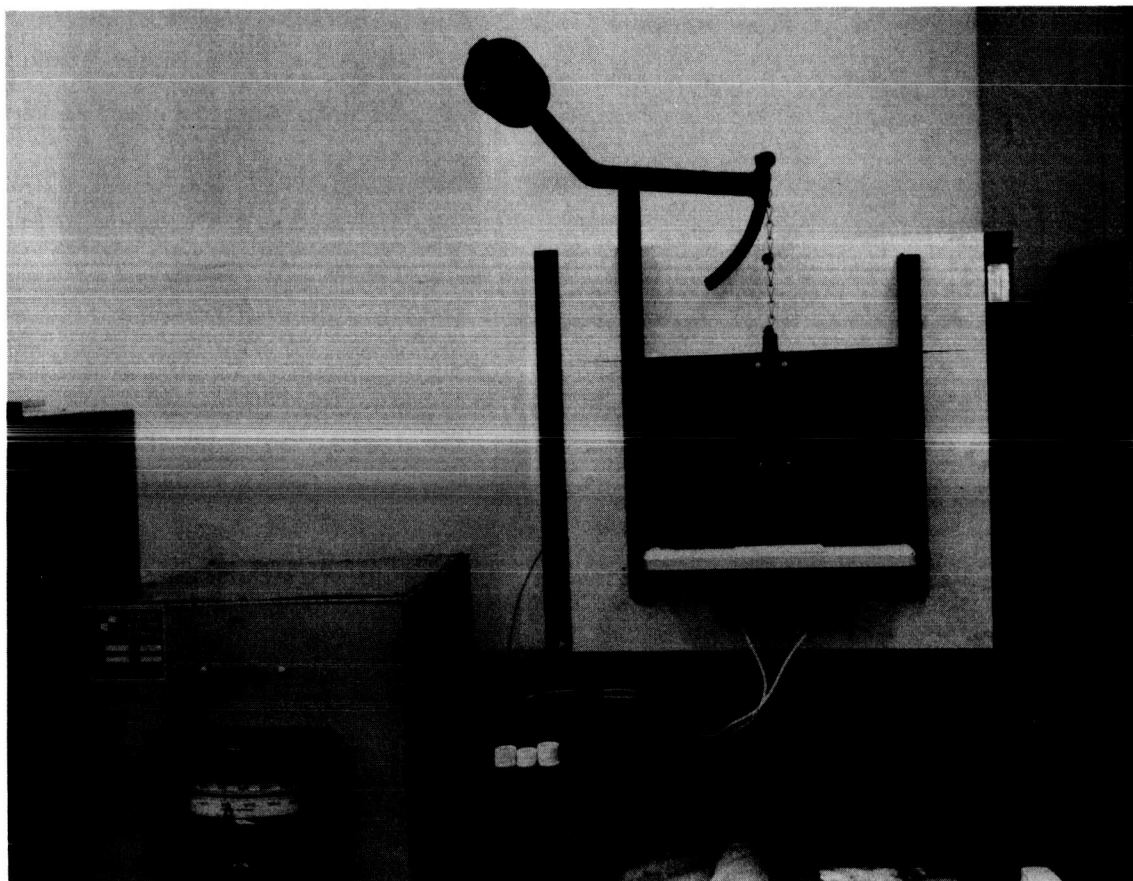


Figure 32. Sintering Furnace for Inorganic Fuel Cell Membranes

APPENDIX B

TRANSVERSE STRENGTH MEASUREMENTS

## APPENDIX B

### TRANSVERSE STRENGTH MEASUREMENTS

Transverse strength or modulus of rupture was chosen as the measure of membrane strength. The reasons for the choice of this characteristic include the fact that modulus of rupture is a measure of both compressive and tensile strength and it is readily determined as compared to compressive strength or tensile strength. Transverse strength was also selected as the measurement for categorizing membranes for strength as the use of membranes in the fuel cell would subject them to transverse loading characteristics.

Modulus of rupture is calculated from the formula  $M = \frac{SC}{I}$  where  $M$  is the modulus of rupture,  $S$  is the maximum bending moment,  $C$  is the distance to the fiber carrying the greatest stress, and  $I$  is the moment of inertia. Applying this equation specifically to a rectangular prism it becomes  $M = \frac{3Wl}{2bh^2}$  where  $M$  is the modulus of rupture (transverse strength) in lbs/in<sup>2</sup>,  $W$  is the load in lbs,  $l$  is the distance between the knife edges in inches,  $b$  is the specimen width in inches, and  $h$  is the thickness of the specimen in inches. The apparatus originally designed and constructed for measuring transverse strength is shown in Figure 33. Specimens having dimensions of 4x1x0.030 in. were cut from experimental membranes and supported on two knife edges spaced 1.5 inches apart on one pan of a double beam trip balance. By adding water to the beaker placed on the opposite pan of the balance at a fixed rate of 45 grams/min, a load increasing at a constant rate was applied at the center of the membrane. Water flow was stopped at the break point, and the weight required to break the test specimen was determined. The transverse strength was calculated from the weight required to break the sample and the observed physical dimensions of the test specimen.

The modulus of rupture data which was obtained was reported along with standard deviation from the mean. Standard deviation gives the interval in which the true average probably lies 68% of the time.

Although adequate for the preliminary screening of compositions for strength, it was found that this test equipment introduced numerous variables and errors. Accordingly, the test method was revised so the variables

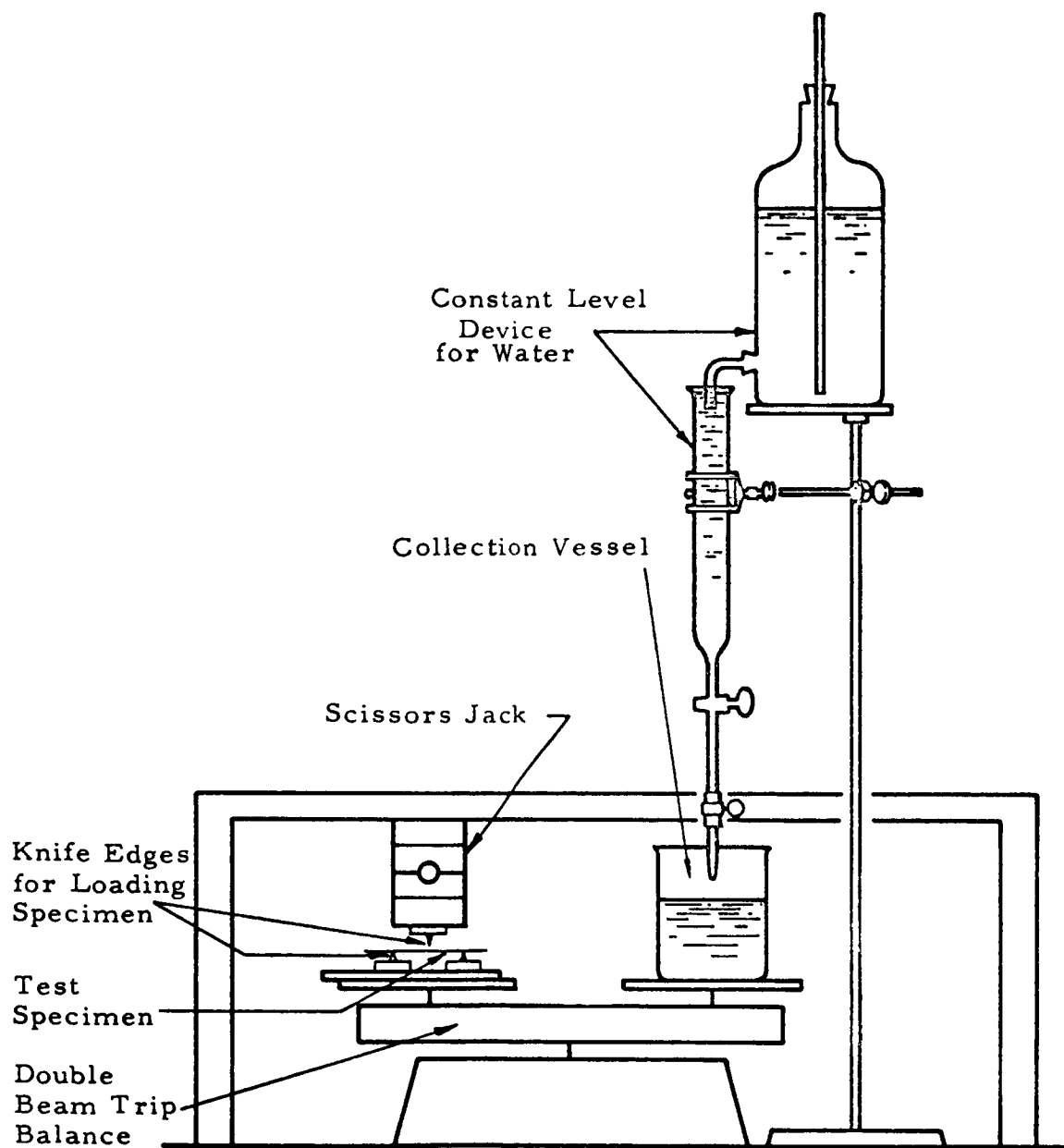


Figure 33. Apparatus for Measuring Transverse Strength of Zeolite Membranes

could be controlled and the errors substantially reduced. The revised transverse strength apparatus is shown in Figure 34. It consisted of a rigid supporting beam holding the two sample supporting knife edges. These knife edges were attached to the beam so as to provide a 1 inch test span. The third knife edge is a 1/8 inch drill rod attached to a wire saddle. A plastic beaker hung from the wire saddle is used to catch the water which is added at constant rate, loading the test piece until it breaks. The redesigned test equipment was checked for squaredness of loading and calibrated using samples of 96% aluminum oxide of known strength.

Along with the redesign of the transverse strength test equipment substantial improvements were also made in the preparation of transverse strength samples. The improved method of sample preparation consisted of cementing the experimental membrane to a porous ceramic tile using a 1:1 mixture of rosin and beeswax. The surface of the tile was coated with a thin, uniform layer of the cement and the experimental membrane was then pressed against the wax coated tile. Upon cooling, the membrane was firmly held to the tile. The transverse strength samples were cut from the experimental membrane using a 0.012 in. thick, bonded diamond wheel. The wheel was mounted on a Hamco metal saw equipped with a power infeed. Water containing a small amount of soluble oil was used as a coolant. Transverse strength samples prepared by this technique were free from edge chipping and cracking and could be cut precisely so that exact dimensional specifications could be maintained. Three 1/2 in. wide samples were cut from each experimental membrane disc making it possible to readily increase the number of transverse strength measurements which could be made for any given composition. After cutting, the wax was removed by soaking the assembly in acetone. The transverse strength samples were washed in clean acetone and oven dried at 150°C for one hour prior to testing.

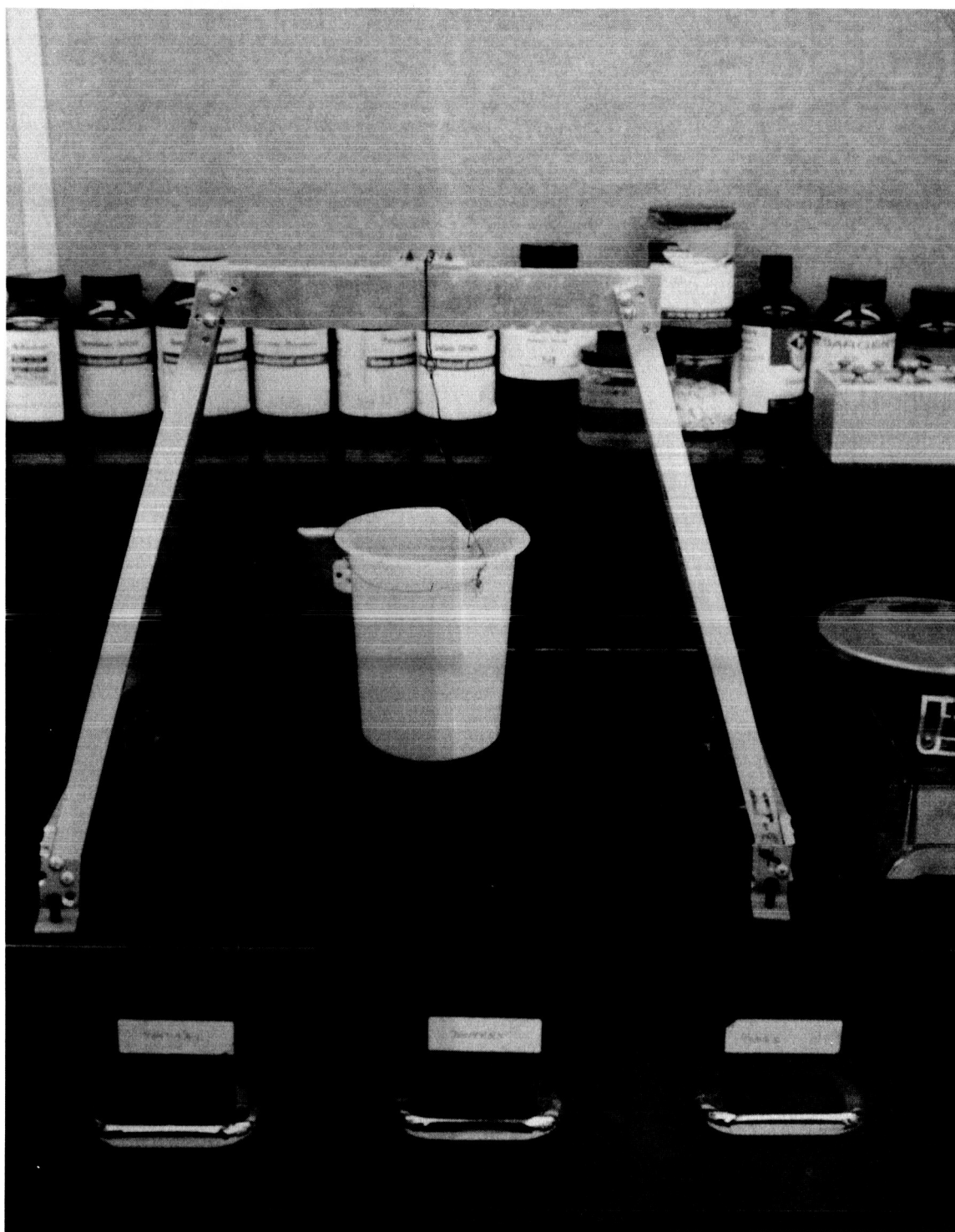


Figure 34. Improved Modulus of Rupture Test Apparatus

APPENDIX C

OPERATING PROCEDURE FOR FUEL CELL



## APPENDIX C

### OPERATING PROCEDURE FOR FUEL CELL

#### A. Cleaning and Assembly

1. Remove "O" rings and Teflon insulating inserts from the steel housings. Dislodge loose dirt with brush and/or air hose. Scrape off traces of hardened grease and/or epoxy resin. Clean the interior surfaces of the housings with acetone. Blow out gas inlets and outlets with the air hose.
2. Scrape epoxy resin from the steel electrode back-up plates. Clean holes in plate and plate surfaces with pipe-cleaners and acetone. Sand both surfaces of the plates lightly with emery cloth to insure good electrical contact with electrodes and with cell leads.
3. Position cleaned Teflon inserts, O-rings, and central Teflon gasket.
4. Assemble the electrode-membrane combination as follows:
  - a. Cut with scissors two 2.0" diameter electrodes from American Cyanamid No. AA-1 membrane electrode materials.
  - b. Using one horizontal steel electrode back-up plate (diameter 2.14") as a support, place upon it the 2.0" ceramic membrane to be used in the fuel cell run. Sprinkle platinum black through a 200 mesh sieve to cover the membrane uniformly. ( $12-14 \text{ mg/cm}^2$ ) Cover the 2.0" membrane with one 2.0" electrode, followed by the other steel back-up plate, and invert the resulting sandwich. Remove the now-uppermost plate, sprinkle the exposed membrane surface in a like manner with platinum black, cover the treated surface with the other 2.0" electrode and replace the steel back-up plate. Clamp the sandwich with a C-clamp.

- c. Fill around the central grove of the "sandwich" with epoxy cement previously prepared in the following way: Mix well, equal parts of genepoxy 190 and versamid 140 and let stand at room temperature 4 to 6 hours (or at 90°C 2-4 min.) until the properly tacky consistency is achieved.
  - d. Allow the epoxy cement to harden (2-4 hours). If necessary, scrape off excess epoxy cement to permit the cemented sandwich to fit into the lower housing. Check the resistance of the assembly with a meter to insure the absence of shorts, etc.
5. If the electrode assembly is to be pre-conditioned by immersion, dip the back-up plate - electrode-membrane "sandwich" into distilled water (immersion time: 10 Sec.). After the immersion, remove the excess water from the holes in the back-up plates with an air stream and dry the assembly. Re-measure the resistance of the assembly, which will have been sharply decreased.
6. Connect the lower electrical lead to the lower back-up plate and insert the assembly into the O-ring seal in the lower housing. Fill the circumferential narrow aperture between assembly and housing with vacuum grease. Bring the upper housing to a position above the lower housing, thread the upper electrical lead through the coil spring and connect the lead to the upper back-up plate. Position the spring and lower the upper housing carefully into position, which operation will slightly compress the spring. Secure the housings with four (4) bolts and nuts.
7. Check the electrical lead exits through the copper T-fittings at the top of the copper tubing gas exit lines, to insure that the Teflon spaghetti insulation protrudes above the corks in the upper ends of the T-fittings. Seal the corks around with vacuum grease so that the exit gases will flow exclusively out the exit lines. Once again, check the cell resistance across the cell leads to guard against loose connections or invisible shorts between cell leads and copper tubing.

8. Submerge the cell in position in the sand bath (the air stream through the bath must be on) and clamp in position by the vertical copper tubing gas lines. Connect the gas inflow lines by copper fitting to the copper tubing lines leading from rotometers to cell.
9. Connect electrical leads to circuit diagrammed in Figure 35.
10. To begin operation of the cell, proceed as follows:
  - a. Turn on voltmeter, air and heater to sand bath, power supply (operates as a constant current device) and gas cylinders.
  - b. Set sand bath temperature controller and gas flowmeters to desired values.
  - c. Set the cell on short circuit across the ammeter (i. e., eliminate the constant current device from the circuit).
  - d. When the current generated by the cell on short circuit has built up to several hundred milliamperes (time required about 30 minutes in the case of preconditioned cells, about 2-3 hours or longer in unconditioned cells) put the constant-current device (Power designs, Inc.) into the circuit, setting the current at the desired level.
  - e. Permit the cell to rise to maximum voltage at the assigned current and proceed.

APPENDIX D

APPARATUS FOR MEASURING CONDUCTIVITY  
AND WATER ABSORPTION OF MEMBRANES

## APPENDIX D

### APPARATUS FOR MEASURING CONDUCTIVITY AND WATER ABSORPTION OF MEMBRANES

A controlled atmosphere thermobalance was constructed in order to carry out these experiments. Basically it consisted of a McBain balance employing a quartz spring. The membrane is suspended in a tube furnace. The balance system is isolated from the room air, and the water vapor content of the gas in the system is controlled. Thus, the temperature and humidity of the atmosphere can be independently varied, and the water adsorbed by the membrane can be measured as a weight change. A photograph of the apparatus is shown in Figure 36 and a functional diagram in Figure 37.

The gas containment system consists of two sections of 3-in. diameter pipe. The main portion is a length of copper pipe inside the furnace. Its heavy walls and high thermal conductivity aid in obtaining a uniform temperature in the furnace. A small copper thermocouple trace tube is silver-soldered inside the copper pipe. A movable thermocouple is placed in this tube so that the temperature at any point along the length of the furnace can be measured. This chromel-alumel thermocouple is connected, through an ice bath cold junction, to a Leeds & Northrup potentiometer. The lower end of the copper pipe is closed with a copper plate through which the gas inlet tube is connected. A gas exit is provided near the upper end of the copper pipe. The upper end of the copper pipe, above the furnace, is bolted to a section of 3-in. glass pipe. The upper end of the glass pipe is closed and contains a hook for the quartz spring. Condensation of water in this portion of the apparatus is prevented by the use of heating tapes and infrared heat lamps.

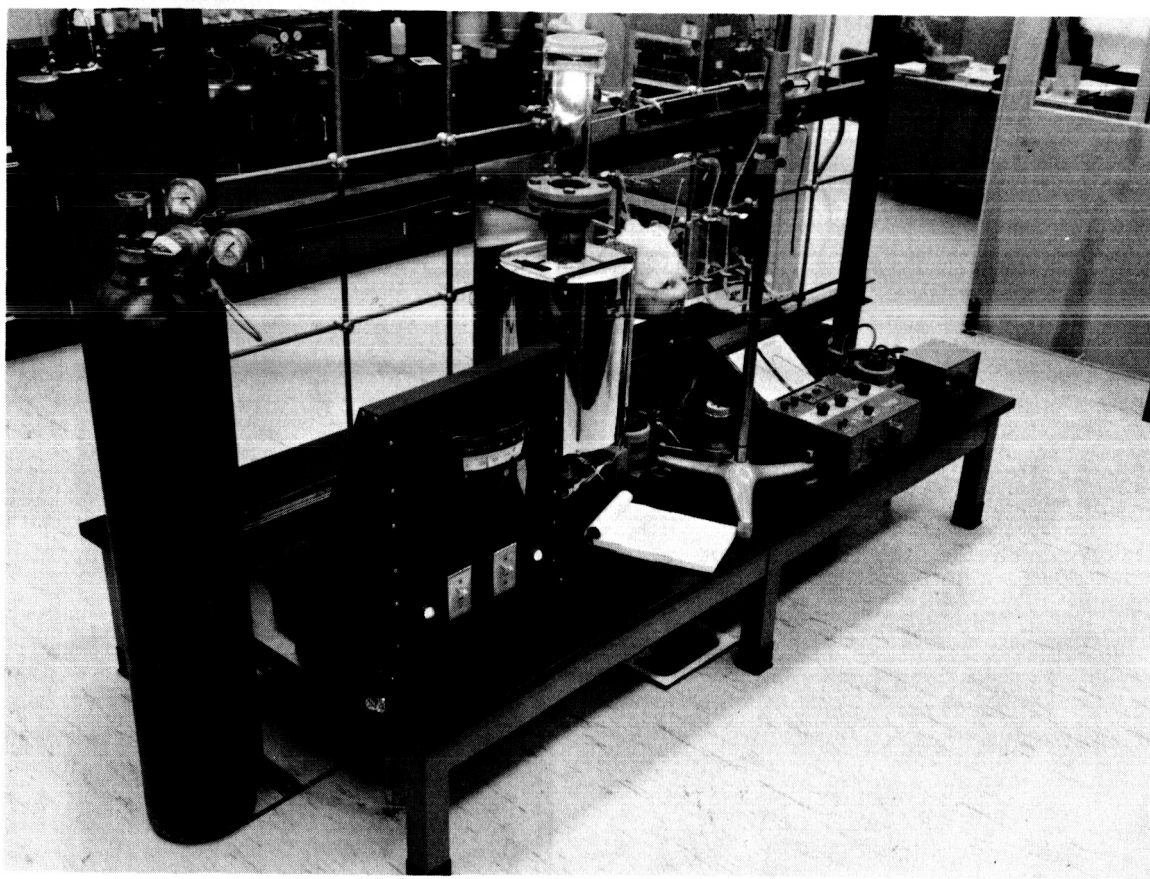


Figure 36. Controlled Atmosphere Thermobalance

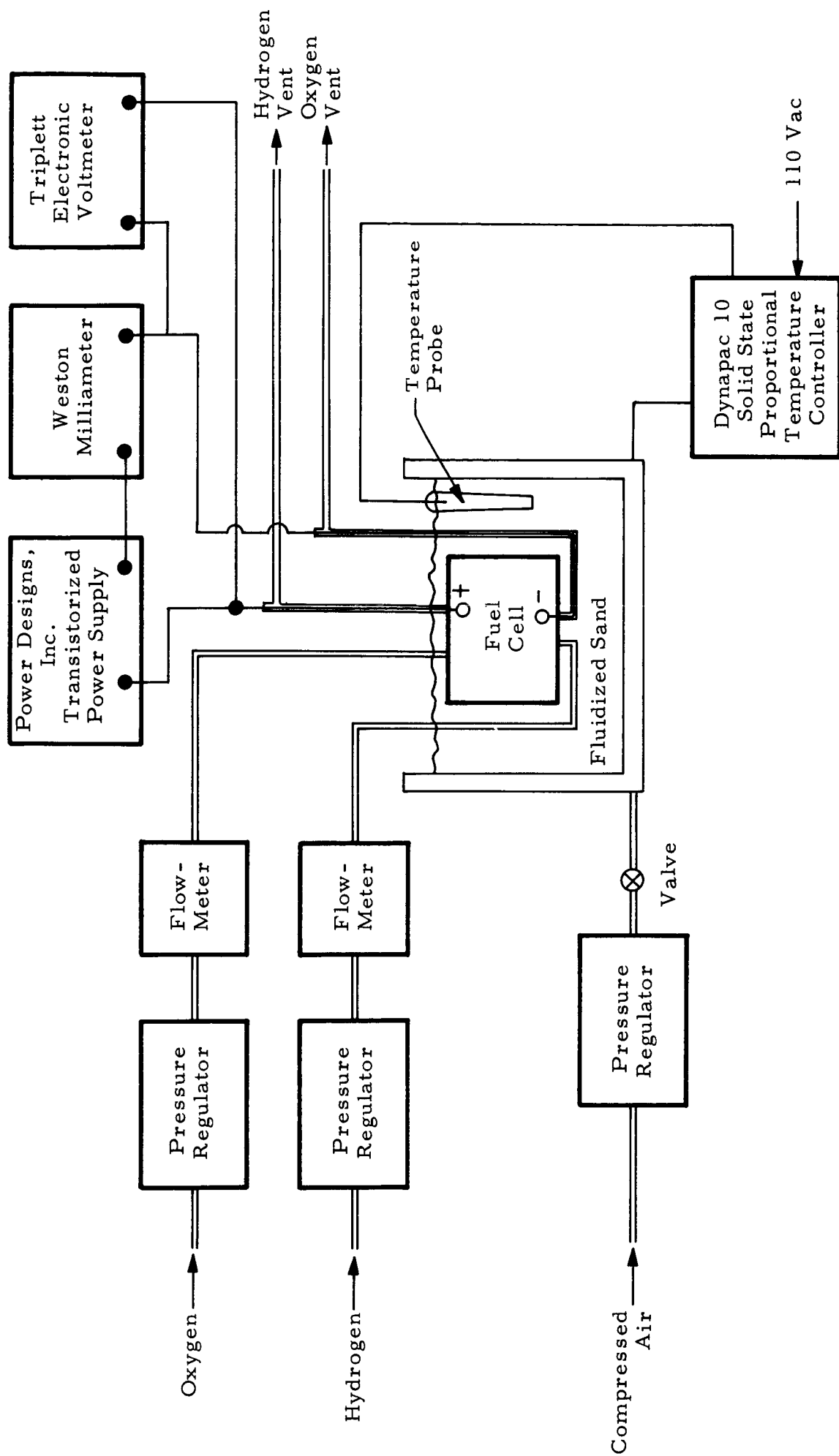


Figure 35. Electrical Circuit of the Inorganic Membrane Analytical Fuel Cell.

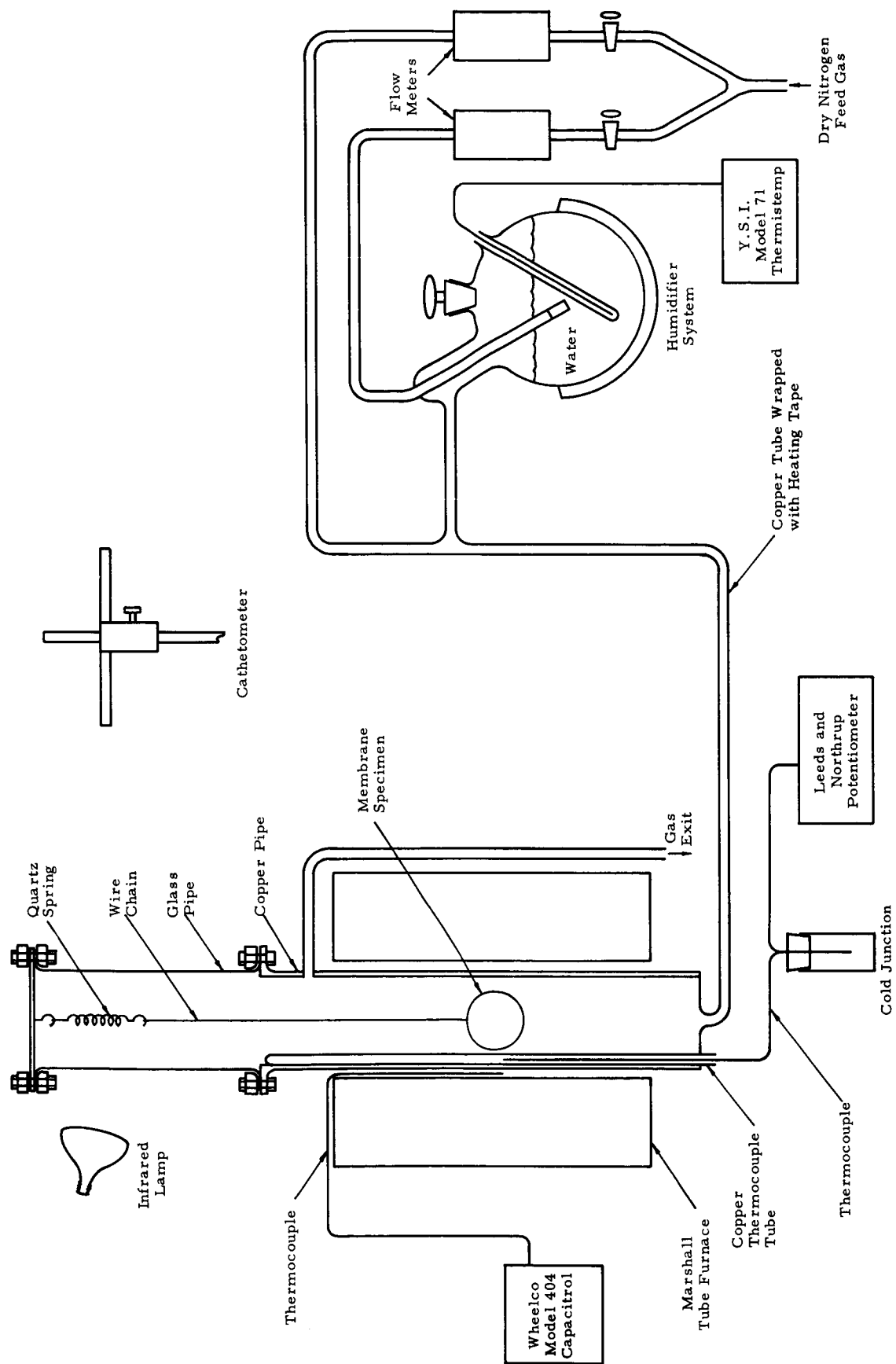


Figure 37. Controlled Atmosphere Thermobalance



APPENDIX E  
BASIC CONDUCTIVITY DATA

## APPENDIX E

### BASIC CONDUCTIVITY DATA

The apparatus employed for measuring water adsorption equilibrium was adapted in order to determine the influence of the partial pressure of water vapor upon the conductivity of membranes at various temperatures, including temperatures above 100°C. The glass assembly employed in the water adsorption apparatus was removed and replaced by a brass plate on the top of the tube furnace. By means of three threaded rods mounted in this brass plate, a series of electrodes was held in a horizontal position in the tube furnace. A photograph of the electrode assembly is shown in Figure 38, and the entire apparatus is shown in Figure 39. Temperature control and measurement, as well as humidity control, were accomplished as described previously.

The electrical resistance of membrane materials was measured by the alternating current bridge and auxiliary electronic equipment described in the body of this report. Platinized platinum electrodes were employed in the measurement of the alternating current resistance for all materials. Resistance was measured directly without using any capacity compensation at each of three frequencies (1000, 400, and 100 cycles/sec). For uniformity, all resistance measurements were reported at 1000 cycles/sec.

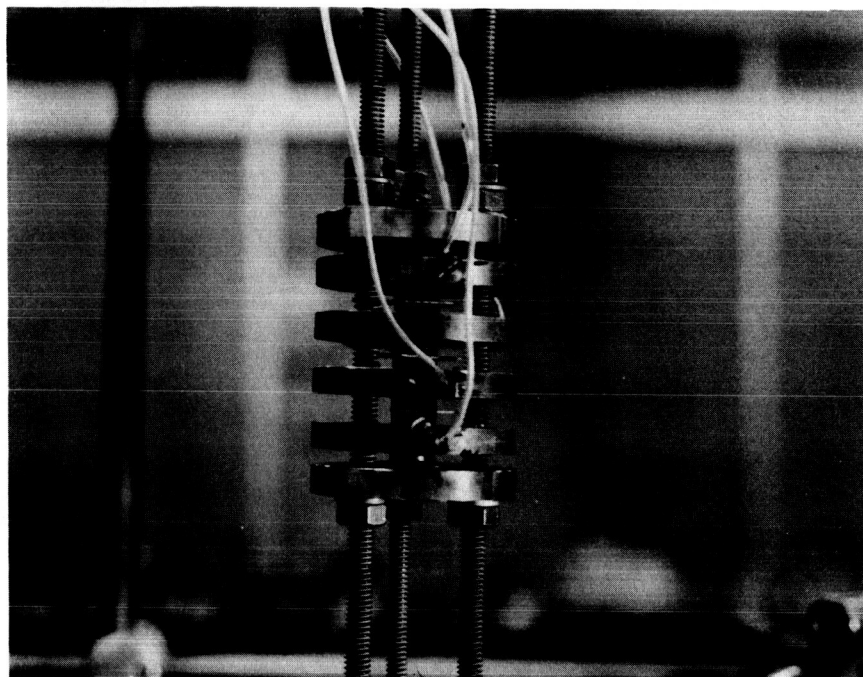


Figure 38. Electrode Assembly

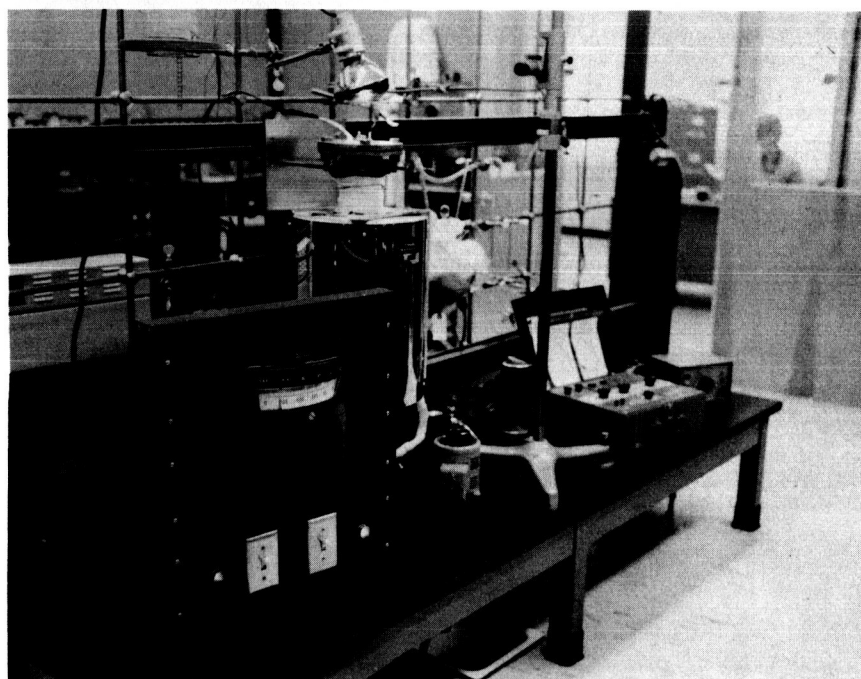


Figure 39. High Temperature Conductivity Apparatus

TABLE I

PROPERTIES OF ZEOLITE MATERIALS INVESTIGATED

<u>Manufacturer</u>	<u>Designation</u>	<u>Cation(s)</u>	<u>Effective Pore Diameter (AU)</u>	<u>Solution Stability (pH)</u>	<u>Maximum Thermal Stability (°C)</u>
Linde	3A	70% K <sup>+</sup> , 30% Na <sup>+</sup>	3	5-12	500
Linde	4A	100% Na <sup>+</sup>	4	5-12	700
Linde	5A	70% Ca <sup>++</sup> , 30% Na <sup>+</sup>	5	5-12	700
Linde	10X	70% Ca <sup>++</sup> , 30% Na <sup>+</sup>	9	--	500
Linde	13X	100% Na <sup>+</sup>	10	--	700
Linde	4A XW	(Improved type of 4A)			
Linde	AW-500	Not known	4-5	> 2.5	500
Norton	Zeolon H	H <sup>+</sup>	9-10	Acid-stable	775

TABLE II  
EVALUATION OF ORGANIC BINDERS

<u>Binder</u>	<u>Zeolite</u>	<u>Preparative Technique</u>	<u>Membrane Strength</u>
1. <u>Epoxy Resin</u>			
20% Hysol 4314	4A	Hot press	Strong
20% Hysol 4314	4A	Cold press-free sinter	Weak
16% Coraline 530	4A	Hot press	Moderate strength
30% G190/V140	4A	Cast and fired	Strong
15% G190/V140	4A	Cast and fired	Strong
10% G190/V140	4A	Cast and fired	Strong
5% G190/V140	4A	Cast and fired	Strong
10% G190/V140	4A	Cold press-free sinter	Strong
20% G190/V140	4A	Cold press-free sinter	Strong
10% G190/V140	13X	Hot press	Strong
2. <u>Teflon</u>			
10% Teflon	4A	Hot press	No strength
10% Teflon	4A	Cold press-free sinter	No strength
3. <u>Polyvinyl Chloride Resin</u>			
30% Pliovic S-50	4A	Hot press	No strength
4. <u>Phenolic Resins</u>			
30% Durez 1400	4A	Hot press	Fragile
5. <u>Silicone Resins</u>			
20% Eccosil 4712	4A	Hot press	No strength
20% D-C 2105A	4A	Hot press	No strength

TABLE III  
EVALUATION OF SILICATE BINDERS

<u>Binder</u>	<u>Mfr.</u>	<u>Zeolite</u>	<u>Preparative Technique</u>	<u>Membrane Strength</u>
20% "STAR" solution	(1)	4A	Hot press	Fragile
10% "GD" powder	(1)	4A	Hot press	Fragile
10% "GD" powder	(1)	4A	Gold press-free sinter	Fragile
10% Eccoceram E-21	(2)	"Zeolon H"	Cast and fired	No strength
20% Eccoceram E-21	(2)	"Zeolon H"	Cast and fired	No strength
40% Eccoceram E-21	(2)	"Zeolon H"	Cast and fired	No strength
10% Sauereisen #30	(3)	"Zeolon H"	Cast and fired	Weak
20% Sauereisen #30	(3)	"Zeolon H"	Cast and fired	Weak
40% Sauereisen #30	(3)	"Zeolon H"	Cast and fired	Weak
10% Eccoceram QC	(2)	"Zeolon H"	Cast and fired	No strength
20% Eccoceram QC	(2)	"Zeolon H"	Cast and fired	No strength
40% Eccoceram QC	(2)	"Zeolon H"	Cast and fired	No strength
"G" sodium silicate	(1)	"Zeolon H"	Cold press at 5 to 13 tons/in <sup>2</sup>	No strength

- 
- (1) Philadelphia Quartz Co.  
(2) Emerson and Cumings, Inc.  
(3) Sauereisen Cements Co.

TABLE III (CONT'D)  
EVALUATION OF SILICATE BINDERS

<u>Binder</u>	<u>Mfr.</u>	<u>Zeolite</u>	<u>Preparative Technique</u>	<u>Membrane Strength</u>
"G" sodium silicate	(1)	"Zeolon H"	Cold press plus 10% H <sub>2</sub> O at 5 to 13 tons/in <sup>2</sup>	No strength
"G" sodium silicate	(1)	"Zeolon H"	Cold press at 7 to 10 tons/in <sup>2</sup>	No strength
"G" sodium silicate	(1)	"Zeolon H"	Cold press plus 10 to 30% H <sub>2</sub> O at 8 tons/in <sup>2</sup>	No strength
"GD" sodium silicate	(1)	"Zeolon H"	Cold press at 5 to 8 tons/in <sup>2</sup>	No strength
"GD" sodium silicate	(1)	"Zeolon H"	Cold press plus 10 to 20% H <sub>2</sub> O at 8 tons/in <sup>2</sup>	No strength
"E" sodium silicate	(1)	"Zeolon H"	Cold press at 5 tons/in <sup>2</sup>	No strength
"E" sodium silicate	(1)	"Zeolon H"	Cold press plus 20% H <sub>2</sub> O at 5 tons/in <sup>2</sup>	No strength
"K" sodium silicate	(1)	"Zeolon H"	Cold press at 5 tons/in <sup>2</sup>	No strength
"K" sodium silicate	(1)	"Zeolon H"	Cold press plus 20% H <sub>2</sub> O at 5 tons/ft <sup>2</sup>	No strength
Kasil #1 potassium silicate	(1)	"Zeolon H"	Cold press at 5 tons/in <sup>2</sup>	No strength
Kasil #1 potassium silicate	(1)	"Zeolon H"	Cold press plus 20% H <sub>2</sub> O at 5 tons/in <sup>2</sup>	No strength

(1) Philadelphia Quartz Co.

TABLE IV

EFFECT OF TYPE OF ZIRCONIA USED ON TRANSVERSE  
STRENGTH OF INORGANIC MEMBRANES

<u>Zirconia Type</u>	<u>Composition</u>			<u>Transverse Strength After Sintering (psi)</u>
	<u>%ZrO<sub>2</sub></u>	<u>%H<sub>3</sub>PO<sub>4</sub></u>	<u>%"Zeolon H"</u>	
CP (Reactive)	33.3	33.3	33.3	785 ± 55
CP (Low reactivity)	33.3	33.3	33.3	2284 ± 84
5% CaO Stabilized	33.3	33.3	33.3	2771 ± 89



TABLE V  
PHYSICAL PROPERTIES OF CALCIA-STABILIZED  
ZIRCONIA FIBERS\*

Stabilized zirconia, 4 to 6% calcia

Fiber length	1-3 in.
Fiber diameter	0.0001-0.0003 in.
Cross section	Circular
Grain size	0.1 micron
Specific gravity	4.5-5.2
Melting point	2550°C
Tensile strength	35,000-150,000 psi
Modulus of elasticity	30-50 x 10 <sup>6</sup> psi
Surface area	200 m <sup>2</sup> /g

---

\* H. I. Thompson Fiber Glass Co. Technical Bulletin  
No. 1-1B.

TABLE VI

PHYSICAL PROPERTIES OF CAST OXIDE-PHOSPHATE-  
ZEOLITE MIXTURES SINTERED AT 500°C

Chemical Composition (Parts by Weight)				Phosphoric Acid (85 w% H <sub>3</sub> PO <sub>4</sub> )	General Physical Properties	Transverse Strength (lb/in <sup>2</sup> )
Metal Oxide						
<u>Al<sub>2</sub>O<sub>3</sub></u>	<u>ZnO</u>	<u>ZrO<sub>2</sub></u>	<u>Zeolon H</u>			
		4	0	2	Poor	N. R.
		3	2	1	Poor	N. R.
		3	1	2	Fair	N. R.
		3	0	3	Good	1453±274
		2	4	0	Poor	N. R.
		2	3	1	Poor	N. R.
		2	2	2	Good	1165±154
		2	1	3	Fair	660±47
		2	0	4	Poor	N. R.
		1.5	2.5	2	Good	1095±40
		1.5	2.0	2.5	Good	588±62
		1.5	1.5	3	Poor	N. R.
		1.5	1.0	3.5	Poor	N. R.
		1	3	2	Fair	N. R.
		1	2.5	2.5	Good	1177±67
		1	2	3	Fair	N. R.
		0.5	3	2.5	Poor	N. R.
		0	4	2	Fair	479±76
4			2	0	Poor	N. R.
3			2	1	Poor	N. R.
3			1	2	Poor	N. R.
2			3	1	Poor	N. R.
2			2	2	Poor	N. R.
2			1	3	Fair	N. R.
2			0	4	Poor	N. R.
1.5			3.5	1	Fair	N. R.
1.5			3	1.5	Poor	N. R.
1.5			2.5	2	Poor	N. R.
1.5			2	2.5	Poor	N. R.
1.5			1	3.5	Poor	N. R.
1			3	2	Fair	515±32
1			2.5	2.5	Fair	964±59
1			2	3	Fair	N. R.
0.5			3	2.5	Good	N. R.
0.5			2.5	3	Poor	N. R.
0.5			2	2.5	Good	1223±456
4			2	0	Poor	N. R.
3			2	1	Poor	N. R.

TABLE VI (CONT'D)

PHYSICAL PROPERTIES OF CAST OXIDE-PHOSPHATE-  
ZEOLITE MIXTURES SINTERED AT 500°C

Chemical Composition (Parts by Weight)					General Physical Properties	Transverse Strength (lb/in <sup>2</sup> )
Metal Oxide			Zeolon H	Phosphoric Acid (85 w% H <sub>3</sub> PO <sub>4</sub> )		
<u>Al<sub>2</sub>O<sub>3</sub></u>	<u>ZnO</u>	<u>ZrO<sub>2</sub></u>				
3						
3			1	2	Poor	N. R.
2			3	1	Poor	N. R.
2			2	2	Fair	N. R.
2			1	3	Fair	N. R.
2			0	4	Poor	N. R.
1.5			2.5	2	Fair	316±7
1.5			2	2.5	Fair	351±75
1.5			1.5	3	Poor	N. R.
1.5			1	3.5	Poor	N. R.
1			3	2	Fair	447±103
1			2.5	2.5	Good	912±83
1			2	3	Fair	N. R.
0.5			3	2.5	Fair	622(single specimen)

TABLE VII

EFFECT OF SINTERING TEMPERATURE ON THE TRANSVERSE  
STRENGTH OF INORGANIC FUEL CELL MEMBRANES

<u>Material No.</u>	<u>Composition</u>	<u>Sintering Temperature (°C)</u>	<u>Modulus of Rupture (psi)</u>
048-001	1 ZrO <sub>2</sub> : 1 H <sub>3</sub> PO <sub>4</sub> : 1 "Zeolon H"	250	2910±90
		350	4120±124
		450	4150±115
		550	3900±151
		650	3680±140
		750	2955±79
191-050	1 ZrO <sub>2</sub> -H <sub>3</sub> PO <sub>4</sub> : 1 H <sub>3</sub> PO <sub>4</sub> : 1 "Zeolon H"	250	1450±89
		500	2760±90
		750	1950±118
		1000	1640±102
	1 ZrO <sub>2</sub> : 1 H <sub>3</sub> PO <sub>4</sub> : 1 "Zeolon H"	300	2153±69
		500	2288±42
		700	2127±159
		1037	2063

TABLE VIII

STATISTICAL PLAN OF EXPERIMENTS $X_1$  = Percentage of  $H_3PO_4$  $X_2$  = Hours of Drying Time $X_3$  = Drying Temperature in  $^{\circ}C$ 

(N = 3)

<u>Treatments</u>	<u><math>X_1</math></u>	<u><math>X_2</math></u>	<u><math>X_3</math></u>
1	23	40	160
2	23	60	150
3	23	40	150
4	27-1/6	52	144
5	23	40	150
6	18-5/6	52	156
7	30	40	150
8	23	40	150
9	23	40	150
10	18-5/6	28	144
11	27-1/6	28	156
12	23	20	150
13	18-5/6	28	156
14	23	40	150
15	27-1/6	28	144
16	18-5/6	52	144
17	27-1/6	52	156
18	16	40	150
19	23	40	140
20	23	40	150

TABLE IX

RESISTIVITIES OF INORGANIC MEMBRANES PREPARED  
FOR STATISTICAL EVALUATION

Membrane No.	Table No.	Resistivity, (Ohm-Cm) at 50% Relative Humidity		Resistivity, (Ohm-Cm) at 100% Relative Humidity	
		105°C	70°C	105°C	70°C
131-021	31	1.00x10 <sup>3</sup>	2.54x10 <sup>3</sup>	2.26x10 <sup>2</sup>	3.35x10 <sup>2</sup>
131-022	32	6.20x10 <sup>2</sup>	1.48x10 <sup>3</sup>	1.45x10 <sup>2</sup>	2.14x10 <sup>2</sup>
131-023	33	4.50x10 <sup>2</sup>	1.38x10 <sup>3</sup>	5.80x10 <sup>2</sup>	1.68x10 <sup>2</sup>
131-024	34	1.92x10 <sup>2</sup>	5.10x10 <sup>2</sup>	3.30x10 <sup>1</sup>	7.60x10 <sup>1</sup>
131-025	35	6.4x10 <sup>2</sup>	1.60x10 <sup>3</sup>	9.8x10 <sup>1</sup>	2.26x10 <sup>2</sup>
131-026	36	1.93x10 <sup>3</sup>	6.90x10 <sup>3</sup>	9.60x10 <sup>1</sup>	6.90x10 <sup>2</sup>
131-027	37	1.00x10 <sup>2</sup>	3.10x10 <sup>2</sup>	1.84x10 <sup>1</sup>	5.10x10 <sup>1</sup>
131-028	38	2.53x10 <sup>2</sup>	1.28x10 <sup>3</sup>	3.29x10 <sup>1</sup>	1.36x10 <sup>2</sup>
131-029	39	2.95x10 <sup>2</sup>	1.48x10 <sup>3</sup>	3.36x10 <sup>1</sup>	1.55x10 <sup>2</sup>
131-030	40	1.64x10 <sup>3</sup>	5.60x10 <sup>3</sup>	1.02x10 <sup>2</sup>	5.30x10 <sup>2</sup>
131-031	41	1.70x10 <sup>2</sup>	5.60x10 <sup>2</sup>	3.20x10 <sup>1</sup>	9.40x10 <sup>1</sup>
131-032	42	6.20x10 <sup>2</sup>	1.68x10 <sup>3</sup>	1.23x10 <sup>2</sup>	2.60x10 <sup>2</sup>
131-033	43	6.80x10 <sup>2</sup>	2.34x10 <sup>3</sup>	1.04x10 <sup>2</sup>	3.14x10 <sup>2</sup>
131-034					
131-035	44	1.24x10 <sup>2</sup>	2.72x10 <sup>2</sup>	2.13x10 <sup>1</sup>	6.80x10 <sup>1</sup>
131-036	45	1.34x10 <sup>3</sup>	3.56x10 <sup>3</sup>	2.20x10 <sup>2</sup>	6.10x10 <sup>2</sup>
131-037	46	8.10x10 <sup>2</sup>	2.36x10 <sup>3</sup>	9.60x10 <sup>1</sup>	2.60x10 <sup>2</sup>
131-038	47	4.00x10 <sup>3</sup>	1.47x10 <sup>4</sup>	6.40x10 <sup>2</sup>	2.15x10 <sup>3</sup>
131-039	48	4.30x10 <sup>2</sup>	1.00x10 <sup>3</sup>	6.90x10 <sup>1</sup>	1.66x10 <sup>2</sup>
131-040	49	5.20x10 <sup>2</sup>	1.42x10 <sup>3</sup>	8.60x10 <sup>1</sup>	1.85x10 <sup>2</sup>

TABLE X  
RESISTIVITIES OF INORGANIC FUEL CELL MEMBRANES AT 50% AND 100% RELATIVE  
HUMIDITY AT ELEVATED TEMPERATURES

Membrane No.	Table No.	Resistivity (Ohm-Cm)		Temp. °C	Composition		Temp °C	Time Hr.	Temp °C	Time Hr.	$\frac{\text{H}_3\text{PO}_4}{\text{ZrO}_2}$	
		Rel. Humidity @ 50 Percent	Rel. Humidity @ 100% Rel. Humidity		$\frac{\text{ZrO}_2}{\text{in weight percent}}$	$\frac{\text{H}_3\text{PO}_4}{\text{Zeolon H}}$					$\frac{\text{H}_3\text{PO}_4}{\text{Zeolon H}}$	$\frac{\text{H}_3\text{PO}_4}{\text{Zeolon H}}$
191-047	19	$1.03 \times 10^{-1}$	$4.00 \times 10^0$	110	16.7 + 5% $\text{ZrO}_2$ Fibers	33.3	500	15	160	15	2.99	1.50
191-017	20	$2.60 \times 10^{-1}$	$3.70 \times 10^0$	110	22.2 + 5% $\text{ZrO}_2$ Fibers	33.3	300	24	160	15	2.00	1.33
98-051*	21	$3.8 \times 10^{-1}$	$(2.0 \times 10^0)^*$	110	20 40	40	300	18	150	8	2.00	1.00
191-007	22	$5.70 \times 10^{-1}$	$5.40 \times 10^0$	105	33.3	33.3	300	24	160	15	1.00	1.00
191-051	23	$6.10 \times 10^{-1}$	$2.10 \times 10^1$	110	33.3 + 5% $\text{ZrO}_2$ Fibers	33.3	500	15	160	15	1.00	1.00
191-042	24	$6.40 \times 10^{-1}$	$2.06 \times 10^1$	105	33.3 + 5% $\text{ZrO}_2$ Fibers	33.3	500	24	160	15	1.00	1.00
191-053	25	$6.90 \times 10^{-1}$	$3.00 \times 10^1$	110	30 30	40	500	15	140	20	1.00	0.75
191-016	26	$1.14 \times 10^{-2}$	$1.16 \times 10^1$	110	40 20	40	300	24	160	15	0.50	0.50
191-032	27	$1.28 \times 10^{-2}$	$4.10 \times 10^1$	105	33.3 + 5% aluminosilicate fibers	33.3	300	24	160	15	1.00	1.00
191-059	28	$1.53 \times 10^{-2}$	$1.57 \times 10^1$	105	30.3 30.3	39.4	500	15	140	40	1.00	0.77
191-057	29	$1.85 \times 10^{-2}$	$2.53 \times 10^1$	105	33.3 Zircon" B" stabilized zirconia	33.3	500	15	160	15	1.00	1.00
191-019	30	$1.84 \times 10^{-3}$	$2.82 \times 10^2$	105	50 50	0	300	24	160	15	1.00	$\infty$

\* These data are less reliable than the other values reported in this table due to operating difficulties with the apparatus during this run.

TABLE XI  
ANALYSIS OF LOG RESISTIVITY DATA

ANALYSIS OF VARIANCE

<u>Term</u>	<u>Coefficient</u>	<u>Sum of Squares</u>	<u>Degrees of Freedom</u>	<u>Mean Square</u>
Mean	2.611872	148.261797	1	148.261797
$X_1$ (Comp.)	-.412883	2.328116	1	2.328116
$X_2$ (Time)	.090301	.111362	1	.111362
$X_3$ (Temp.)	.084557	.097645	1	.097645
$X_1^2$	.053213	.099893	3	.033298
$X_2^2$	.050158			
$X_3^2$	.058765			
$X_1X_2$	.062826	.031577	1	.031577
$X_2X_3$	.128619	.132343	1	.132343
$X_1X_3$	.123261	.121546	1	.121546
Error	-	.113935	4	.028484
Lack of Fit	-	.144926	5	.028985
Total	-	151.443140	19	-

Fitted Response Surface:

$$\text{Log } R = 2.6119 - .4129X_1 + .0903X_2 + .0846X_3 + .0532X_1^2 + .0502X_2^2 + .0588X_3^2 + .0628X_1X_2 + .1286X_2X_3 + .1233X_1X_3$$



TABLE XII

ANALYSIS OF STRENGTH DATA: QUADRATIC SURFACEANALYSIS OF VARIANCE

<u>Term</u>	<u>Coefficient</u>	<u>Sum of Squares</u>	<u>Degree of Freedom</u>	<u>Mean Square</u>
Mean	2,902.542	163,584.370	1	163,584.370
$X_1$ (Comp.)	132.279	238,975	1	238,975
$X_2$ (Time)	-176.156	423,802	1	423,802
$X_3$ (Temp.)	343.767	1,611,197	1	1,611,197
$X^2$	-53.595	84,144	3	28,048
$X_2^2$	-43.815			
$X_3^2$	34.839			
$X_1X_2$	-47.750	18,240	1	18,240
$X_2X_3$	12.083	1,168	1	1,168
$X_1X_3$	179.084	256,568	1	256,568
Error	-	9,434	5	1,887
Lack of Fit	-	1,415,430	5	283,086
Total	-	167,643,328	20	-

TABLE XIII

ANALYSIS OF STRENGTH DATA: HIGHER ORDER SURFACEANALYSIS OF VARIANCE

<u>Term</u>	<u>Coefficient</u>	<u>Sum of Squares</u>	<u>Degrees of Freedom</u>	<u>Mean Square</u>
Mean	2,882.766	163,584,370	1	163,584,370
$X_1$ (Comp.)	132.279	238,975	1	238,975
$X_2$ (Time)	-176,158	423,802	1	423,802
$X_3$ (Temp.)	343.767	1,611,197	1	1,611,197
$X_1X_3$	179.084	256,568	1	256,568
$X_1X_2X_3$	-117.000	109,512	1	109,512
$X_1^2+X_2^2+X_3^2$	-207.346	1,200,456	2	600,228
$X_1^4+X_2^4+X_3^4$	111.645			
Error	-	9,434	5	1,887
Lack of Fit	-	209,014	7	29,858
Total	-	167,643,328	20	-

Fitted Response Surface:

$$S = 2883 + 132X_1 - 176X_2 + 344X_3 + 179X_1X_3 - 117X_1X_2X_3 - 207(X_1^2 + X_2^2 + X_3^2) + 112(X_1^4 + X_2^4 + X_3^4)$$

TABLE XIV  
INORGANIC MEMBRANE FUEL CELL OPERATING DATA

Run No.	Membrane No.	Thickness Mn.	Electrode Area Cm <sup>2</sup>	Temp. °C	ma/cm <sup>2</sup> at 0.5V	Resistivity at 100%Rel. Humidity Ohm-Cm	Observed Fuel Cell Resistance Ohms	Calculated* Electrode-Membrane Contact Resistance Ohms	Open Circuit Voltage Volts	Remarks
1	98-051-2	-	13.4	90	7.0	9	3.3	-	.79	-
2	191-002	-	13.4	68	12.3	-	2.1	-	.84	-
3	191-002	-	13.4	85	17.9	-	1.4	-	.91	-
6	191-002	-	13.4	90	30.8	-	1.0	-	.90	First day
				95	27.3	-	1.1	-	.94	Second day
				100	17.4	-	1.6	-	.86	Second day
				105	14.5	-	1.9	-	.90	Second day
				110	11.2	-	2.2	-	.88	Second day
				115	10.1	-	2.5	-	.84	Second day
				120	8.1	-	2.9	-	.84	Second day
				90	18.6	-	1.7	-	.92	Third day
				90	16.6	-	1.8	-	.90	Fourth day
7	191-042	0.80	13.4	30	5.1	-	4.1	-	.77	First day
				90	7.5	31	3.9	3.7	.85	First day
				89	6.3	31	5.9	5.7	.96	Fourth day
8	191-042	0.53	13.4	90	7.1	31	5.5	5.3	1.09	First day
				25	4.9	-	6.6	-	.99	Second day
9	191-042	-	13.4	90	23.1	31	1.4	1.2	.95	First day
				68	20.2	33	1.5	1.3	.97	Second day
				67	14.2	33	2.4	2.2	.94	Third day
				67	26.8	33	1.3	1.1	1.05	First day
				90	18.3	31	1.8	1.6	.95	First day
				67	18.3	33	1.7	1.5	1.02	Second day
				90	16.4	31	1.9	1.7	.93	Second day
				67	18.5	33	1.8	1.6	1.01	Third day
				67	19.3	33	1.7	1.5	1.02	Fourth day
				90	11.2	31	2.4	2.2	.88	Fifth day
				90	12.3	31	2.2	2.10	.88	Sixth day
				67	20.5	33	1.6	1.4	1.04	Seventh day
11	191-050	1.31	13.4	89	14.2	31	2.0	1.8	.90	Seventh day
				67	25.7	15	1.29	1.14	1.04	First day
				66	24.6	15	1.31	1.16	1.04	Second day
				90	24.3	15	1.31	1.16	1.02	Second day
				95	21.3	15	1.36	1.21	.94	Second day
19	191-019	0.98	13.4	75	8.8	310	3.96	1.70	.98	First Day
				64	6.9	310	4.13	1.92	.94	Second day
19-A	200-011	-	20.2	75	6.9	310	4.13	1.92	.94	Second day
				65	5.7	-	2.74	1.92	.81	Zeolon H-H <sub>3</sub> PO <sub>4</sub> membrane
20	191-019	1.09	13.4	67	10.4	310	3.13	.87	.94	Humidified membrane

\* Calculated electrode-membrane contact resistance is obtained by subtracting the membrane resistance (calculated from the membrane dimensions plus the resistivity at 100% relative humidity) from the observed cell resistance.

TABLE XIV (CONT'D)  
INORGANIC MEMBRANE FUEL CELL OPERATING DATA

Run No.	Membrane No.	Thickness Mm.	Electrode Area Cm <sup>2</sup>	Temp. °C	ma/cm <sup>2</sup> at 0.5V	Resistivity at 100% Rel. Humidity Ohm-Cm	Observed Fuel Cell Resistance Ohms	Calculated* Electrode-Membrane Contact Resistance Ohms	Open Circuit Voltage Volts	Remarks
25	191-050	0.61	20.2	65	28.4	15	.51	.46	.80	First day-humidified membrane
				89	31.9	15	.41	.36	.78	First day
				95	33.3	15	.41	.36	.77	First day
26	191-032	0.72	20.2	65	28.1	110	.78	.39	1.06	One electrode reused
				89	23.7	74	1.00	.74	1.01	Assembly baked 30-min. at 120°C
27	191-032	-	13.4	65	17.2	110	1.81	1.42	1.04	Membrane humidified
				89	13.8	74	2.19	1.93	.96	Assembly baked 30-min. at 150°C and 50-min. at 120°C
28	191-068	0.79	13.4	65	16.1	-	1.81	-	.99	Morning
				89	17.5	-	1.65	-	.98	Afternoon
30	191-050	0.99	20.2	65	24.6	-	1.24	-	.97	No platinum black
32	191-050	-	20.2	64	12.4	15	1.43	1.36	.93	Experimental unified assembly
				64	8.5	15	2.25	7.18	.90	
33	191-050	0.85	20.2	65	50.0	15	.41	.35	.92	250° sintered membrane
				90	25.2	15	.38	.32	.66	
34	191-050	0.80	20.2	65	40.0	15	.46	.40	.92	750° sintered membrane
35	191-050	0.83	20.2	65	34.7	15	.51	.45	.96	500° sintered membrane
				89	7.9	15	2.00	1.94	.82	
37	148-001	0.90	20.2	65	63.2	20	.33	.24	.97	350° sintered membrane
										1st day assembly dipped in water
				90	53.3	15	.37	.30	.91	After 1.0 hr at 90°C
				90	45.0	15	.36	.29	.82	After 1.25 hr at 90°C
				91	39.6	15	.40	.33	.84	After 2.25 hr at 90°C
				97	32.6	-	.48	-	.80	After 0.8 hrs at 97°C
				97	29.9	-	.47	-	.80	After 1.8 hrs at 97°C
				97	25.7	-	.53	-	.78	After 3.0 hrs at 97°C
				107	19.5	4	.52	.50	.71	After 0.2 hrs at 107°C
				107	7.4	4	.63	.61	.59	After 0.4 hrs at 107°C
				107	1.5	4	.83	.81	.52	After 0.6 hrs at 107°C
				66	51.4	20	.35	.26	.94	Second day
				91	23.9	15	.60	.53	.86	Second day after 2.25 hr
				91	23.3	15	.62	.55	.86	Second day after 4.5 hr

\*Calculated electrode-membrane contact resistance is obtained by subtracting the membrane resistance (calculated from the membrane dimensions plus the resistivity at 100% relative humidity) from the observed cell resistance.

TABLE XIV (CONT'D)  
INORGANIC MEMBRANE FUEL CELL OPERATING DATA

Run No.	Membrane No.	Thickness Mm.	Electrode Area $\text{cm}^2$	Temp. $^{\circ}\text{C}$	ma/cm <sup>2</sup> at 0.5V	Resistivity at 100% Rel. Humidity Ohm-Cm	Observed Fuel Cell Resistance Ohms	Calculated* Electrode-Membrane Contact Resistance Ohms	Open Circuit Voltage Volts	Remarks
38	191-042	0.83	20.2	66	45.0	33	.41	.27	.96	Assembly dipped in water
				90	36.9	31	.45	.32	.85	
				97	19.1	-	.80	-	.84	
				66	51.5	33	.35	.21	.92	Second day
				90	13.3	31	1.23	1.10	.88	
				66	46.7	33	.37	.23	.92	Third day
				66	36.2	33	.45	.31	.92	Fifth day
				66	37.1	33	.47	.33	.92	Sixth day, Beg. 8th day cell failed

\* Calculated electrode-membrane contact resistance is obtained by subtracting the membrane resistance (calculated from the membrane dimensions plus the resistivity at 100% relative humidity) from the observed cell resistance.

TABLE XV

THE EFFECT OF MEMBRANE SINTERING TEMPERATURE  
ON FUEL CELL OPERATION

<u>Run No.</u>	<u>Membrane No.</u>	<u>Operating Temperature</u>	<u>Membrane Sintering Temperature</u>	<u>Current Density at 0.5 Volts</u>
33	191-050	65°C	250°C	50.0 Ma/Cm <sup>2</sup>
35	191-050	65	500	34.4
25	191-050	65	500	25.7
34	191-050	65	750	40.0
37	48-001	65	350	63.2 First Day
		66		51.4 Second Day
38	191-042	66	500	45.0 First Day
		66		51.5 Second Day

TABLE XVI

THE EFFECT ON FUEL CELL OPERATION OF OMITTING "ZEOLON H"  
FROM THE INORGANIC MEMBRANE COMPOSITION

Run No.	Membrane Comp.	Membrane No.	Electrode Area Cm <sup>2</sup>	Temperature	Cell Resistance	Resistivity at 100% Rel. Hum. ohm-cm
19	50% ZrO <sub>2</sub>	191-019	13.4	75°	3.96	310
	50% H <sub>3</sub> PO <sub>4</sub>					
10	31.7 ZrO <sub>2</sub>	191-042	13.4	67	1.32	33
	31.7 H <sub>3</sub> PO <sub>4</sub>					
	31.7 Zeolon H					
	5.0 ZrO <sub>2</sub> fibers					
11	33.3%(ZrO) <sub>3</sub> (PO <sub>4</sub> ) <sub>2</sub>	191-050	13.4	67	1.29	15
	33.3%H <sub>3</sub> PO <sub>4</sub>					
	33.3% Zeolon H					
28	30% ZrO <sub>2</sub>	191-068	13.4	65	1.24	-
	24% H <sub>3</sub> PO <sub>4</sub>					
	46% Zeolon H					

TABLE XVII

THE EFFECT OF ALUMINO-SILICATE FIBER ADDITIONS ON THE FUEL CELL  
PERFORMANCE OF INORGANIC MEMBRANES

Run No.	Membrane Comp.	Membrane No.	Electrode Area Cm <sup>2</sup>	Temperature	Resistance	Resistivity at 100% Rel. Hum. ohm-cm
26	31. 7% ZrO <sub>2</sub>	191-032	20.2	65	0.78	110
	31. 7% H <sub>3</sub> PO <sub>4</sub>					
	31. 7% Zeolon H					
	5% Fiberfrax fibers					
25	33. 3%(ZrO) <sub>3</sub> (PO <sub>4</sub> ) <sub>2</sub>	191-050	20.2	65	0.51	15
	33. 3% H <sub>3</sub> PO <sub>4</sub>					
	33. 3% Zeolon H					
34	33. 3%(ZrO) <sub>3</sub> (PO <sub>4</sub> ) <sub>2</sub>	191-050	20.2	65	0.46	15
	33. 3% H <sub>3</sub> PO <sub>4</sub>					
	33. 3% Zeolon H					
35	33. 3%(ZrO) <sub>3</sub> (PO <sub>4</sub> ) <sub>2</sub>	191-050	20.2	65	0.52	15
	33. 3% H <sub>3</sub> PO <sub>4</sub>					
	33. 3% Zeolon H					



TABLE XVIII  
RESISTIVITIES AT THREE TEMPERATURES  
(MEMBRANE NO. 191-047)

Composition: 1 ZrO<sub>2</sub>: 1 H<sub>3</sub>PO<sub>4</sub> (1:1 parts by wt)  
H<sub>3</sub>PO<sub>4</sub>, "Zeolon H" (1:1:1 parts by  
wt) + 5% ZrO<sub>2</sub> Fibers.

<u>Relative Humidity</u> (%)	<u>Resistivity</u> (Ohm-Cm)
<u>Temperature 70.3°C</u>	
48	$(7.38 \pm 2.34) \times 10^1$
23	$(1.57 \pm 0.34) \times 10^2$
14	$(9.16 \pm 1.51) \times 10^2$
11	$(9.41 \pm 1.49) \times 10^2$
0	$(7.83 \pm 1.26) \times 10^4$
<u>Temperature 90.8°C</u>	
46	$(1.06 \pm 0.19) \times 10^2$
30	$(1.73 \pm 0.28) \times 10^2$
18	$(2.72 \pm 0.39) \times 10^2$
10	$(5.19 \pm 0.77) \times 10^2$
0	$(2.38 \pm 0.44) \times 10^4$
<u>Temperature 109.5°C</u>	
51	$(1.01 \pm 0.22) \times 10^2$
34	$(1.39 \pm 0.30) \times 10^2$
22	$(1.74 \pm 0.38) \times 10^2$
15	$(2.35 \pm 0.49) \times 10^2$
9	$(2.97 \pm 0.58) \times 10^2$
5	$(3.79 \pm 0.69) \times 10^2$
0	$(7.80 \pm 4.3) \times 10^6$

TABLE XIX  
RESISTIVITIES AT THREE TEMPERATURES  
(MEMBRANE NO. 191-017-1)

Composition:  $\text{ZrO}_2$ ,  $\text{H}_3\text{PO}_4$ , "Zeolon H"  
 (1:2: $\frac{3}{2}$  parts by weight)

<u>Relative Humidity</u> (%)	<u>Resistivity</u> (Ohm-Cm)
<u>Temperature 69°C</u>	
69	$(3.12 \pm 0.18) \times 10^1$
56	$(3.31 \pm 0.22) \times 10^1$
42	$(3.48 \pm 0.26) \times 10^1$
25	$(4.44 \pm 0.44) \times 10^1$
15	$(7.72 \pm 0.95) \times 10^1$
0	$(8.94 \pm 0.80) \times 10^2$
<u>Temperature 90°C</u>	
70	$(2.88 \pm 0.24) \times 10^1$
49	$(2.94 \pm 0.29) \times 10^1$
28	$(5.04 \pm 0.63) \times 10^1$
20	$(6.11 \pm 0.83) \times 10^1$
11	$(8.81 \pm 1.27) \times 10^1$
0	$(2.47 \pm 0.57) \times 10^3$
<u>Temperature 110°C</u>	
57	$(2.47 \pm 0.15) \times 10^1$
32	$(4.12 \pm 0.29) \times 10^1$
14	$(1.05 \pm 0.09) \times 10^2$
9	$(1.25 \pm 0.12) \times 10^2$
7	$(1.33 \pm 0.14) \times 10^2$
5	$(1.65 \pm 0.67) \times 10^2$
0	$(2.90 \pm 0.38) \times 10^2$

TABLE XX  
RESISTIVITIES AT TWO TEMPERATURES  
(MEMBRANE NO. 98-051-1)

Composition:  $\text{ZrO}_2$ ,  $\text{H}_3\text{PO}_4$ , "Zeolon H" (1/2:1:1  
parts by weight)

<u>Relative Humidity</u> <u>(%)</u>	<u>Resistivity</u> <u>(Ohm-Cm)</u>
<u>Temperature 87°C</u>	
80	$(2.45 \pm 0.17) \times 10^1$
61	$(7.57 \pm 0.84) \times 10^1$
46	$(10.7 \pm 1.3) \times 10^1$
<u>Temperature 110°C</u>	
57.8	$(2.4 \pm 0.3) \times 10^1$
22.5	$(2.3 \pm 0.7) \times 10^2$
15.3	$(3.3 \pm 1.0) \times 10^2$
9.1	$(3.7 \pm 1.0) \times 10^2$

TABLE XXI

RESISTIVITIES AT THREE TEMPERATURES  
(MEMBRANE NO. 191-007)

Composition:  $\text{ZrO}_2$ ,  $\text{H}_3\text{PO}_4$ , "Zeolon H" (1:1:1  
 parts by weight)

<u>Relative Humidity</u> (%)	<u>Resistivity</u> (Ohm-Cm)
<u>Temperature 69.8°C</u>	
78.9	$(1.30 \pm 0.32) \times 10^2$
65.6	$(1.68 \pm 0.42) \times 10^2$
39.6	$(2.55 \pm 0.75) \times 10^2$
14.2	$(3.33 \pm 0.91) \times 10^2$
<u>Temperature 89.8°C</u>	
82.5	$(3.97 \pm 0.56) \times 10^1$
68.9	$(6.53 \pm 0.58) \times 10^1$
46.5	$(1.55 \pm 0.43) \times 10^2$
30.0	$(4.91 \pm 0.46) \times 10^2$
10.0	$(6.92 \pm 0.56) \times 10^2$
<u>Temperature 105.0°C</u>	
70.3	$(2.67 \pm 0.69) \times 10^1$
59.1	$(2.97 \pm 0.81) \times 10^1$
46.6	$(6.77 \pm 2.93) \times 10^1$
25.6	$(1.97 \pm 0.65) \times 10^2$
10.1	$(3.45 \pm 1.25) \times 10^2$

TABLE XXII

RESISTIVITIES AT THREE TEMPERATURES  
(MEMBRANE NO. 191-051)

Composition:  $\text{ZrO}_2$ ,  $\text{H}_3\text{PO}_4$ , "Zeolon H" (1:1:1  
 parts by weight) + 5%  $\text{ZrO}_2$  Fibers

<u>Relative Humidity</u> (%)	<u>Resistivity</u> (Ohm-Cm)
<u>Temperature 70.3°C</u>	
48	$(4.36 \pm 0.13) \times 10^1$
23	$(1.06 \pm 0.06) \times 10^2$
14	$(5.62 \pm 0.04) \times 10^2$
11	$(5.67 \pm 0.09) \times 10^2$
0	$(1.74 \pm 0.32) \times 10^4$
<u>Temperature 90.8°C</u>	
46	$(6.28 \pm 0.36) \times 10^1$
30	$(1.02 \pm 0.07) \times 10^2$
18	$(1.50 \pm 0.07) \times 10^2$
10	$(2.90 \pm 0.26) \times 10^2$
0	$(6.05 \pm 1.26) \times 10^3$
<u>Temperature 109.5°C</u>	
51	$(6.11 \pm 0.28) \times 10^1$
34	$(8.59 \pm 0.47) \times 10^1$
22	$(1.05 \pm 0.04) \times 10^2$
15	$(1.34 \pm 0.03) \times 10^2$
9	$(1.75 \pm 0.06) \times 10^2$
5	$(2.10 \pm 0.07) \times 10^2$
0	$>(1.09 \pm 0.23) \times 10^7$

TABLE XXIII

## RESISTIVITIES AT THREE TEMPERATURES

(MEMBRANE NO. 191-042)

Composition:  $\text{ZrO}_2$ ,  $\text{H}_3\text{PO}_4$ , Zeolon H" (1:1:1 parts by weight)  
with addition of 5% of total weight of  $\text{ZrO}_2$  Fibers

Relative Humidity (%)	Resistivity (Ohm-Cm)
<u>Temperature 69.5°C</u>	
70	$(8.33 \pm 1.01) \times 10^1$
40	$(6.81 \pm 0.57) \times 10^1$
20	$(1.09 \pm 0.07) \times 10^2$
14	$(2.18 \pm 0.19) \times 10^2$
0	$(2.38 \pm 0.20) \times 10^3$
<u>Temperature 89.0°C</u>	
71	$(5.52 \pm 0.57) \times 10^1$
50	$(6.36 \pm 0.69) \times 10^1$
31	$(8.92 \pm 0.62) \times 10^1$
15	$(1.34 \pm 0.08) \times 10^2$
11	$(2.18 \pm 0.16) \times 10^2$
7.9	$(2.96 \pm 0.18) \times 10^2$
0	$(3.96 \pm 0.27) \times 10^2$
<u>Temperature 104.2°C</u>	
78	$(3.82 \pm 0.37) \times 10^1$
66	$(3.79 \pm 0.29) \times 10^1$
41	$(7.70 \pm 0.39) \times 10^1$
27	$(1.11 \pm 0.06) \times 10^2$
17	$(1.68 \pm 0.14) \times 10^2$
11	$(2.36 \pm 0.13) \times 10^2$
6.4	$(4.40 \pm 0.26) \times 10^2$
0	$(1.59 \pm 0.08) \times 10^5$

TABLE XXIV  
RESISTIVITIES AT THREE TEMPERATURES  
(MEMBRANE NO. 191-053)

Composition:  $\text{ZrO}_2$ ,  $\text{H}_3\text{PO}_4$ , "Zeolon H"  
 (1:1:4/3 parts by weight)

<u>Relative Humidity</u> (%)	<u>Resistivity</u> (Ohm-Cm)
<u>Temperature 70.3°C</u>	
48	$(5.88 \pm 0.37) \times 10^1$
23	$(7.37 \pm 0.77) \times 10^1$
14	$(4.59 \pm 1.27) \times 10^2$
11	$(7.54 \pm 3.32) \times 10^2$
0	$(7.56 \pm 1.87) \times 10^3$
<u>Temperature 90.8°C</u>	
46	$(6.26 \pm 0.87) \times 10^1$
30	$(1.11 \pm 0.20) \times 10^2$
18	$(3.13 \pm 1.22) \times 10^2$
10	$(4.58 \pm 1.76) \times 10^2$
0	$(2.97 \pm 0.79) \times 10^3$
<u>Temperature 109.5°C</u>	
51	$(6.80 \pm 1.63) \times 10^1$
34	$(8.63 \pm 2.12) \times 10^1$
22	$(1.13 \pm 0.32) \times 10^2$
15	$(1.73 \pm 0.54) \times 10^2$
9	$(2.07 \pm 0.65) \times 10^2$
5	$(2.53 \pm 1.17) \times 10^2$
0	$>(1.04 \pm 0.14) \times 10^7$

TABLE XXV  
RESISTIVITIES AT THREE TEMPERATURES  
(MEMBRANE NO. 191-016)

Composition:  $\text{ZrO}_2$ ,  $\text{H}_3\text{PO}_4$ , "Zeolon H"  
 (2:1:2 parts by weight)

<u>Relative Humidity</u> (%)	<u>Resistivity</u> (Ohm-Cm)
<u>Temperature 69°C</u>	
69	$(7.61 \pm 1.13) \times 10^1$
56	$(1.13 \pm 0.20) \times 10^2$
42	$(1.59 \pm 0.31) \times 10^2$
25	$(2.91 \pm 0.18) \times 10^2$
15	$(6.16 \pm 1.51) \times 10^2$
0	$(2.26 \pm 0.82) \times 10^4$
<u>Temperature 90°C</u>	
70	$(0.92 \pm 0.16) \times 10^2$
49	$(1.62 \pm 0.28) \times 10^2$
28	$(3.81 \pm 0.85) \times 10^2$
20	$(4.66 \pm 1.09) \times 10^2$
11	$(7.17 \pm 1.85) \times 10^2$
0	$(2.68 \pm 0.92) \times 10^4$
<u>Temperature 110°C</u>	
57	$(0.92 \pm 0.14) \times 10^2$
32	$(2.43 \pm 0.44) \times 10^2$
14	$(5.98 \pm 1.20) \times 10^2$
9	$(7.34 \pm 1.41) \times 10^2$
7	$(8.13 \pm 1.65) \times 10^2$
5	$(9.95 \pm 1.98) \times 10^2$
0	$(4.35 \pm 0.42) \times 10^3$



TABLE XXVI

RESISTIVITIES AT THREE TEMPERATURES  
(MEMBRANE NO. 191-032)

Composition:  $\text{ZrO}_2$ ,  $\text{H}_3\text{PO}_4$ , "Zeolon H" (1:1:1 parts by weight)  
 with addition of 5% of total weight of fiberfrax fibers

<u>Relative Humidity</u> (%)	<u>Resistivity</u> (Ohm-Cm)
<u>Temperature 69.4°C</u>	
70	$(2.07 \pm 0.26) \times 10^2$
40	$(1.77 \pm 0.17) \times 10^2$
20	$(2.25 \pm 0.16) \times 10^2$
14	$(4.23 \pm 0.39) \times 10^2$
0	$(4.38 \pm 0.78) \times 10^4$
<u>Temperature 89.0°C</u>	
71	$(1.13 \pm 0.10) \times 10^2$
50	$(1.50 \pm 0.19) \times 10^2$
31	$(1.79 \pm 0.20) \times 10^2$
15	$(2.77 \pm 0.17) \times 10^2$
11	$(1.14 \pm 0.03) \times 10^3$
7.9	$(2.29 \pm 0.14) \times 10^3$
0	$(7.10 \pm 1.50) \times 10^3$
<u>Temperature 104.2°C</u>	
78	$(7.17 \pm 0.57) \times 10^1$
66	$(8.28 \pm 0.60) \times 10^1$
41	$(1.51 \pm 0.09) \times 10^2$
27	$(2.23 \pm 0.09) \times 10^2$
17	$(1.34 \pm 0.07) \times 10^3$
11	$(2.82 \pm 0.08) \times 10^3$
6.4	$(8.65 \pm 0.22) \times 10^3$
0	$(2.11 \pm 0.27) \times 10^6$

TABLE XXVII

RESISTIVITIES AT THREE TEMPERATURES  
(MEMBRANE NO. 191-059)

Composition:  $\text{ZrO}_2$ ,  $\text{H}_3\text{PO}_4$ , "Zeolon H"  
 (1:1:1.3 parts by weight)

<u>Relative Humidity</u> <u>(%)</u>	<u>Resistivity</u> <u>(Ohm-Cm)</u>
<u>Temperature 69.8°C</u>	
78.9	$(4.54 \pm 0.34) \times 10^2$
65.6	$(4.84 \pm 0.29) \times 10^2$
39.6	$(6.37 \pm 0.33) \times 10^2$
14.2	$(8.56 \pm 0.67) \times 10^2$
<u>Temperature 89.8°C</u>	
82.5	$(9.89 \pm 0.29) \times 10^1$
68.9	$(2.11 \pm 0.14) \times 10^2$
46.5	$(3.89 \pm 0.22) \times 10^2$
30.0	$(6.59 \pm 0.41) \times 10^2$
10.0	$(1.18 \pm 0.09) \times 10^3$
<u>Temperature 105.0°C</u>	
70.3	$(5.27 \pm 0.77) \times 10^1$
59.1	$(1.13 \pm 0.26) \times 10^2$
46.6	$(2.00 \pm 0.22) \times 10^2$
25.6	$(5.95 \pm 1.20) \times 10^2$
10.1	$(7.26 \pm 1.10) \times 10^2$

TABLE XXVIII

RESISTIVITIES AT THREE TEMPERATURES  
(MEMBRANE NO. 191-057)

Composition:  $\text{ZrO}_2$ ,  $\text{H}_3\text{PO}_4$ , "Zeolon H"  
 (1:1:1 parts by weight)

<u>Relative Humidity</u> (%)	<u>Resistivity</u> (Ohm-Cm)
<u>Temperature 69.8°C</u>	
78.9	$(4.47 \pm 0.05) \times 10^2$
65.6	$(4.80 \pm 0.06) \times 10^2$
39.6	$(6.34 \pm 0.11) \times 10^2$
14.2	$(8.64 \pm 0.15) \times 10^2$
<u>Temperature 89.8°C</u>	
82.5	$(9.08 \pm 0.01) \times 10^1$
68.9	$(1.94 \pm 0.004) \times 10^2$
46.5	$(3.88 \pm 0.02) \times 10^2$
30.0	$(8.03 \pm 0.34) \times 10^2$
10.0	$(1.08 \pm 0.11) \times 10^3$
<u>Temperature 105.0°C</u>	
70.3	$(8.42 \pm 0.25) \times 10^1$
59.1	$(1.26 \pm 0.00) \times 10^2$
46.6	$(1.80 \pm 0.04) \times 10^2$
25.6	$(5.31 \pm 0.02) \times 10^2$
10.1	$(8.30 \pm 0.61) \times 10^2$

TABLE XXIX

RESISTIVITIES AT THREE TEMPERATURES  
(MEMBRANE NO. 191-019)

Composition:  $\text{ZrO}_2$ ,  $\text{H}_3\text{PO}_4$  (1:1 parts by weight)

<u>Relative Humidity</u> (%)	<u>Resistivity</u> (Ohm-Cm)
<u>Temperature 69.8°C</u>	
78.9	$(4.18 \pm 0.73) \times 10^3$
65.6	$(4.62 \pm 0.81) \times 10^3$
39.6	$(6.44 \pm 1.17) \times 10^3$
14.2	$(9.49 \pm 1.76) \times 10^3$
<u>Temperature 89.8°C</u>	
82.5	$(1.43 \pm 0.26) \times 10^3$
68.9	$(1.96 \pm 0.34) \times 10^3$
46.5	$(4.20 \pm 0.68) \times 10^3$
30.0	$(7.41 \pm 1.22) \times 10^3$
10.0	$(8.90 \pm 1.49) \times 10^3$
<u>Temperature 105.0°C</u>	
70.3	$(8.87 \pm 1.58) \times 10^2$
59.1	$(1.24 \pm 0.21) \times 10^3$
46.6	$(2.12 \pm 0.11) \times 10^3$
25.6	$(4.81 \pm 0.25) \times 10^3$
10.1	$(7.60 \pm 0.93) \times 10^3$

TABLE XXX

RESISTIVITIES AT THREE TEMPERATURES  
(MEMBRANE NO. 131-021)

Composition:  $\text{ZrO}_2$ ,  $\text{H}_3\text{PO}_4$ , "Zeolon H" (30, 23,  
 47 percent by weight)  
 Drying Conditions: 40 hours at 160°C

<u>Relative Humidity</u> (%)	<u>Resistivity</u> (Ohm-Cm)
<u>Temperature 70.4°C</u>	
75.6	$(1.58 \pm 0.27) \times 10^3$
38.3	$(3.61 \pm 0.57) \times 10^3$
13.7	$(4.71 \pm 0.64) \times 10^3$
0	$(1.78 \pm 0.33) \times 10^4$
<u>Temperature 90.1°C</u>	
83.1	$(4.91 \pm 0.79) \times 10^2$
68.6	$(1.00 \pm 0.14) \times 10^3$
45.6	$(2.29 \pm 0.20) \times 10^3$
27.9	$(3.18 \pm 0.45) \times 10^3$
9.6	$(4.18 \pm 0.64) \times 10^3$
0	$(9.47 \pm 2.45) \times 10^3$
<u>Temperature 105.2°C</u>	
64.0	$(6.35 \pm 0.44) \times 10^2$
58.5	$(6.33 \pm 0.95) \times 10^2$
48.2	$(1.11 \pm 0.17) \times 10^3$
26.5	$(2.14 \pm 0.42) \times 10^3$
9.2	$(3.29 \pm 0.74) \times 10^3$
0	$(1.65 \pm 0.42) \times 10^5$

TABLE XXXI

RESISTIVITIES AT THREE TEMPERATURES  
(MEMBRANE NO. 131-002)

Composition:  $\text{ZrO}_2$ ,  $\text{H}_3\text{PO}_4$ , "Zeolon H"  
(30, 23, 47 percent by weight)  
Drying Conditions: 60 hours at  $150^\circ\text{C}$

<u>Relative Humidity</u> <u>(%)</u>	<u>Resistivity</u> <u>(Ohm-Cm)</u>
<u>Temperature <math>70.4^\circ\text{C}</math></u>	
75.6	$(8.96 \pm 2.33) \times 10^2$
38.3	$(1.84 \pm 0.49) \times 10^3$
13.7	$(3.04 \pm 0.76) \times 10^3$
0	$(1.08 \pm 0.25) \times 10^4$
<u>Temperature <math>90.1^\circ\text{C}</math></u>	
83.1	$(3.54 \pm 0.41) \times 10^2$
68.6	$(6.24 \pm 0.83) \times 10^2$
45.6	$(1.40 \pm 0.21) \times 10^3$
27.9	$(1.92 \pm 0.30) \times 10^3$
9.6	$(2.53 \pm 0.41) \times 10^3$
0	$(5.80 \pm 1.10) \times 10^3$
<u>Temperature <math>105.2^\circ\text{C}</math></u>	
64.0	$(3.90 \pm 0.64) \times 10^2$
58.5	$(4.21 \pm 0.83) \times 10^2$
48.5	$(6.93 \pm 1.23) \times 10^2$
26.5	$(1.30 \pm 0.25) \times 10^3$
9.2	$(1.98 \pm 0.41) \times 10^3$
0	$(5.44 \pm 1.17) \times 10^4$

TABLE XXXII

RESISTIVITIES AT THREE TEMPERATURES  
(MEMBRANE NO. 131-023)

Composition: (30, 23, 47 percent by weight)  
 Drying Conditions: 40 hours at 150°C

<u>Relative Humidity</u> <u>(%)</u>	<u>Resistivity</u> <u>(Ohm-Cm)</u>
<u>Temperature 70.7°C</u>	
84	$(7.80 \pm 1.68) \times 10^2$
37	$(1.84 \pm 0.21) \times 10^3$
13	$(2.47 \pm 0.24) \times 10^3$
0	$(1.78 \pm 0.08) \times 10^4$
<u>Temperature 89.8°C</u>	
85	$(2.84 \pm 0.70) \times 10^2$
46	$(1.10 \pm 0.20) \times 10^3$
30	$(1.77 \pm 0.29) \times 10^3$
10	$(2.42 \pm 0.32) \times 10^3$
0	$(2.92 \pm 0.31) \times 10^4$
<u>Temperature 104.3°C</u>	
72	$(1.83 \pm 0.36) \times 10^2$
61	$(2.89 \pm 0.61) \times 10^2$
51	$(5.07 \pm 0.90) \times 10^2$
26	$(1.30 \pm 0.22) \times 10^3$
11	$(2.09 \pm 0.29) \times 10^3$
0	$(2.41 \pm 1.02) \times 10^5$

TABLE XXXIII

RESISTIVITIES AT THREE TEMPERATURES

(MEMBRANE NO. 131-024)

Composition:  $\text{ZrO}_2$ ,  $\text{H}_3\text{PO}_4$ , "Zeolon H" (30, 27.2,  
42.8 percent by weight)

Drying Conditions: 52 hours at  $144^\circ\text{C}$

<u>Relative Humidity</u> <u>(%)</u>	<u>Resistivity</u> <u>(Ohm-Cm)</u>
<u>Temperature <math>70.7^\circ\text{C}</math></u>	
84	$(3.02 \pm 0.51) \times 10^2$
37	$(6.70 \pm 0.58) \times 10^2$
13	$(8.76 \pm 0.72) \times 10^2$
0	$(5.85 \pm 0.18) \times 10^3$
<u>Temperature <math>89.8^\circ\text{C}</math></u>	
85	$(1.22 \pm 0.08) \times 10^2$
46	$(4.31 \pm 0.53) \times 10^2$
30	$(6.82 \pm 0.73) \times 10^2$
10	$(9.28 \pm 0.84) \times 10^2$
0	$(7.44 \pm 0.71) \times 10^3$
<u>Temperature <math>104.3^\circ\text{C}</math></u>	
61	$(1.19 \pm 0.12) \times 10^2$
51	$(2.06 \pm 0.20) \times 10^2$
26	$(4.47 \pm 0.70) \times 10^2$
11	$(7.59 \pm 1.04) \times 10^2$
0	$(4.57 \pm 1.33) \times 10^4$



TABLE XXXIV

RESISTIVITIES AT THREE TEMPERATURES  
(MEMBRANE NO. 131-025)

Composition:  $\text{ZrO}_2$ ,  $\text{H}_3\text{PO}_4$ , "Zeolon H" (30, 23, 47  
 percent by weight)

Drying Conditions: 40 hours at  $150^\circ\text{C}$

<u>Relative Humidity</u> (%)	<u>Resistivity</u> (Ohm-Cm)
<u>Temperature <math>70.4^\circ\text{C}</math></u>	
75.6	$(1.07 \pm 0.43) \times 10^3$
38.3	$(1.94 \pm 0.76) \times 10^3$
13.7	$(2.83 \pm 1.24) \times 10^3$
0	$(5.84 \pm 1.89) \times 10^3$
<u>Temperature <math>90.1^\circ\text{C}</math></u>	
83.1	$(3.84 \pm 1.50) \times 10^2$
68.6	$(6.34 \pm 2.07) \times 10^2$
45.6	$(1.34 \pm 0.41) \times 10^3$
27.9	$(2.16 \pm 1.05) \times 10^3$
9.6	$(3.55 \pm 2.33) \times 10^3$
0	$(5.91 \pm 1.68) \times 10^3$
<u>Temperature <math>105.2^\circ\text{C}</math></u>	
64.0	$(3.77 \pm 1.96) \times 10^2$
58.5	$(4.49 \pm 2.56) \times 10^2$
48.2	$(6.99 \pm 3.70) \times 10^2$
26.5	$(1.60 \pm 0.93) \times 10^3$
9.2	$(2.97 \pm 2.11) \times 10^3$
0	$(1.98 \pm 1.91) \times 10^4$

TABLE XXXV

RESISTIVITIES AT THREE TEMPERATURES  
(MEMBRANE NO. 131-026)

Composition:  $\text{ZrO}_2$ ,  $\text{H}_3\text{PO}_4$ , "Zeolon H" (30, 18.8,  
 51.2 percent by weight)  
 Drying Conditions: 52 hours at  $156^\circ\text{C}$

<u>Relative Humidity</u> <u>(%)</u>	<u>Resistivity</u> <u>(Ohm-Cm)</u>
<u>Temperature <math>70.7^\circ\text{C}</math></u>	
84	$(3.49 \pm 0.99) \times 10^3$
37	$(9.94 \pm 3.56) \times 10^3$
13	$(1.47 \pm 0.60) \times 10^4$
0	$(1.65 \pm 1.07) \times 10^5$
<u>Temperature <math>89.9^\circ\text{C}</math></u>	
85	$(1.24 \pm 0.23) \times 10^3$
46	$(5.70 \pm 1.82) \times 10^3$
30	$(1.01 \pm 0.37) \times 10^4$
10	$(1.45 \pm 0.49) \times 10^4$
0	$(2.57 \pm 0.74) \times 10^5$
<u>Temperature <math>104.3^\circ\text{C}</math></u>	
72	$(4.97 \pm 1.43) \times 10^2$
61	$(1.04 \pm 0.14) \times 10^3$
51	$(2.27 \pm 0.48) \times 10^3$
26	$(6.53 \pm 1.75) \times 10^3$
11	$(1.16 \pm 0.30) \times 10^4$
0	$(2.80 \pm 0.79) \times 10^6$

TABLE XXXVI

RESISTIVITIES AT THREE TEMPERATURES  
(MEMBRANE NO. 131-027)

Composition:  $\text{ZrO}_4$ ,  $\text{H}_3\text{PO}_4$ , "Zeolon H"  
 (30, 30, 40 percent by weight)  
 Drying Conditions: 40 hours at 150°C

<u>Relative Humidity</u> (%)	<u>Resistivity</u> (Ohm-Cm)
<u>Temperature 70.4°C</u>	
75.6	$(2.17 \pm 0.37) \times 10^2$
38.3	$(3.77 \pm 0.61) \times 10^2$
13.7	$(5.05 \pm 0.93) \times 10^2$
0	$(1.53 \pm 0.23) \times 10^3$
<u>Temperature 90.1°C</u>	
83.1	$(7.50 \pm 1.26) \times 10^1$
68.6	$(1.22 \pm 0.23) \times 10^2$
45.6	$(2.53 \pm 0.49) \times 10^2$
27.9	$(3.38 \pm 0.72) \times 10^2$
9.6	$(4.37 \pm 0.85) \times 10^2$
0	$(1.02 \pm 0.13) \times 10^3$
<u>Temperature 105.2°C</u>	
64.0	$(6.81 \pm 1.05) \times 10^1$
58.5	$(6.94 \pm 1.06) \times 10^1$
48.2	$(1.11 \pm 0.18) \times 10^2$
26.5	$(2.48 \pm 0.41) \times 10^2$
9.2	$(3.64 \pm 0.64) \times 10^2$
0	$(6.64 \pm 1.64) \times 10^3$

TABLE XXXVII  
RESISTIVITIES AT THREE TEMPERATURES  
(MEMBRANE NO. 131-028)

Composition:  $\text{ZrO}_2$ ,  $\text{H}_3\text{PO}_4$ , "Zeolon H"  
 (30, 23, 47 percent by weight)  
 Drying Conditions: 40 hours at 150°C

<u>Relative Humidity</u> (%)	<u>Resistivity</u> (Ohm-Cm)
<u>Temperature 69.8°C</u>	
78.9	$(9.52 \pm 0.63) \times 10^2$
65.6	$(1.03 \pm 0.06) \times 10^3$
39.6	$(1.32 \pm 0.05) \times 10^3$
14.2	$(2.12 \pm 0.16) \times 10^3$
<u>Temperature 89.8°C</u>	
82.5	$(2.30 \pm 0.18) \times 10^2$
68.9	$(4.11 \pm 0.26) \times 10^2$
46.5	$(7.50 \pm 0.54) \times 10^2$
30.0	$(1.72 \pm 0.12) \times 10^3$
10.0	$(2.21 \pm 0.20) \times 10^3$
<u>Temperature 105.0°C</u>	
70.3	$(1.09 \pm 0.16) \times 10^2$
59.1	$(1.81 \pm 0.26) \times 10^2$
46.6	$(3.40 \pm 0.50) \times 10^2$
25.6	$(7.04 \pm 0.87) \times 10^2$
10.1	$(1.27 \pm 0.21) \times 10^3$

TABLE XXXVIII

RESISTIVITIES AT THREE TEMPERATURES  
(MEMBRANE NO. 131-029)

Composition:  $\text{ZrO}_2$ ,  $\text{H}_3\text{PO}_4$ , "Zeolon H" (30, 23,  
 47 percent by weight)  
 Drying Conditions: 40 hours at  $150^\circ\text{C}$

<u>Relative Humidity</u> <u>(%)</u>	<u>Resistivity</u> <u>(Ohm-Cm)</u>
<u>Temperature <math>69.8^\circ\text{C}</math></u>	
78.9	$(1.07 \pm 0.08) \times 10^3$
65.6	$(1.17 \pm 0.08) \times 10^3$
39.6	$(1.49 \pm 0.09) \times 10^3$
14.2	$(2.59 \pm 0.19) \times 10^3$
<u>Temperature <math>89.8^\circ\text{C}</math></u>	
82.5	$(2.61 \pm 0.14) \times 10^2$
68.9	$(4.87 \pm 0.28) \times 10^2$
46.5	$(8.95 \pm 0.55) \times 10^2$
30.0	$(2.17 \pm 0.13) \times 10^3$
10.0	$(2.67 \pm 0.24) \times 10^3$
<u>Temperature <math>105.0^\circ\text{C}</math></u>	
70.3	$(1.18 \pm 0.18) \times 10^2$
59.1	$(2.08 \pm 0.28) \times 10^2$
46.6	$(3.95 \pm 0.44) \times 10^2$
25.6	$(8.88 \pm 1.22) \times 10^2$
10.1	$(1.62 \pm 0.22) \times 10^3$

TABLE XXXIX

RESISTIVITIES AT THREE TEMPERATURES  
(MEMBRANE NO. 131-030)

Composition:  $\text{ZrO}_2$ ,  $\text{H}_3\text{PO}_4$ , "Zeolon H" (30, 18.8,  
51.2 percent by weight)  
Drying Conditions: 28 hours at  $144^\circ\text{C}$

<u>Relative Humidity</u> <u>(%)</u>	<u>Resistivity</u> <u>(Ohm-Cm)</u>
<u>Temperature <math>70.7^\circ\text{C}</math></u>	
84	$(2.90 \pm 1.37) \times 10^3$
37	$(7.83 \pm 3.54) \times 10^3$
13	$(1.11 \pm 0.49) \times 10^4$
0	$(1.15 \pm 0.57) \times 10^5$
<u>Temperature <math>89.8^\circ\text{C}</math></u>	
85	$(9.74 \pm 3.63) \times 10^2$
46	$(4.74 \pm 2.43) \times 10^3$
30	$(8.30 \pm 4.27) \times 10^3$
10	$(1.16 \pm 0.52) \times 10^4$
0	$(2.62 \pm 2.22) \times 10^5$
<u>Temperature <math>104.3^\circ\text{C}</math></u>	
72	$(4.41 \pm 0.84) \times 10^2$
61	$(9.94 \pm 1.63) \times 10^2$
51	$(2.44 \pm 0.74) \times 10^3$
26	$(7.52 \pm 2.92) \times 10^3$
11	$(1.26 \pm 0.37) \times 10^4$
0	$(4.65 \pm 3.19) \times 10^6$

TABLE XL

RESISTIVITIES AT THREE TEMPERATURES(MEMBRANE NO. 131-031)

Composition:  $\text{ZrO}_2$ ,  $\text{H}_3\text{PO}_4$ , "Zeolon H" (30, 27.2,  
42.8 percent by weight)

Drying Conditions: 28 hours at 156°C

<u>Relative Humidity</u> (%)	<u>Resistivity</u> (Ohm-Cm)
<u>Temperature 70.4°C</u>	
75.6	$(3.70 \pm 0.52) \times 10^2$
38.3	$(6.79 \pm 0.93) \times 10^2$
13.7	$(9.97 \pm 1.60) \times 10^2$
0	$(3.32 \pm 0.51) \times 10^3$
<u>Temperature 90.1°C</u>	
83.1	$(1.37 \pm 0.21) \times 10^2$
68.6	$(2.27 \pm 0.37) \times 10^2$
45.6	$(4.62 \pm 0.65) \times 10^2$
27.9	$(6.21 \pm 0.65) \times 10^2$
9.6	$(8.00 \pm 0.59) \times 10^2$
0	$(1.81 \pm 0.30) \times 10^3$
<u>Temperature 105.2°C</u>	
64.0	$(1.01 \pm 0.21) \times 10^2$
58.5	$(1.17 \pm 0.16) \times 10^2$
48.2	$(1.97 \pm 0.33) \times 10^2$
26.5	$(4.08 \pm 0.64) \times 10^2$
9.2	$(6.29 \pm 0.89) \times 10^2$
0	$(9.29 \pm 1.29) \times 10^3$

TABLE XLI

RESISTIVITIES AT THREE TEMPERATURES(MEMBRANE NO. 131-032)Composition:  $\text{ZrO}_2$ ,  $\text{H}_3\text{PO}_4$ , "Zeolon H" (30, 23,

47 percent by weight)

Drying Conditions: 20 hours at 150°C

<u>Relative Humidity</u> (%)	<u>Resistivity</u> (Ohm-Cm)
<u>Temperature 70.4°C</u>	
75.6	$(1.13 \pm 0.20) \times 10^3$
38.3	$(2.12 \pm 0.43) \times 10^3$
13.7	$(2.92 \pm 0.72) \times 10^3$
0	$(1.07 \pm 0.31) \times 10^4$
<u>Temperature 90.1°C</u>	
83.1	$(3.95 \pm 0.60) \times 10^2$
68.6	$(6.65 \pm 1.07) \times 10^2$
45.6	$(1.45 \pm 0.28) \times 10^3$
27.9	$(1.93 \pm 0.37) \times 10^3$
9.6	$(2.52 \pm 0.53) \times 10^3$
0	$(6.96 \pm 1.54) \times 10^3$
<u>Temperature 105.2°C</u>	
64.0	$(3.75 \pm 0.52) \times 10^2$
58.5	$(4.26 \pm 0.64) \times 10^2$
48.2	$(6.99 \pm 1.21) \times 10^2$
26.5	$(1.41 \pm 0.28) \times 10^3$
9.2	$(2.14 \pm 0.45) \times 10^3$
0	$(5.85 \pm 1.28) \times 10^4$



TABLE XLII

RESISTIVITIES AT THREE TEMPERATURES  
(MEMBRANE NO. 131-033)

Composition:  $\text{ZrO}_2$ ,  $\text{H}_3\text{PO}_4$ , "Zeolon H" (30, 18.8,  
 51.2 percent by weight)  
 Drying Conditions: 28 hours at 156°C

<u>Relative Humidity</u> (%)	<u>Resistivity</u> (Ohm-Cm)
<u>Temperature 70.4°C</u>	
75.6	$(1.59 \pm 0.09) \times 10^3$
38.3	$(2.98 \pm 0.22) \times 10^3$
13.7	$(3.89 \pm 0.40) \times 10^3$
0	$(1.60 \pm 0.29) \times 10^4$
<u>Temperature 90.1°C</u>	
83.1	$(4.89 \pm 0.13) \times 10^2$
68.6	$(8.32 \pm 0.44) \times 10^2$
45.6	$(1.94 \pm 0.15) \times 10^3$
27.9	$(2.64 \pm 0.23) \times 10^3$
9.6	$(3.47 \pm 0.35) \times 10^3$
0	$(1.01 \pm 0.13) \times 10^4$
<u>Temperature 105.2°C</u>	
64.0	$(3.65 \pm 0.16) \times 10^2$
58.5	$(4.76 \pm 0.18) \times 10^2$
48.2	$(8.19 \pm 0.32) \times 10^2$
26.5	$(1.84 \pm 0.13) \times 10^3$
9.2	$(2.84 \pm 0.23) \times 10^3$
0	$(8.47 \pm 1.49) \times 10^4$

TABLE XLIII

## RESISTIVITIES AT THREE TEMPERATURES

(MEMBRANE NO. 131-035)

Composition:  $\text{ZrO}_2$ ,  $\text{H}_3\text{PO}_4$ , "Zeolon H" (30, 27.2,

42.8, percent by weight)

Drying Conditions: 28 hours at  $144^\circ\text{C}$ 

Relative Humidity (%)	Resistivity (Ohm-Cm)
<u>Temperature <math>70.1^\circ\text{C}</math></u>	
64.6	$(2.24 \pm 0.01) \times 10^2$
39.0	$(3.13 \pm 0.11) \times 10^2$
13.4	$(4.19 \pm 0.18) \times 10^2$
<u>Temperature <math>89.8^\circ\text{C}</math></u>	
84.2	$(9.61 \pm 0.21) \times 10^1$
68.9	$(1.48 \pm 0.04) \times 10^2$
45.1	$(2.24 \pm 0.04) \times 10^2$
29.4	$(4.35 \pm 0.10) \times 10^2$
10.4	$(5.27 \pm 0.25) \times 10^2$
<u>Temperature <math>105.7^\circ\text{C}</math></u>	
70.5	$(5.95 \pm 0.45) \times 10^1$
55.6	$(9.32 \pm 0.21) \times 10^1$
47.0	$(1.42 \pm 0.05) \times 10^2$
24.6	$(2.81 \pm 0.11) \times 10^2$
10.0	$(5.70 \pm 0.09) \times 10^2$

TABLE XLIV

RESISTIVITIES AT THREE TEMPERATURES(MEMBRANE NO. 131-036)Composition:  $\text{ZrO}_2$ ,  $\text{H}_3\text{PO}_4$ , "Zeolon H" (30, 18.8,

51.2 percent by weight)

Drying Conditions: 52 hours at  $144^\circ\text{C}$ 

<u>Relative Humidity (%)</u>	<u>Resistivity (Ohm-Cm)</u>
<u>Temperature <math>70.1^\circ\text{C}</math></u>	
64.6	$(2.95 \pm 0.89) \times 10^3$
39.0	$(4.12 \pm 1.24) \times 10^3$
13.4	$(5.38 \pm 1.47) \times 10^3$
<u>Temperature <math>89.8^\circ\text{C}</math></u>	
84.2	$(8.83 \pm 3.63) \times 10^2$
68.9	$(1.60 \pm 0.56) \times 10^3$
45.1	$(3.94 \pm 1.39) \times 10^3$
29.4	$(6.06 \pm 2.22) \times 10^3$
10.4	$(5.68 \pm 1.92) \times 10^3$
<u>Temperature <math>105.7^\circ\text{C}</math></u>	
70.5	$(5.32 \pm 2.37) \times 10^2$
55.6	$(8.69 \pm 3.83) \times 10^2$
47.0	$(1.89 \pm 0.69) \times 10^3$
24.6	$(3.53 \pm 1.55) \times 10^3$
10.0	$(5.33 \pm 2.00) \times 10^3$

TABLE XLV

RESISTIVITIES AT THREE TEMPERATURES

(MEMBRANE NO. 131-037)

Composition:  $\text{ZrO}_2$ ,  $\text{H}_3\text{PO}_4$ , "Zeolon H" (30, 27.2,

42.8 percent by weight)

Drying Conditions: 52 hours at  $156^\circ\text{C}$

<u>Relative Humidity</u> <u>(%)</u>	<u>Resistivity</u> <u>(Ohm-Cm)</u>
<u>Temperature <math>70.1^\circ\text{C}</math></u>	
64.6	$(1.87 \pm 0.32) \times 10^3$
39.0	$(2.84 \pm 0.56) \times 10^3$
13.4	$(3.81 \pm 0.83) \times 10^3$
<u>Temperature <math>89.8^\circ\text{C}</math></u>	
84.2	$(4.05 \pm 0.86) \times 10^2$
68.9	$(7.60 \pm 1.51) \times 10^2$
45.1	$(2.69 \pm 0.40) \times 10^3$
29.4	$(4.01 \pm 0.91) \times 10^3$
10.4	$(4.22 \pm 1.13) \times 10^3$
<u>Temperature <math>105.7^\circ\text{C}</math></u>	
70.5	$(3.02 \pm 0.11) \times 10^2$
55.6	$(5.23 \pm 0.35) \times 10^2$
47.0	$(1.10 \pm 0.11) \times 10^3$
24.6	$(2.56 \pm 0.18) \times 10^3$
10.0	$(4.19 \pm 0.54) \times 10^3$

TABLE XLVI

RESISTIVITIES AT THREE TEMPERATURES

(MEMBRANE NO. 131-038)

Composition:  $\text{ZrO}_2$ ,  $\text{H}_3\text{PO}_4$ , "Zeolon H" (30, 16,

54 percent by weight)

Drying Conditions: 40 hours at  $150^\circ\text{C}$

<u>Relative Humidity (%)</u>	<u>Resistivity (Ohm-Cm)</u>
<u>Temperature <math>70.1^\circ\text{C}</math></u>	
64.6	$(1.17 \pm 0.06) \times 10^4$
39.0	$(1.78 \pm 0.08) \times 10^4$
13.4	$(2.41 \pm 0.10) \times 10^4$
<u>Temperature <math>89.8^\circ\text{C}</math></u>	
84.2	$(3.07 \pm 0.25) \times 10^3$
68.9	$(5.57 \pm 0.38) \times 10^3$
45.1	$(1.09 \pm 0.07) \times 10^4$
29.4	$(1.64 \pm 0.27) \times 10^4$
10.4	$(2.30 \pm 0.14) \times 10^4$
<u>Temperature <math>105.7^\circ\text{C}</math></u>	
70.5	$(1.33 \pm 0.03) \times 10^3$
55.6	$(2.79 \pm 0.04) \times 10^3$
47.0	$(5.72 \pm 0.40) \times 10^3$
24.6	$(1.01 \pm 0.03) \times 10^4$
10.0	$(1.77 \pm 0.04) \times 10^4$

TABLE XLVII

## RESISTIVITIES AT THREE TEMPERATURES

(MEMBRANE NO. 131-039)

Composition:  $\text{ZrO}_2$ ,  $\text{H}_3\text{PO}_4$ , "Zeolon H" (30, 23,  
47 percent by weight)

Drying Conditions: 40 hours at  $140^\circ\text{C}$

Relative Humidity (%)	Resistivity (Ohm-Cm)
<u>Temperature <math>70.1^\circ\text{C}</math></u>	
64.6	$(8.24 \pm 0.47) \times 10^2$
39.0	$(1.19 \pm 0.08) \times 10^3$
13.4	$(1.52 \pm 0.12) \times 10^3$
<u>Temperature <math>89.8^\circ\text{C}</math></u>	
84.2	$(2.47 \pm 0.18) \times 10^2$
68.9	$(4.54 \pm 0.57) \times 10^2$
45.1	$(8.85 \pm 0.40) \times 10^2$
29.4	$(1.32 \pm 0.15) \times 10^3$
10.4	$(1.60 \pm 0.21) \times 10^3$
<u>Temperature <math>105.7^\circ\text{C}</math></u>	
70.5	$(2.42 \pm 0.59) \times 10^2$
55.6	$(3.15 \pm 0.50) \times 10^2$
47.0	$(5.23 \pm 0.52) \times 10^2$
24.6	$(1.23 \pm 0.29) \times 10^3$
10.0	$(1.74 \pm 0.27) \times 10^3$

TABLE XLVIII  
RESISTIVITIES AT THREE TEMPERATURES  
(MEMBRANE NO. 131-040)

Composition:  $\text{ZrO}_2$ ,  $\text{H}_3\text{PO}_4$ , "Zeolon H" (32, 23,  
47 percent by weight)  
Drying Conditions: 40 hours at  $150^\circ\text{C}$

<u>Relative Humidity</u> (%)	<u>Resistivity</u> (Ohm-Cm)
<u>Temperature <math>70.1^\circ\text{C}</math></u>	
64.6	$(1.14 \pm 0.56) \times 10^3$
39.0	$(1.69 \pm 0.83) \times 10^3$
13.4	$(2.22 \pm 1.09) \times 10^3$
<u>Temperature <math>89.8^\circ\text{C}</math></u>	
84.2	$(3.15 \pm 1.46) \times 10^2$
68.9	$(5.92 \pm 2.93) \times 10^2$
45.1	$(1.36 \pm 0.72) \times 10^3$
29.4	$(2.19 \pm 1.22) \times 10^3$
10.4	$(2.28 \pm 1.13) \times 10^3$
<u>Temperature <math>105.7^\circ\text{C}</math></u>	
70.5	$(2.37 \pm 1.79) \times 10^2$
55.6	$(3.57 \pm 2.09) \times 10^2$
47.0	$(7.11 \pm 3.83) \times 10^2$
24.6	$(1.31 \pm 0.87) \times 10^3$
10.0	$(2.27 \pm 1.17) \times 10^3$